

ENERGY METABOLISM AND MECHANOTRANSDUCTION  
IN OSTEOARTHRITIC CHONDROCYTES:  
TARGETED METABOLIC PROFILING AND FLUX ANALYSIS

by

Ayten Ebru Erdogan

A thesis submitted in partial fulfillment  
of the requirements for the degree

of

Master of Science

in

Chemical Engineering

MONTANA STATE UNIVERSITY  
Bozeman, Montana

August 2023

©COPYRIGHT

by

Ayten Ebru Erdogan

2023

All Rights Reserved

## DEDICATION

This thesis, first and foremost, is dedicated in loving memory to one of the most important people that raised me. I will forever be grateful for Hatice Gulhan and her beautiful heart.

I also dedicate this to my mother who, through thick and thin, never stopped believing in me and taught me how to be a dreamer.

I would also like to express my deepest appreciation to my family and friends who has been supporting me throughout this journey. I am forever grateful.

## TABLE OF CONTENTS

1. INTRODUCTION .....	1
Background and Project Rationale.....	1
Chondrocyte Metabolism, Articular Cartilage and Collagen .....	4
Targeted Metabolomics and Flux Analysis .....	8
References.....	10
 2. IDENTIFICATION OF CARBON SOURCES IN OA PRIMARY HUMAN CHONDROCYTES USING <sup>13</sup> C-ISOTOPIC LABELING AND MASS SPECTROMETRY .....	16
Contributions of Authors and Co-authors.....	16
Manuscript Information .....	17
Abstract.....	18
Introduction.....	19
Materials and Methods.....	22
Chondrocyte Harvest and Culture with Isotopic Conditions .....	22
Untargeted Metabolomics .....	23
Targeted Metabolomics and Statistical Analysis .....	24
Results.....	25
Temporal Analysis of OA Primary Human Chondrocytes .....	25
Targeted Qualitative Analysis of Regular Labeled Media .....	27
Targeted Qualitative Analysis of Alternately Labeled Media .....	29
Discussion.....	32
<sup>13</sup> C labeling Has Minimal Effects on Metabolomic Profiles .....	32
TCA Cycle Metabolite Isotopes were Detected within Different Time Windows.....	33
OA PHC have Different Responses to Different Carbon Sources.....	33
Conclusion .....	33
References.....	35
 3. AN IMPROVED STOICHIOMETRIC MODEL OF CHONDROCYTE CENTRAL METABOLISM: FLUX BALANCE ANALYSIS AND INITIAL MECHANOTRANSDUCTION RESULTS .....	37
Contributions of Authors and Co-authors.....	37
Manuscript Information .....	38
Abstract.....	39
Introduction.....	40
Materials and Methods.....	42
Stoichiometric Model Building.....	42
Chondrocyte Harvest and Culture.....	43
Agarose Encapsulation and Chondrocyte Loading.....	44
LC-MS Method Development and Targeted Metabolomics .....	46

## TABLE OF CONTENTS CONTINUED

Results.....	46
Model Predictions of ATP Yields.....	46
O <sub>2</sub> Dependent Type II Collagen and Type VI Collagen Predictions .....	47
Mapping Collagen Production on Lactate via FBA.....	48
Accumulation of Four Targets under OA Mechanotransduction .....	49
Discussion .....	50
Conclusion .....	52
References.....	54
4. CONCLUSION AND FUTURE WORK .....	57
REFERENCES CITED.....	59
APPENDICES .....	70
APPENDIX A: SUPPLEMENTAL INFORMATION FOR CHAPTER 2.....	71
APPENDIX B: SUPPLEMENTAL INFORMATION FOR CHAPTER 3 .....	81

## LIST OF TABLES

Table	Page
1. Table 2.1. ANOVA and clustergram .....	26
2. Table 3.1. List of targeted central carbon metabolism compounds .....	45
3. Table A.1. Library for targeted metabolites and their isotopes .....	72

## LIST OF FIGURES

Figure	Page
1. Figure.1.1. Basic biological structure of articular chondrocytes .....	6
2. Figure.1.2. Cells obtain nutrients and energy from glucose, which is metabolized into amino acid precursors that help make up collagen II. Two possible source of carbon is depicted to be glucose and glutamine when the pathways are traced .....	7
3. Figure.2.1. Production of Collagen via Central Carbon Metabolism. Key amino acid precursors (3-Pyruvateglycerate, Pyruvate and Oxaloacetate) that majorly contribute to Collagen production were depicted in yellow .....	20
4. Figure 2.2. Collagen-II and Collagen-VI within ECM and PCM.....	21
5. Figure 2.3. Experimental designs for Regular Labeled and Alternately Labeled experimental sets .....	22
6. Figure 2.4. Label-dependent PCA that covers nearly 50% of the dataset variance indicates minimal kinetic effect of isotopic labeling.....	25
7. Figure 2.5. Detected metabolites key to TCA cycle. Orange depicts metabolites that are only detected in their unlabeled structure, green depicts metabolites that are detected in their isotopic states, and blue depicts metabolites that were not detected.....	27
8. Figure 2.6. Repeated measures ANOVA results for temporal analysis, experimental set 1 .....	28
9. Figure 2.7. Repeated measures ANOVA results for between-label analysis, experimental set 1 .....	29
10. Figure 2.8. Repeated measures ANOVA results for temporal analysis, experimental set 2 .....	30
11. Figure 2.9. Repeated measures ANOVA results for between-label analysis, experimental set 2 .....	31

## LIST OF FIGURES CONTINUED

12. Figure 3.1. Key amino acid precursors produced by Glycolysis and TCA Cycle play an important role in the production and maintenance of Collagen. In turn, Collagen provides articular cartilage, that is degenerated in OA, with the necessary mechanical strength, flexibility, and resistance to mechanical forces .....	41
13. Figure 3.2. Carbon source dependent ATP yield predictions in the presence and absence of available O <sub>2</sub> .....	47
14. Figure 3.3. Yields of Collagen-II and Collagen-VI on Glucose and Glutamine with oxidative phosphorylation.....	47
15. Figure 3.4. Maximized production of Collagen-II in varying levels of lactate production .....	48
16. Figure 3.5. Maximized production of Collagen-VI in varying levels of lactate production .....	49
17. Figure 3.6. Accumulations of four targeted metabolites.....	50
18. Figure 3.7. Essential and non-essential amino acid needs of Collagen-II and Collagen-VI.....	51
19. Figure A.1. Clustering of median metabolite intensities finds 3 distinct groups that vary between timepoints .....	80

## ABSTRACT

Osteoarthritis (OA) is a prevalent and debilitating disease that affects hundreds of millions of people worldwide. One of OA's major consequences is the degradation of articular cartilage, leading to joint pain, stiffness, and loss of function. Currently, there is no treatment for OA. The existing interventions are mostly for suppressing the symptoms: physical therapy, anti-inflammatories, and pain management. The last resort is total joint replacement, which has long-term consequences especially for early-onset OA patients. Thus, researchers are focusing on understanding this complex disease and its molecular components to develop better treatments. Chondrocytes, the sole cell type in articular cartilage, play a crucial role in maintaining tissue homeostasis and responding to mechanical stimuli via synthesis of key structural components like collagen. However, the intracellular pathways underlying chondrocyte mechanotransduction are not fully understood, especially those related to central carbon metabolism. This thesis uses  $^{13}\text{C}$  isotopic labeling to trace carbon sources and downstream metabolites related to energy metabolism *in vitro*. Primary human articular chondrocytes from OA patients exposed to labeled glucose and glutamine, and their global and targeted metabolite profiles are assessed. The results show how both glucose and glutamine utilization as carbon sources flows through the TCA cycle. This work also develops a comprehensive model of mammalian carbon metabolism in OA primary human chondrocytes. The model integrates energy metabolism, amino acid synthesis, and transport reactions contributing to Collagen-II and Collagen-VI production. Using flux balance analysis (FBA), trade-offs between Collagen-II and Collagen-VI synthesis are evaluated based on ATP and carbon source requirements under different oxidative stress conditions. Then, these model predictions are presented with experimental data obtained from OA chondrocytes subjected to shear and compressive mechanical stimulation, which can be integrated in the model later on. These data shed new light on the metabolism of primary OA chondrocytes and provide insight into potential therapeutic targets for OA intervention.

## CHAPTER ONE

## INTRODUCTION

Background and Project Rationale

Osteoarthritis (OA) is a complex disease that affects more than 500 million people globally [1]. It results from the degradation of articular cartilage and associated pathological changes in nearby joint tissues [2]. Interventions that currently exist are anti-inflammatories, pain management, and as a last resort, joint replacement. The healthcare costs for OA are \$81 billion in United States alone [3]. In spite of advances in the field, researchers need a better understanding of the molecular underpinnings of the disease to develop interventions that reduce the need for joint replacement surgery. The current research is focused on studying the cellular properties of chondrocytes.

Articular cartilage is solely composed of specialized type of cells, the chondrocytes. The chondrocytes are surrounded by a PCM and a denser ECM that envelopes both [4]. Cartilage is avascular (possessing no blood vessel) and chondrocytes exhibit mechanotransductive properties. “Mechanotransduction” refers to the cellular responses triggered by mechanical loading. We can think of these mechanical stimuli as resulting from the physical activities that we perform in our everyday life. Walking, running, standing, etc. are all examples of activities that provide mechanical loads on our various joints. As a result of these activities, transmission of forces occurs and result in strains throughout the respective joint tissues they have an effect on. For articular cartilage, these strains include shear, compression, and tension [5]. The responses

elucidated from chondrocytes as a result of these loads and deformations vary between a healthy sample compared to a diseased one [6][7].

The pathogenesis of OA is also affected by several different risk factors, which elevates the complexity of the disease. Although counterintuitive, heavy manual labor is associated with decreased osteoarthritis in elderly patients [8]. This is likely an example of the benefits of chondrocyte mechanotransduction. In another example, the force acting on the joints of two adults doing the same activities but have different body weights will be different. Thus, the body mass index (BMI) [9] as well as the age [10], sex [11], genetic factors [12], environment and comorbidities vary between donor samples, affecting the etiology of OA on the cellular level. Interestingly, obese individuals have elevated rates of OA in both weight-bearing and non-weight-bearing joints [13]. Therefore, studying OA samples from different donors with or without loading is necessary to characterize chondrocyte mechanotransduction and the pathways playing role in the maintenance of the cell.

The resulting change in biochemical responses can be characterized using several complementary techniques. These techniques are classified as “omics” approaches. The availability of different omics such as genomics, transcriptomics, proteomics and metabolomics offers us an opportunity to study cellular pathways. Genomics maps the DNA sequence and structure of the organism of interest. Transcriptomics uses RNA, which are copied pieces of DNA (e.g. messenger mRNA), to study the information expressed through the RNA transcripts [14]. Proteomics is the large study and characterization of proteomes and their interactions with each other in an organism [15].

A newly emerged technique is metabolomics which is the study of small molecule substrates, intermediates, and products that are generated from the myriad of biochemical reactions in the cell. A metabolomic profile describes the unique physiological fingerprint of a biological sample at a specific point in time. Metabolites have a vital role in biological systems and represent important candidates to understand disease phenotypes. They are low-molecular-weight (<1000 Da) and include lipids, amino acids, peptides, nucleic acids, organic acids, vitamins, thiols, and carbohydrates. The diversity of these metabolites makes the global analysis of cellular metabolome a challenge [16], yet is an emerging and promising field [17].

There are two main techniques for metabolomics – nuclear magnetic resonance (NMR) and mass spectrometry (MS). NMR spectroscopy can be used for the identification and quantification of the chemical composition of a sample – which can be in liquid or solid form, or a tissue sample. Because it can help study molecular structures as well as molecular dynamics under biological conditions, NMR can be used as a method in metabolomics applications. However, NMR metabolomics are only capable of detecting ~100s of metabolites and also requires large sample volumes (>1mL). On the other hand, a mass spectrometer characterizes thousands of metabolites through their mass-to-charge ratio ( $m/z$ ) from small <100 $\mu$ L samples. Ions are generated by inducing either the loss or gain of a charge from a neutral species. Once formed, ions are electrostatically directed into a mass analyzer where they are separated according to  $m/z$  and finally detected. The combination of different molecular ionization, ion separation, and ion detection techniques results in a spectrum that can provide molecular mass and even structural information for ~1000s of metabolite features [18]. While NMR has a higher reproducibility compared to MS, for targeted approaches such as this project, MS is the superior

choice [19]. MS methods provide higher sensitivity and higher selectivity compared to NMR and require less volume per sample.

Here we developed a targeted HPLC-MS method for detecting central energy metabolites and amino acid pathways. In Chapter 2, this method is combined with qualitative isotopic labeling to provide additional insight into OA articular chondrocyte metabolism under different mechanotransduction conditions for different donors. In Chapter 3, the qualitative results obtained with this method are analyzed and a core scale metabolic model of articular chondrocytes are introduced. These analyses further the field of OA by exploring the role of the citric acid cycle and oxygen consumption in collagen synthesis and cell maintenance.

### Chondrocyte Metabolism, Articular Cartilage and Collagen

For decades, the field has perceived chondrocyte metabolism as only utilizing anaerobic glycolysis [20]. This assumption was based on three main points: (1) low oxygen tension of articular joints at baseline, (2) low number of mitochondria per cell, and (3) strong dependence of chondrocytes upon glucose for energy. This led the researchers to ascribe chondrocyte metabolism to a phenomenon called the “Warburg effect”, usually associated with cancer cells, where they retain high levels of glycolysis even in an aerobic environment [21][22][23]. This perspective suggested that because of its low-oxygen environment, articular chondrocytes would use glucose as the main energy source but would then use lactate fermentation because of the low oxygen levels. The studies that were done within these limitations show that chondrocytes have low levels of oxygen consumption and exhibit patterns that suggest that ATP is generated predominantly by substrate-level phosphorylation in the glycolytic pathway.

However, recent studies show a more complex picture, preventing us from seeing them as solely anaerobic glycolytic. Despite their low O<sub>2</sub> environment, chondrocytes have abundant and active mitochondria that contribute to ATP production [24]. Moreover, articular cartilage has different zones defined by the depth from the articular surface – superficial zone, middle zone, and deep zone. The ability to consume and use oxygen, as well as the mitochondrial density depends on which zone the cells are present in [25]. With new observations like so, the field is heading in new directions.

Studies done by Coleman Lab [26] demonstrate the importance of mitochondria in post-traumatic osteoarthritis (PTOA). Hypoxic cells under normal conditions are introduced to a flow of blood and oxygen, creating the possibility of producing energy in ways other than anaerobic glycolysis. Articular chondrocytes have a burst of mitochondrial activity and produce damaging amounts of reactive oxygen species (ROS) immediately after *in vivo* injury. In addition to drastic changes after injury, ROS production should also be considered alongside natural factors like aging, BMI, constant mechanical loading etc. since these factors can also play a role in matrix degradation and OA progression [27]. Production of ROS elevates the oxidative stress in a cellular level and articular chondrocytes will respond to the stress of the environment via biochemical changes. It is important to know how the biomechanical properties are altered in OA articular chondrocytes compared to healthy cells.

Recent work by the June Lab has calculated fluxes from experimental metabolomic data, comparing compressed and uncompressed SW1353 human chondrocytes [28]. The paper studies the short-term effects of an *in vitro* model of chondrocyte undergoing cyclical compression. The results suggest that physiological compression of SW1353 chondrocytes causes central energy

metabolism to change in a manner consistent with increased production of amino acid precursors for ECM and PCM proteins as an early-time (<30 min) response [29]. Another study from our group finds that cyclical compression results in changes in central energy metabolism in primary human chondrocytes. Five (n=5) OA primary human chondrocyte donors were subjected to 0, 15, or 30 minutes of cyclical compression, revealing that even grade IV OA cells are capable of synthesizing non-essential amino acid precursors as a response to cyclical compression [30]. However, a complete understanding of how OA chondrocyte central energy metabolism responds to mechanical loads for multiple donors (male and female), and what pathways and carbon sources play a role in maintaining the cells remains to be determined.

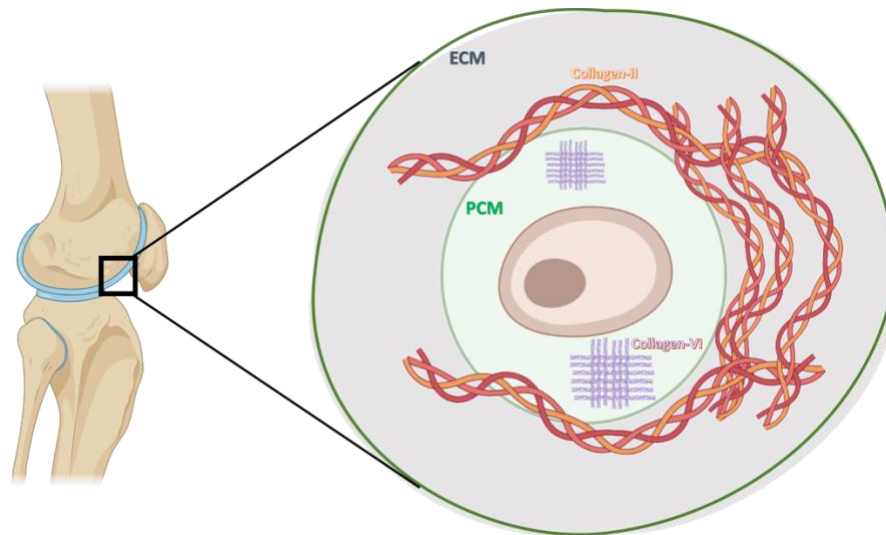


Figure 1.1: Basic biological structure of articular chondrocytes.

In Chapter 3, we focused on the production of two collagen types using a core scale metabolic model. Collagen is the most abundant structural macromolecule in ECM (Figure 1.1). It makes up around 60% of the dry weight of cartilage. Collagen types I, IV, V, VI, IX, and XI (minor collagens) contribute to the fibril network, while Collagen Type II has a major role in the

cartilage ECM [31]. It comprises 90% to 95% of the total collagen in ECM in articular cartilage and is responsible of forming fibrils and fibers that are intertwined with proteoglycan aggregates to provide the unique mechanical function of the tissue. On the other hand, within the minor collagens, Collagen Type VI has an important role regulating PCM and mechanotransduction properties via TRPV4 signaling or other ion channels independent from Ca(2+) signaling in articular cartilage [32]. Thus, Collagen-II and Collagen-VI are the main contributors we were focused on while studying articular cartilage properties in Chapter 2.

All collagen primary sequences contain a frequent motif consisting of a sequence of 3 amino acids that facilitate formation of a triple helix. This motif is glycine (Gly, G), proline (Pro, p) and hydroxyproline (Hyp, O). Hydroxyproline provides stability via hydrogen bonds along the length of the molecule while the triple helix structure provides articular cartilage with shear and tensile properties, which help to stabilize the matrix [4]. The precursors to these amino acids are produced within central energy metabolism (Figure 1.2). Thus, two possible carbon sources that contribute to the composition of Collagen II are glucose (via the glycolysis pathway) and glutamine (as a contributor to TCA cycle and by itself).

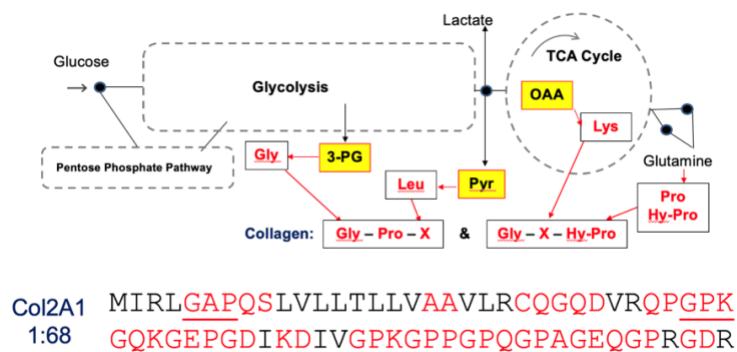


Figure 1.2. Cells obtain nutrients and energy from glucose, which is metabolized into amino acid precursors that help make up collagen II. Two possible source of carbon is depicted to be glucose and glutamine when the pathways are traced.

### Targeted Metabolomics and Flux Analysis

Metabolism assumes a pivotal role across various domains of biology, spanning from ecology and bioengineering to disease research. It helps specify the metabolic pathways that play a role in the maintenance and function of the cell of interest [33]. However, this big picture point of view also comes with more complexity than other approaches such as proteomics, a much more established field. The identification of the resulting metabolites depends on the method used to extract the metabolites, and the accuracy and the sensitivity of the instruments used, where specific libraries and different methods must be prespecified for the analysis of different sample types. Even then, there are many unidentified metabolite features to consider. For targeted metabolomics, where a set of metabolite features are preselected for analysis, overcoming these limitations mostly depend on optimizing the extraction method and developing an accurate targeted method to detect the metabolite features of interest with appropriate sensitivity and specificity.

In Chapter 2, we utilized  $^{13}\text{C}$  isotopic labeling to trace different carbon sources in OA articular chondrocytes. Isotopic labeling is an identification method, where one can trace the heavier isotopes (e.g. glucose synthesized with  $^{13}\text{C}$  instead of  $^{12}\text{C}$ ) of targeted metabolites through a network of different biological reactions [34]. This way, results for the patterns of the label of interest, as well as downstream metabolite products, can be detected and identified more accurately. In our two experimental setups, we used labeled glucose and glutamine as carbon sources for OA primary human articular chondrocytes to detect if they will be utilized by the TCA cycle. In the future, this qualitative method can be integrated in the comprehensive model we have established in Chapter 3.

Measuring the metabolite feature abundances, however, tells only half of the story. Because the upregulated and downregulated features are a part of much bigger and complex network of metabolic pathways, we need an established model to accurately interpret the consumption and the production rates of these molecules. In Chapter 2, we have expanded on previous metabolic modeling work from the June Lab. Our more comprehensive model has more metabolites and reactions, takes oxygen and electron flow into consideration, and the transport reactions are included.

References

- [1] D. J. Hunter, L. March, and M. Chew, “Osteoarthritis in 2020 and beyond: a Lancet Commission,” *The Lancet*, vol. 396, no. 10264, pp. 1711–1712, 2020, doi: 10.1016/S0140-6736(20)32230-3.
- [2] J. S. Mort and C. J. Billington, “Articular cartilage and changes in arthritis matrix degradation,” *Arthritis Res*, vol. 3, no. 6, pp. 337–341, 2001, doi: 10.1186/ar325.
- [3] K. E. Barbour, C. G. Helmick, M. Boring, and T. J. Brady, “Vital Signs: Prevalence of Doctor-Diagnosed Arthritis and Arthritis-Attributable Activity Limitation — United States, 2013–2015,” *MMWR Morb Mortal Wkly Rep*, vol. 66, no. 9, pp. 246–253, 2017, doi: 10.15585/mmwr.mm6609e1.
- [4] A. J. Sophia Fox, A. Bedi, and S. A. Rodeo, “The basic science of articular cartilage: Structure, composition, and function,” *Sports Health*, vol. 1, no. 6, pp. 461–468, 2009, doi: 10.1177/1941738109350438.
- [5] D. D. Chan, L. Cai, K. D. Butz, S. B. Trippel, E. A. Nauman, and C. P. Neu, “In vivo articular cartilage deformation: Noninvasive quantification of intratissue strain during joint contact in the human knee,” *Sci Rep*, vol. 6, no. August 2015, pp. 1–14, 2016, doi: 10.1038/srep19220.
- [6] F. Meyer *et al.*, “Chondrocytes From Osteoarthritic and Chondrocalcinosis Cartilage Represent Different Phenotypes,” *Front Cell Dev Biol*, vol. 9, no. April, pp. 1–9, 2021, doi: 10.3389/fcell.2021.622287.
- [7] A. Villalvilla, R. Gómez, R. Largo, and G. Herrero-Beaumont, “Lipid transport and metabolism in healthy and osteoarthritic cartilage,” *Int J Mol Sci*, vol. 14, no. 10, pp. 20793–20808, 2013, doi: 10.3390/ijms141020793.
- [8] R. J. Goekoop *et al.*, “Determinants of absence of osteoarthritis in old age,” *Scand J Rheumatol*, vol. 40, no. 1, pp. 68–73, 2011, doi: 10.3109/03009742.2010.500618.
- [9] S. O., G. G., G. K., and M. F.D., “Investigation of the relationships between knee osteoarthritis and obesity via untargeted metabolomics analysis,” *Clin Rheumatol*, pp. 1351–1360, 2019, [Online]. Available:

<http://www.embase.com/search/results?subaction=viewrecord&from=export&id=L625994783%0Ahttp://dx.doi.org/10.1007/s10067-019-04428-1>

- [10] K. M. Clements, Z. C. Bee, G. V. Crossingham, M. A. Adams, and M. Sharif, “How severe must repetitive loading be to kill chondrocytes in articular cartilage?,” *Osteoarthritis Cartilage*, vol. 9, no. 5, pp. 499–507, 2001, doi: 10.1053/joca.2000.0417.
- [11] M. Tschon, D. Contartese, S. Pagani, V. Borsari, and M. Fini, “Gender and Sex Are Key Determinants in Osteoarthritis Not Only Confounding Variables. A Systematic Review of Clinical Data,” *J Clin Med*, vol. 10, no. 14, p. 10, Jul. 2021, doi: 10.3390/JCM10143178.
- [12] N. Chinzei *et al.*, “Evidence for Genetic Contribution to Variation in Posttraumatic Osteoarthritis in Mice,” *Arthritis and Rheumatology*, vol. 71, no. 3, pp. 370–381, 2019, doi: 10.1002/art.40730.
- [13] B. Mohajer *et al.*, “Metabolic Syndrome and Osteoarthritis Distribution in the Hand Joints: A Propensity Score Matching Analysis From the Osteoarthritis Initiative,” *J Rheumatol*, vol. 48, no. 10, pp. 1608–1615, Oct. 2021, doi: 10.3899/JRHEUM.210189.
- [14] R. Lowe, N. Shirley, M. Bleackley, S. Dolan, and T. Shafee, “Transcriptomics technologies,” *PLoS Comput Biol*, vol. 13, no. 5, pp. 1–23, 2017, doi: 10.1371/journal.pcbi.1005457.
- [15] S. Al-Amrani, Z. Al-Jabri, A. Al-Zaabi, J. Alshekaili, and M. Al-Khabori, “Proteomics: Concepts and applications in human medicine,” *World J Biol Chem*, vol. 12, no. 5, pp. 57–69, 2021, doi: 10.4331/wjbc.v12.i5.57.
- [16] S. J. Kim, S. H. Kim, J. H. Kim, S. Hwang, and H. J. Yoo, “Understanding metabolomics in biomedical research,” *Endocrinology and Metabolism*, vol. 31, no. 1, pp. 7–16, 2016, doi: 10.3803/EnM.2016.31.1.7.
- [17] B. Lin, “A roadmap for interpreting <sup>13</sup>C metabolite labeling patterns from cells,” *Physiol Behav*, vol. 176, no. 12, pp. 139–148, 2017, doi: 10.1016/j.copbio.2015.02.003.A.
- [18] S. Edition, “The Expanding Role of Mass Spectrometry in Biotechnology, Second Edition [Paperback],” p. 257, 2006, [Online]. Available: [http://www.amazon.com/dp/0974245127/ref=cm\\_sw\\_su\\_dp](http://www.amazon.com/dp/0974245127/ref=cm_sw_su_dp)

- [19] A. H. M. Emwas, *The strengths and weaknesses of NMR spectroscopy and mass spectrometry with particular focus on metabolomics research*, vol. 1277. 2015. doi: 10.1007/978-1-4939-2377-9\_13.
- [20] R. E. Marcus and L. Sokoloff, "The effect of low oxygen concentration on growth, glycolysis, and sulfate incorporation by articular chondrocytes in monolayer culture," *Arthritis Rheum*, vol. 16, no. 5, pp. 646–656, 1973, doi: 10.1002/art.1780160509.
- [21] H. K. Heywood and D. A. Lee, "Monolayer expansion induces an oxidative metabolism and ROS in chondrocytes," *Biochem Biophys Res Commun*, vol. 373, no. 2, pp. 224–229, 2008, doi: 10.1016/j.bbrc.2008.06.011.
- [22] O. Rosentiaal, M. A. Bowte, and G. Wagoner, "STUDIES IN THE METABOLISM OF ARTICULAR CARTILAGE," pp. 221–233.
- [23] R. A. J. Windhaber, R. J. Wilkins, and D. Meredith, "Functional characterisation of glucose transport in bovine articular chondrocytes," *Pflugers Arch*, vol. 446, no. 5, pp. 572–577, 2003, doi: 10.1007/s00424-003-1080-5.
- [24] R. Terkeltaub, K. Johnson, A. Murphy, and S. Ghosh, "Invited review: The mitochondrion in osteoarthritis," *Mitochondrion*, vol. 1, no. 4, pp. 301–319, 2002, doi: 10.1016/S1567-7249(01)00037-X.
- [25] H. K. Heywood, M. M. Knight, and D. A. Lee, "Both superficial and deep zone articular chondrocyte subpopulations exhibit the crabtree effect but have different basal oxygen consumption rates," *J Cell Physiol*, vol. 223, no. 3, pp. 630–639, 2010, doi: 10.1002/jcp.22061.
- [26] M. C. Coleman *et al.*, "Targeting mitochondrial responses to intra-articular fracture to prevent posttraumatic osteoarthritis," *Sci Transl Med*, vol. 10, no. 427, pp. 1–15, 2018, doi: 10.1126/scitranslmed.aan5372.
- [27] J. A. Bolduc, J. A. Collins, and R. F. Loeser, "Reactive oxygen species, aging and articular cartilage homeostasis," *Free Radic Biol Med*, vol. 132, no. August 2018, pp. 73–82, 2019, doi: 10.1016/j.freeradbiomed.2018.08.038.
- [28] D. Salinas, C. A. Minor, R. P. Carlson, C. N. McCutchen, B. M. Mumeay, and R. K. June, "Combining Targeted Metabolomic Data with a Model of Glucose Metabolism: Toward

- Progress in Chondrocyte Mechanotransduction,” *PLoS One*, vol. 12, no. 1, Jan. 2017, doi: 10.1371/JOURNAL.PONE.0168326.
- [29] D. Salinas, C. A. Minor, R. P. Carlson, C. N. McCutchen, B. M. Mumey, and R. K. June, “Combining targeted metabolomic data with a model of glucose metabolism: Toward progress in chondrocyte mechanotransduction,” *PLoS One*, vol. 12, no. 1, pp. 1–16, 2017, doi: 10.1371/journal.pone.0168326.
- [30] D. Salinas, B. M. Mumey, and R. K. June, “Physiological dynamic compression regulates central energy metabolism in primary human chondrocytes,” *Biomech Model Mechanobiol*, vol. 18, no. 1, pp. 69–77, 2019, doi: 10.1007/s10237-018-1068-x.
- [31] J. D. Humphrey, E. R. Dufresne, and M. A. Schwartz, “Mechanotransduction and extracellular matrix homeostasis,” *Nat Rev Mol Cell Biol*, vol. 15, no. 12, p. 802, Dec. 2014, doi: 10.1038/NRM3896.
- [32] N. A. Zelenski *et al.*, “Type VI Collagen Regulates Pericellular Matrix Properties, Chondrocyte Swelling, and Mechanotransduction in Mouse Articular Cartilage,” *Arthritis Rheumatol*, vol. 67, no. 5, pp. 1286–1294, May 2015, doi: 10.1002/ART.39034.
- [33] C. Jang, L. Chen, and J. D. Rabinowitz, “Metabolomics and Isotope Tracing,” *Cell*, vol. 173, no. 4, pp. 822–837, 2018, doi: 10.1016/j.cell.2018.03.055.
- [34] U. Sauer, “Metabolic networks in motion: <sup>13</sup>C-based flux analysis,” *Mol Syst Biol*, vol. 2, pp. 1–10, 2006, doi: 10.1038/msb4100109.
- [35] K. D. Allen, L. M. Thoma, and Y. M. Golightly, “Epidemiology of osteoarthritis,” *Osteoarthritis Cartilage*, vol. 30, no. 2, pp. 184–195, 2022, doi: 10.1016/j.joca.2021.04.020.
- [36] X. Ji and H. Zhang, “Current Strategies for the Treatment of Early Stage Osteoarthritis,” *Front Mech Eng*, vol. 5, p. 480160, Sep. 2019, doi: 10.3389/FMECH.2019.00057/BIBTEX.
- [37] J. W. J. Bijlsma, F. Berenbaum, and F. P. J. G. Lafeber, “Osteoarthritis: an update with relevance for clinical practice,” *The Lancet*, vol. 377, no. 9783, pp. 2115–2126, Jun. 2011, doi: 10.1016/S0140-6736(11)60243-2.

- [38] M. Lotz *et al.*, “Value of biomarkers in osteoarthritis: current status and perspectives,” *Ann Rheum Dis*, vol. 72, no. 11, p. 1756, 2013, doi: 10.1136/ANNRHEUMDIS-2013-203726.
- [39] S. Kundu *et al.*, “Enabling early detection of osteoarthritis from presymptomatic cartilage texture maps via transport-based learning,” *Proc Natl Acad Sci U S A*, vol. 117, no. 40, pp. 24709–24719, Oct. 2020, doi: 10.1073/PNAS.1917405117/SUPPL\_FILE/PNAS.1917405117.SAPP.PDF.
- [40] D. T. Felson and R. Hodgson, “Identifying and Treating Pre-Clinical and Early Osteoarthritis,” *Rheum Dis Clin North Am*, vol. 40, no. 4, p. 699, Nov. 2014, doi: 10.1016/J.RDC.2014.07.012.
- [41] E. G. L. Bywaters and M. MacKinnon, “The metabolism of joint tissues,” *J Pathol Bacteriol*, vol. 44, no. 1, pp. 247–268, Jan. 1937, doi: 10.1002/PATH.1700440119.
- [42] J. W. Kim and C. V. Dang, “Cancer’s Molecular Sweet Tooth and the Warburg Effect,” *Cancer Res*, vol. 66, no. 18, pp. 8927–8930, Sep. 2006, doi: 10.1158/0008-5472.CAN-06-1501.
- [43] P. C. Gomez-Contreras, P. N. Kluz, M. R. Hines, and M. C. Coleman, “Intersections Between Mitochondrial Metabolism and Redox Biology Mediate Posttraumatic Osteoarthritis,” *Curr Rheumatol Rep*, vol. 23, no. 5, 2021, doi: 10.1007/s11926-021-00994-z.
- [44] N. K. Goto and L. E. Kay, “New developments in isotope labeling strategies for protein solution NMR spectroscopy,” *Curr Opin Struct Biol*, vol. 10, no. 5, pp. 585–592, Oct. 2000, doi: 10.1016/S0959-440X(00)00135-4.
- [45] M. R. Antoniewicz, “A guide to <sup>13</sup>C metabolic flux analysis for the cancer biologist,” *Experimental & Molecular Medicine 2018 50:4*, vol. 50, no. 4, pp. 1–13, Apr. 2018, doi: 10.1038/s12276-018-0060-y.
- [46] P. Firdous, T. Hassan, S. Farooq, and K. Nissar, “Applications of proteomics in cancer diagnosis,” *Proteomics*, pp. 257–285, Jan. 2023, doi: 10.1016/B978-0-323-95072-5.00014-6.

- [47] P. P. Brahmachary, H. D. Welhaven, and R. K. June, "Metabolomic Profiling to Understand Chondrocyte Metabolism," *Methods in Molecular Biology*, vol. 2598, pp. 141–156, 2023, doi: 10.1007/978-1-0716-2839-3\_11/FIGURES/5.
- [48] T. Pluskal, S. Castillo, A. Villar-Briones, and M. Orešič, "MZmine 2: modular framework for processing, visualizing, and analyzing mass spectrometry-based molecular profile data," *BMC Bioinformatics*, vol. 11, Jul. 2010, doi: 10.1186/1471-2105-11-395.
- [49] R. Nilsson, "Validity of natural isotope abundance correction for metabolic flux analysis," 2020, doi: 10.1101/2020.05.04.075838.
- [50] Z. Ser, X. Liu, N. N. Tang, and J. W. Locasale, "Extraction parameters for metabolomics from cell extracts," *Anal Biochem*, vol. 475, p. 22, Apr. 2015, doi: 10.1016/J.AB.2015.01.003.
- [51] C. Andresen *et al.*, "Comparison of extraction methods for intracellular metabolomics of human tissues," *Front Mol Biosci*, vol. 9, Aug. 2022, doi: 10.3389/FMOLB.2022.932261/FULL.

CHAPTER TWO

IDENTIFICATION OF CARBON SOURCES IN OA PRIMARY HUMAN CHONDROCYTES  
USING  $^{13}\text{C}$ -ISOTOPIC LABELING AND MASS SPECTROMETRY

Contribution of Authors and Co-Authors

Manuscript in Chapter 2

Author: Ayten Ebru Erdogan

Contributions: Participated in manuscript preparation.

Co-Author: Priyanka Brahmachary

Contributions: Participated in manuscript preparation.

Co-Author: Donald Smith

Contributions: Participated in manuscript preparation.

Co-Author: Ronald K. June

Contributions: Participated in manuscript preparation

Manuscript Information

Ayten Ebru Erdogan, Priyanka Brahmachary, Donald Smith, Ronald K. June

Status of Manuscript:

Prepared for submission to a peer-reviewed journal

Officially submitted to a peer-reviewed journal

Accepted by a peer-reviewed journal

Published in a peer-reviewed journal

Abstract

Osteoarthritis (OA) is a complex degenerative joint disease characterized by the deterioration of articular cartilage, resulting in pain and loss of joint function. The maintenance of articular cartilage is performed by articular chondrocytes, and there is a gap in our understanding of the energy cycles and carbon sources that chondrocytes use to produce cartilage matrix. This study investigates articular chondrocyte metabolism in primary human OA cells by focusing on the carbon sources utilized for energy and the production of key amino acid precursors. By labeling metabolites of interest with  $^{13}\text{C}$  isotopes, this identifies likely carbon sources processed through glycolysis and the tricarboxylic acid (TCA) cycle. The findings provide insight into carbon sources used by OA chondrocytes and may potentially lead to novel therapeutic strategies.

## Introduction

Osteoarthritis (OA) is a widespread degenerative joint condition impacting hundreds of millions of individuals globally [35]. It is a chronic disease characterized by the gradual deterioration and breakdown of joint cartilage. OA results in joint pain, stiffness, and limited mobility. Affecting various joints such as the knees, hips, hands, and spine, OA worsens progressively. Although often associated with aging, it can also arise from joint injuries, obesity, genetic factors, and repetitive joint stress.

The traditional treatment for OA includes pain management via anti-inflammatories, exercise and physical therapy, and eventually joint replacement [36][37]. There are additional co-morbidities (e.g. heart disease) associated with OA, and the long-term effects often include continued pain for a substantial fraction (i.e. 25%) of patients. Importantly, studies focusing on early diagnosis and new intervention practices are emerging and necessary [38][39][40]. However, there are still gaps in our basic knowledge of joint biology including chondrocyte metabolism. Targeting the cellular level underpinnings of OA is one important approach to both better understand and provide novel interventions to this complex disease.

Based on the avascular nature of cartilage, historically the metabolism of cartilage cells (chondrocytes) was thought to be similar to the Warburg effect [41]. The Warburg effect is associated with cancer and stem cells, where the availability of glucose drives the cells to first metabolize glucose via glycolysis but then instead of using the TCA cycle, pyruvate is converted to lactate [42]. However, articular cartilage has different tissue zones, and the availability and usage of oxygen varies between the superficial zone, the middle zone, or the deep zone [25]. Thus, instead of considering chondrocytes as solely anaerobic glycolytic, recent studies

emphasize the importance of mitochondria and associated pathways including the TCA cycle [43]. Mitochondria house the TCA cycle enzymes and associated biochemical reactions, and also produce substantial cellular ROS (reactive oxygen species). This is important because the TCA cycle produces the amino acid precursors oxaloacetate and  $\alpha$ -ketoglutarate, and the resulting amino acids (proline and hydroxyproline) play a key role in the structure of collagen (Figure 2.1). Because collagen is a key component of both the cartilage pericellular and extracellular matrices, collagen production is vital for the maintenance of cartilage (Figure 2.2).

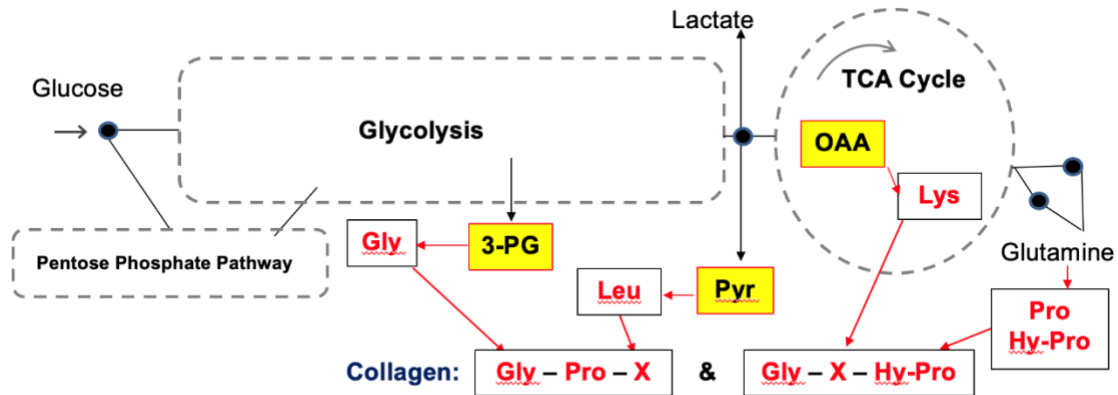


Figure 2.1. Production of Collagen via Central Carbon Metabolism. Key amino acid precursors (3-Pyruvateglycerate, Pyruvate and Oxaloacetate) that majorly contribute to Collagen production were depicted in yellow.

Isotopic labeling in conjunction with mass spectrometry is a widely used method for assessing active metabolic pathways across different disciplines [44][45]. This approach involves feeding cells with carbon sources which have the substitution of specific atoms with isotopes that share the same number of protons but have more neutrons than the original atom (e.g.  $^{13}\text{C}$  instead of  $^{12}\text{C}$ [46]). By tracking downstream metabolites that include the labeled isotopes with mass spectrometry, studies can track active metabolic pathways. Here, we use  $^{13}\text{C}$  isotopic labeling to

trace carbon sources for energy metabolism and production of amino acid precursors that are necessary for collagen production. The objectives of this study are to (1) identify sources of carbon that articular chondrocytes use for energy metabolism and production of amino acid precursors and (2) test if standard carbon sources are metabolized through the TCA cycle.

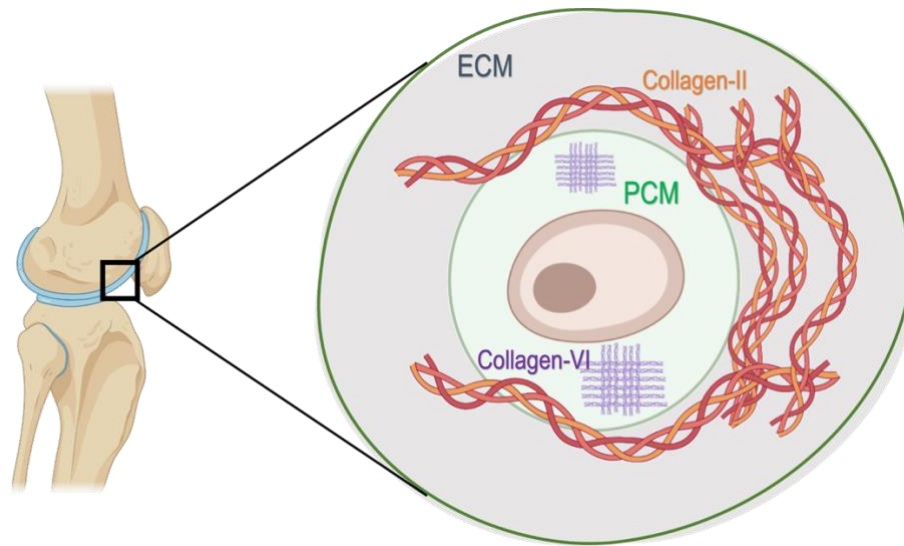


Figure 2.2. Basic biological structure of articular chondrocytes.

To our knowledge, this is one of the first studies to assess the downstream metabolites from the carbon sources of glucose and glutamine using OA primary human chondrocytes and  $^{13}\text{C}$  isotope labeling. Here, we use  $^{13}\text{C}$ -labeled glucose and glutamine to track carbons through central metabolism in OA primary human chondrocytes. We hypothesize that (i) primary monolayer osteoarthritic chondrocytes would utilize both glucose and glutamine as carbon sources flow through the TCA cycle and (ii) lack of glucose and lack of glutamine would have different targeted labeled results within compared group isotopes. After confirming that  $^{13}\text{C}$ -labeling had minimal effects on untargeted metabolomic profiles, we tested this through feeding primary OA chondrocytes different  $^{13}\text{C}$ -labeled carbon sources and tracking the resulting labeled

metabolites. Our results demonstrate that monolayer OA chondrocytes can use both glucose and glutamine as carbon sources by utilizing the TCA cycle. Knowledge of the carbon sources used by OA chondrocytes is important for designing strategies to maximize production of collagen.

## Materials and Methods

### Chondrocyte Harvest and Culture with Isotopic Conditions

Two sets of experiments with chondrocytes from different donors and varying conditions were used to address our hypotheses. For both sets, harvest, culture, and metabolite extractions for OA Human Primary Chondrocytes (OA-HPCs) were performed as described before [47] with minor alterations described below for  $^{13}\text{C}$  compounds for the cultures (Figure 2.3). OA-HPCs were acquired from Grade IV patients that underwent total joint replacement using an IRB-approved consent form.

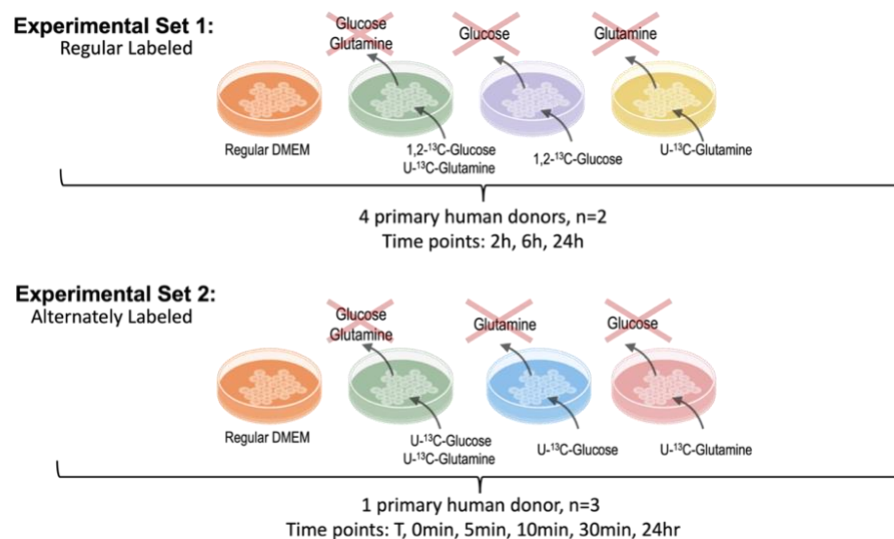


Figure 2.3. Experimental designs for Regular Labeled and Alternately Labeled experimental sets.

For the first set of experiments, after a single expansion two replicates from n=4 primary human donors were plated in 12 well plates (100,000 cells/well) with high glucose DMEM media for 24 hours. Then, the cells were serum starved for 12 hours before experiments. Next, one of each of the following media were fed to all cell lines: (1) control high glucose DMEM, (2) glucose-free DMEM spiked with  $^{13}\text{C}$ -glucose, (3) glutamine-free DMEM spiked with  $^{13}\text{C}$ -glutamine and (4) dual glucose- and glutamine-free DMEM spiked with both  $^{13}\text{C}$ -glucose and  $^{13}\text{C}$ -glutamine. For all spiked conditions,  $^{13}\text{C}$ -glucose and  $^{13}\text{C}$ -glutamine were used at concentrations that matched normal DMEM conditions. Cells were collected at 2, 6, and 24 hours after feeding. Metabolites were extracted with 100% HPLC-grade methanol, and pellets were resuspended in 50:50 Acetonitrile:Water buffer for HPLC-MS analysis.

For the second set of experiments, triplicates of all conditions from a single primary human donor were plated in 24 well plates (30,000 cells/well) with high glucose DMEM media for 24 hours. Then, the cells were serum-starved for 12 hours before experiments. Next, one of each of the following media were fed to all cell lines: (1) high glucose DMEM, (2) glutamine-free DMEM spiked with  $^{13}\text{C}$ -glucose, (3) glucose-free DMEM spiked with  $^{13}\text{C}$ -glutamine and (4) dual glucose- and glutamine-free DMEM spiked with both  $^{13}\text{C}$ -glucose and  $^{13}\text{C}$ -glutamine. As in Experiment 1,  $^{13}\text{C}$ -glucose and  $^{13}\text{C}$ -glutamine were spiked at concentrations that matched normal DMEM conditions. Cells were collected at T (right after starvation), 0-min, 15-min, 30-min and 24-h after feeding. Metabolite extraction and resuspension were performed as in Experiment 1.

### Untargeted Metabolomics

Initially untargeted metabolic profiling was used to test if the  $^{13}\text{C}$ -labeled carbon sources affected general chondrocyte physiology. A total of 96 samples (4 cell lines x 2 replicates each x

3 timepoints x 4 groups) from the first set of experiments were analyzed using MS Q-TOF mass spectrometry with positive ESI as the ion source and HILIC as the column. The resulting raw files were processed for analysis using MS-Convert and XCMS. Metabolomic profiling (ANOVA, PCA, PLS-DA, clustering and heatmap analyses) and pathway enrichment analysis for label-dependent and timepoint-dependent groups were performed using Metaboanalyst 5.0. A single sample was removed as an outlier after an initial analysis found it to be well outside of the 95% confidence interval in its group. Putative metabolite identities were detected using pathway enrichment metabolite feature hits via Mummichog algorithm (in Metaboanalyst), with a 5 ppm tolerance.

#### Targeted Metabolomics and Statistical Analysis

A total of 147 samples from both first and second experiment sets were analyzed using MS Q-TOF mass spectrometry with negative electro-spray injection (ESI) as the ion source and C18 as the column. The resulting raw files were processed for analysis using MS-Convert. A metabolite library was assembled with all possible m/z value identifications of the targeted metabolites with [M]-H and [M]+Cl ionizations and their monoisotopic masses (Table A.1). Mass detection, chromatogram building, retention time normalization, peak alignment, gap filling, and identification using the library was performed on MZmine-2.53 [48]. Normalizations across groups were done in Metaboanalyst. Separate repeated-measures ANOVA for both experiments were performed in SPSS, followed by pairwise comparisons. For the first set of experiments, because the 24-h timepoint didn't have the DMEM group, the analyses were run first between all timepoints excluding DMEM group, and next with DMEM group but without the 24-h timepoint.

## Results

### Temporal Analysis of OA Primary Human Chondrocytes

Principle Components Analysis (PCA) shows substantial overlap between  $^{13}\text{C}$  groups (Figure 2.4) and DMEM controls suggesting that  $^{13}\text{C}$  compounds result in limited alterations of global chondrocyte metabolism, validating their use for heavy carbon labeling. When analyzing potential effects of time after starvation, pathway enrichment analysis finds several time-dependent pathways via ANOVA comparing between 2-, 6- and 24-h timepoints, resulting in 11 significant pathways and multiple IDs for putative metabolite features (Table 2.1).

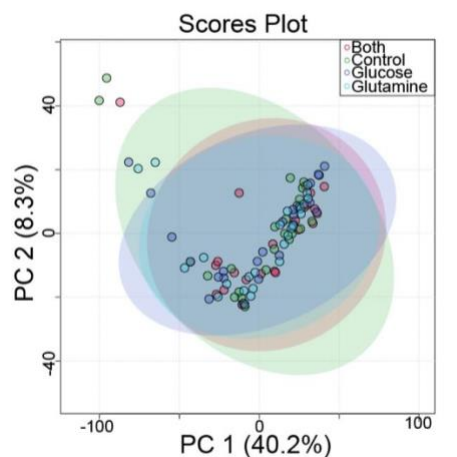


Figure 2.4. Label-dependent PCA that covers nearly 50% of the dataset variance indicates minimal kinetic effect of isotopic labeling.

Some of the significant putative metabolite features that increased in abundance with time include Estrone ( $m/z$ : 309.1257935), L-Glutamic acid ( $m/z$ : 130.050354), D-Proline ( $m/z$ : 116.0706177), Coenzyme A ( $m/z$ : 722.1136819) and FADH2 ( $m/z$ : 826.1379094). In contrast, putative metabolite features that show a descending trend over time include Argininosuccinic acid ( $m/z$ : 219.1086578) and N-Acetylserotonin ( $m/z$ : 218.105957).

Cluster analysis for the median intensities at each timepoint finds additional trends during time after starvation (Figure A.1). Pathway enrichment analysis on Cluster 1 (C1) yielded no pathways. Cluster 2 (C2) metabolites represent leukotriene metabolism and hexose phosphorylation, while Cluster 3 (C3) metabolites represent glycerophospholipid metabolism, purine metabolism, urea cycle/amino group metabolism, ascorbate (vitamin C) and aldarate metabolism, and  $\beta$ -alanine metabolism.

Table 2.2. ANOVA and clustergram. Relative abundance peaking timepoints have been noted unless the increase/decrease is even over time.

ANOVA PATHWAYS	IMPORTANT METABOLITE FEATURE HITS
<b>Androgen and Estrogen Biosynthesis and Metabolism</b>	S-Adenosylhomocysteine (24h $\uparrow$ ), Estrone (24h $\uparrow$ )
<b>Urea Cycle/Amino Group Metabolism</b>	L-Glutamic acid (6h $\uparrow$ ), D/L-Proline (24h $\uparrow$ ), Hippuric acid ( $\uparrow$ ), S-Adenosylhomocysteine (24h $\uparrow$ ), Argininosuccinic acid (6h $\downarrow$ ), Coenzyme A ( $\uparrow$ ), FADH (6h $\uparrow$ ), Epinephrine (24h $\uparrow$ ), Norepinephrine (6h $\uparrow$ ), L-Ornithine (24h $\uparrow$ )
<b>Tryptophan Metabolism</b>	L-Glutamic acid (6h $\uparrow$ ), S-Adenosylhomocysteine (24h $\uparrow$ ), Coenzyme A ( $\uparrow$ ), 2-Aminomuconic acid (6h $\uparrow$ ), N-Acetylserotonin (6h $\downarrow$ ), FADH (6h $\uparrow$ )
<b>Lysine Metabolism</b>	L-Glutamic acid (6h $\uparrow$ ), S-Adenosylhomocysteine (24h $\uparrow$ ), L-Carnitine (24h $\uparrow$ ), Coenzyme A ( $\uparrow$ ), FADH (6h $\uparrow$ )
<b>C21-steroid Hormone Biosynthesis and Metabolism</b>	Estrone (24h $\uparrow$ ), Dihydrocortisol (6h $\uparrow$ )
<b>Saturated Fatty Acids Beta-Oxidation</b>	L-Carnitine (24h $\uparrow$ ), Coenzyme A ( $\uparrow$ ), FADH (6h $\uparrow$ )
<b>Arginine and Proline Metabolism</b>	L-Glutamic acid (6h $\uparrow$ ), D/L-Proline (24h $\uparrow$ ), Argininosuccinic acid (6h $\downarrow$ ), Coenzyme A ( $\uparrow$ ), FADH (6h $\uparrow$ ), L-Glutamine (6h $\uparrow$ )
<b>Leukotriene metabolism</b>	Coenzyme A ( $\uparrow$ )
<b>Fatty Acid Metabolism</b>	L-Carnitine (24h $\uparrow$ ), Coenzyme A ( $\uparrow$ )
<b>Beta-Alanine Metabolism</b>	L-Glutamic acid (6h $\uparrow$ ), Coenzyme A ( $\uparrow$ )
<b>R Group Synthesis</b>	FADH (6h $\uparrow$ )
CLUSTERGRAM	PATHWAYS
<b>Cluster 2 (C2)</b>	Leukotriene metabolism, Hexose phosphorylation
<b>Cluster 3 (C3)</b>	Glycerophospholipid metabolism, Purine metabolism, Urea cycle/amino group metabolism, Ascorbate (Vitamin C) and Aldarate Metabolism, Beta-Alanine metabolism

### Targeted Qualitative Analysis of Regular Labeled Media

To trace the carbon sources in primary OA articular chondrocytes, the first experiment used four conditions with (i) Regular DMEM, (ii) 1,2-<sup>13</sup>C-Glucose replacing Glucose in DMEM, (iii) U-<sup>13</sup>C-Glutamine replacing Glucose in DMEM, and (iv) both 1,2-<sup>13</sup>C-Glucose and U-<sup>13</sup>C-Glutamine replacing glucose and glutamine in DMEM. 12 metabolites (Glucose, Glutamine, Pyruvate, Oxaloacetate, Alpha-ketoglutarate, Fructose-6-Phosphate, Phosphoenolpyruvate, Lactate, Succinate, Malate, Citrate, Acetyl-CoA) were detected in their negatively charged states of either [M]-H or [M]+Cl. Key metabolites for TCA cycle that are detected for both sets of experiments are depicted in Figure 2.5. Out of the 12 the following metabolites were also detected in their various isotopes: Glucose, Glutamine, Pyruvate, Alpha-ketoglutarate (AKG), Fructose-6-Phosphate, Oxaloacetate and Phosphoenolpyruvate (PEP).

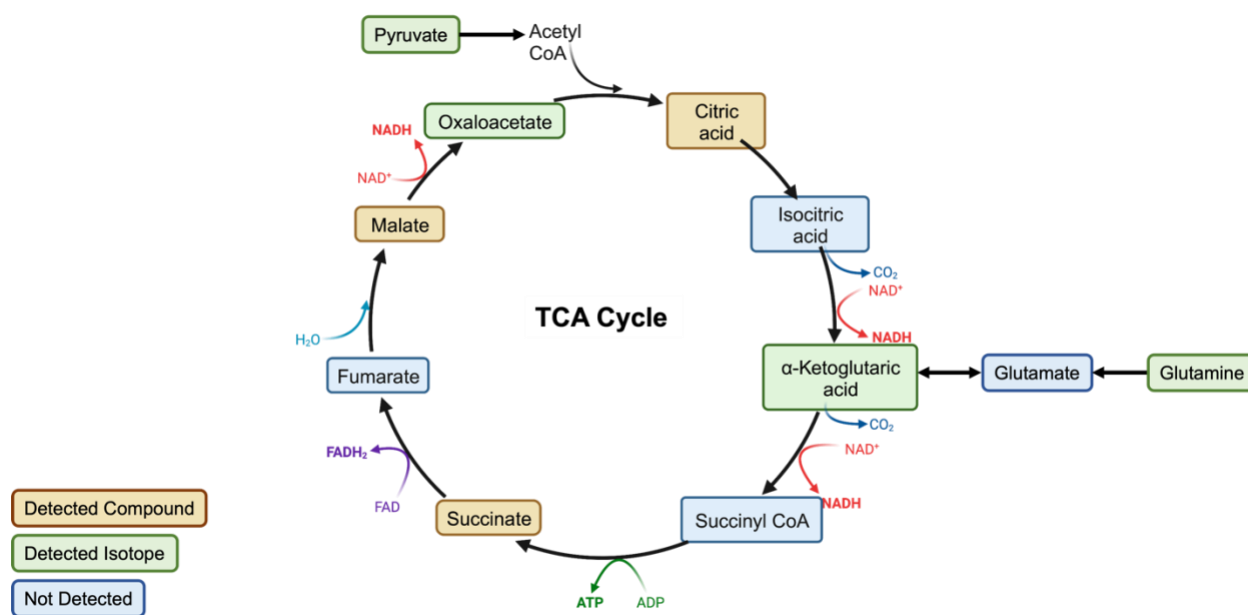


Figure 2.5. Detected metabolites key to TCA cycle. Orange depicts metabolites that are only detected in their unlabeled structure, green depicts metabolites that are detected in their isotopic states, and blue depicts metabolites that were not detected.

Repeated-measures ANOVA determined significant differences ( $p < 0.01$ ) between timepoints for Fructose-6-Phosphate[+Cl+7], Pyruvate[-H+4] and Glucose[-H+1] (Figure 2.6). The analysis of mean normalized relative intensities for Pyruvate[-H+4] has revealed statistically significant differences when comparing all three timepoints in the absence of DMEM ( $p = 0.036$ ), as well as when comparing the mean intensities between the 2-h and 6-h timepoints ( $p = 0.002$ ). Similarly, for Fructose-6-Phosphate[+Cl+7], the comparison between the 2-h and 6-h timepoints also yielded statistical significance ( $p = 0.006$ ). Both Pyruvate[-H+4] ( $p < 0.001$ ) and Fructose-6-Phosphate[+Cl+7] ( $p = 0.032$ ) exhibited a more pronounced effect at the 2-h timepoint when assessing the between-timepoint differences.

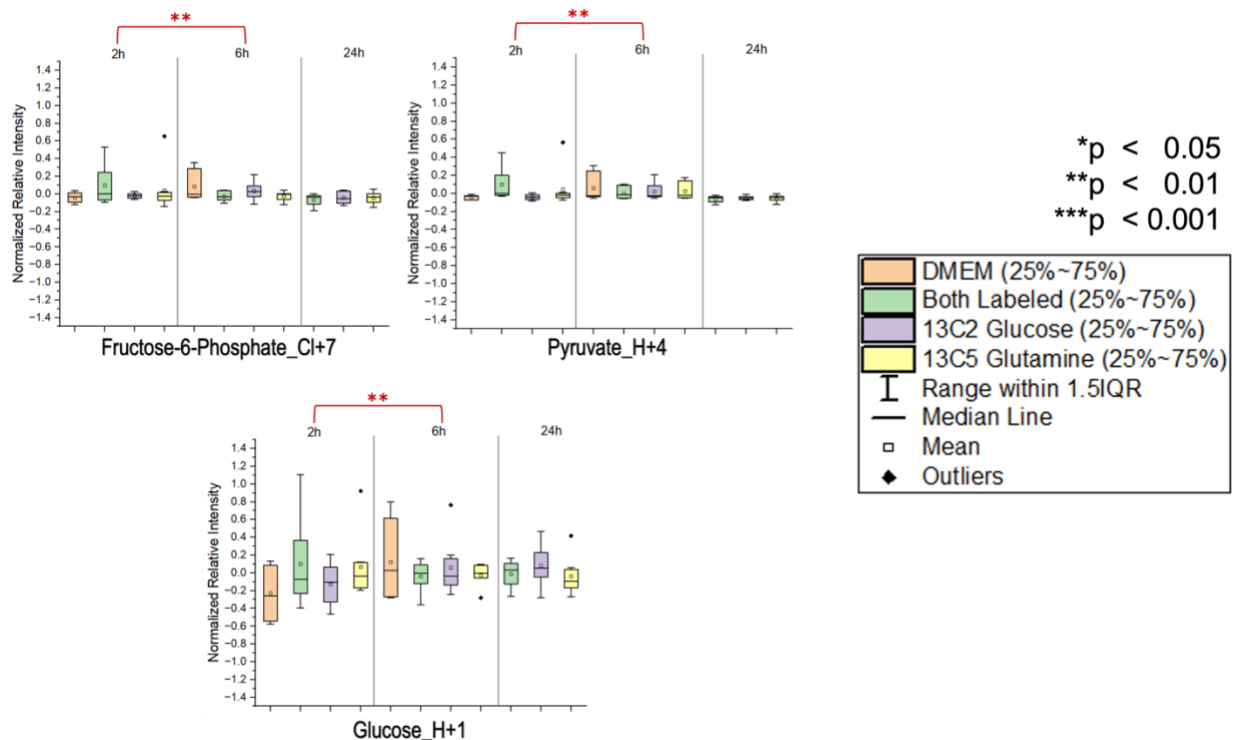


Figure 2.6. Repeated measures ANOVA results for temporal analysis, experimental set 1.

Statistical analysis also found differences between labels in different timepoints for Glucose[+C1+4], Glutamine[-H], Pyruvate[-H+5] and Fructose-6-Phosphate[-C1+6] (Figure 2.7). The within-timepoints differences in differently labeled groups were most significant in Glucose[+C1+4] ( $p=0.002$ ), followed by Glutamine[-H] ( $p=0.019$ ), Fructose-6-Phosphate[-C1+6] ( $p=0.028$ ), and finally Pyruvate[-H+5] ( $p=0.04$ ).

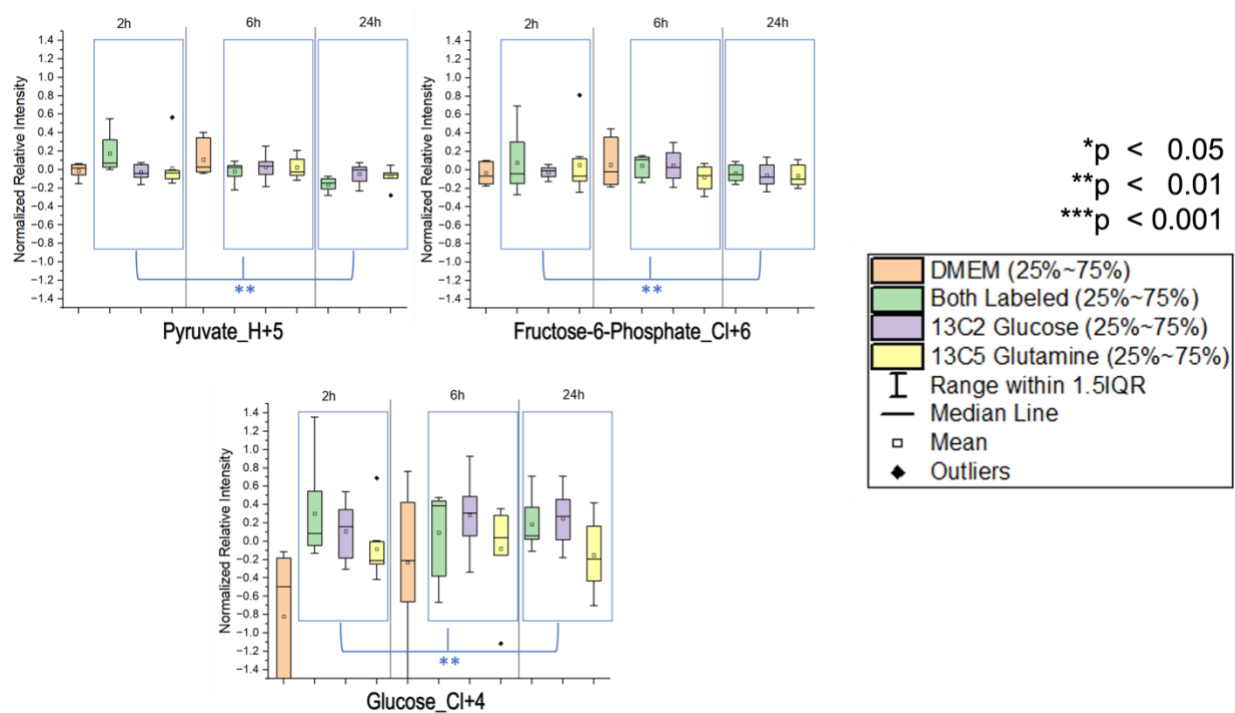


Figure 2.7. Repeated measures ANOVA results for between-label analysis, experimental set 1.

### Targeted Qualitative Analysis of Alternately Labeled Media

The second experiment had four conditions with (i) Regular DMEM, (ii) U-<sup>13</sup>C-Glucose without Glutamine in DMEM, (iii) U-<sup>13</sup>C-Glutamine without glucose in DMEM, and (iv) both U-<sup>13</sup>C-Glucose and U-<sup>13</sup>C-Glutamine replacing glucose and glutamine in DMEM. This way, two groups had alternately labeled carbon sources while lacking the other. The same set of detected

targeted metabolites and their isotopes were sampled in shorter window timepoints of 0-min, 5-min, 10-min, 30-min and 24-h.

Repeated-measures ANOVA determined significant differences between all timepoints for the normalized relative intensities of Glutamine[-H+5], Oxaloacetate[+Cl+4], Pyruvate[-H+4] and Pyruvate[-H+5] (Figure 2.8). Most significant differences were detected for Oxaloacetate[+Cl+4] ( $p < 0.001$ ) and Pyruvate[+Cl+4] ( $p < 0.001$ ), two of the important components of TCA cycle. Another isotope of Pyruvate, Pyruvate[+Cl+5], has also shown a difference of  $p = 0.007$  between all timepoints. Glutamine[-H+5], re-sized for better observing, was the last metabolite to have a significant difference ( $p = 0.045$ ) between short-window timepoints of alternatively labeled media experiment.

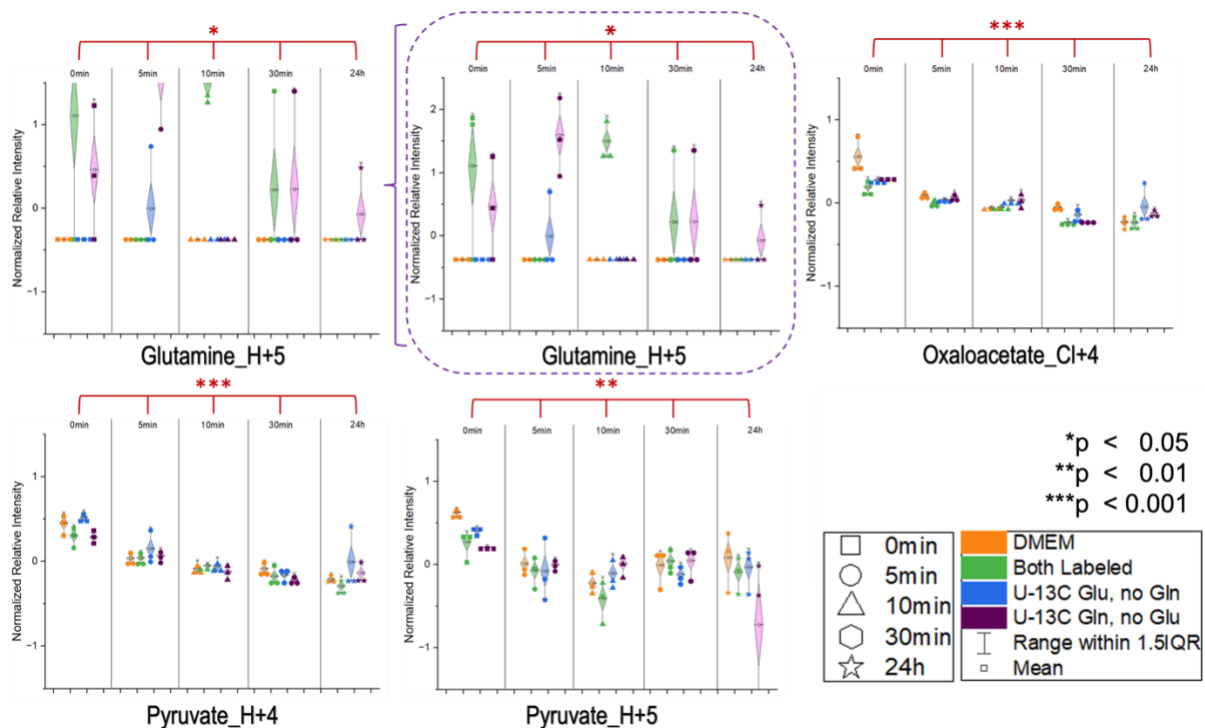


Figure 2.8. Repeated measures ANOVA results for temporal analysis, experimental set 2.

There were also significant differences in normalized relative abundances within labels when comparing them in each timepoint (Figure 2.9). Oxaloacetate[+Cl+4] isotope, one of the key amino acid precursors, was affected by different labels within the timepoints significantly with DMEM and Both Label groups having a pairwise difference of  $p=0.018$ . Relative intensity values of Glutamine[-H+5] within different labeled groups were also affected significantly. Pairwise comparison between DMEM and Both Labeled group had a significant difference of  $p=0.06$ , while DMEM and  $^{13}\text{C}$  Glutamine group lacking Glucose had a difference of  $p=0.009$ . For the same isotope, pairwise comparison has demonstrated statistical significance of  $p=0.011$  between Both Labeled and  $^{13}\text{C}$  Glucose group lacking glutamine.

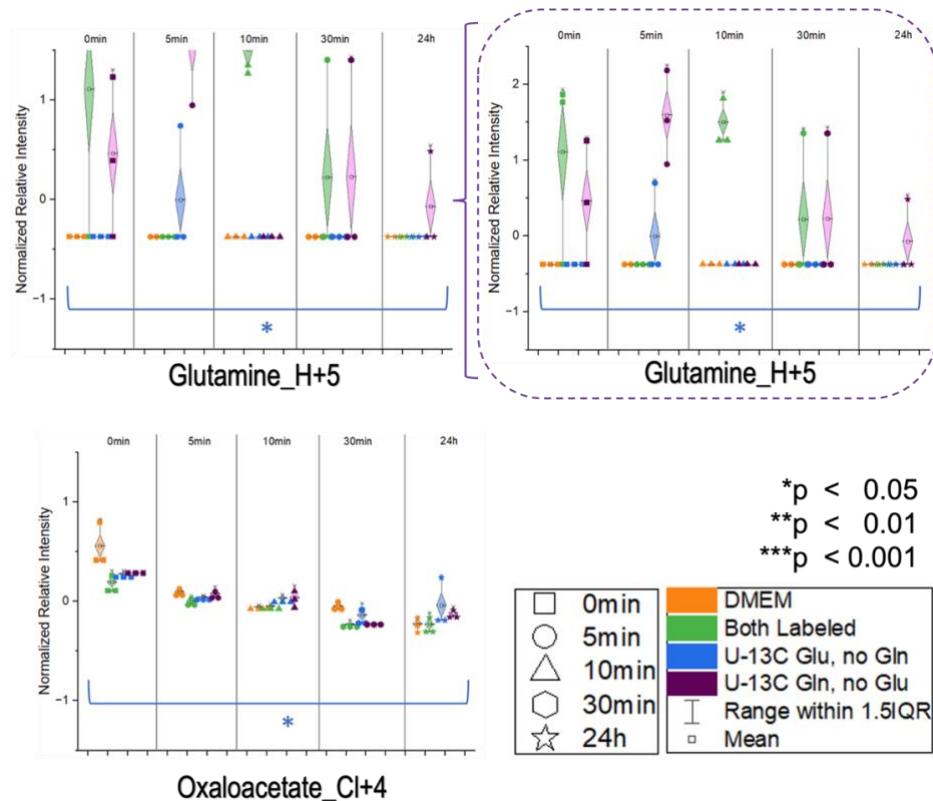


Figure 2.9. Repeated measures ANOVA results for between-label analysis, experimental set 2.

## Discussion

### <sup>13</sup>C labeling Has Minimal Effects on Metabolomic Profiles

Global metabolomic profiles of OA PHCs after starvation (Figure 3) suggests that <sup>13</sup>C compounds result in limited alterations of global chondrocyte metabolism, suggesting minimal kinetic isotope effects and validating their use for heavy carbon labeling in these conditions. Examining the post-starvation time dependent responses suggests that metabolic activity is gradually restored post-starvation by metabolites representing tryptophan metabolism, lysine metabolism, saturated fatty acid  $\beta$ -oxidation, and R group synthesis.

FADH<sub>2</sub> is a common metabolite feature amongst all of them in our analysis, with its relative abundance increasing over time. FADH<sub>2</sub> is generated by TCA cycle and fed into oxidative phosphorylation, aiding the generation of ATP. L-glutamic acid similarly increases in abundance, supporting the targeted investigation into the role of glutamine as a possible carbon source for cartilage matrix collagen formation in OA cells, that was addressed in this paper.

Another key result from the untargeted analysis was the importance of energy metabolism in articular chondrocytes. Multiple CoA-derived metabolite features are also significant, indicating the strong energy metabolism response of the OA PHCs. For an overall assessment of the three timepoints, the median clustergram analysis of time dependence shows great differentiation between 2-, 6-, and 24-h post-starvation: there is a palpable contrast between 2- and 24-h.

### TCA Cycle Metabolite Isotopes were Detected within Different Time Windows

Isotopic steady state in cultured cells is typically achieved over 10 minutes for glycolysis, and over 2 hours for the TCA cycle [33]. Thus, we have detected more dramatic changes in normalized relative intensities of targeted metabolites in the second set of experiments, where we have shorter time windows and altered the carbon sources for energy production. Glutamine and oxaloacetate isotopes, especially, were detected to have more significant changes both timepoint-wise and group label-wise within shorter time windows.

### OA PHC have Different Responses to Different Carbon Sources

It was demonstrated that OA primary human cells have different responses to different carbon sources, both in the presence of each other or lack thereof. Alternately labeled samples have shown the most statistically different responses in within-group comparisons, pointing out to the importance of studying alternative carbon sources in OA.

As a limitation of this study, the normalization for naturally occurring isotopes can be pointed out. For a quantitated analysis, the MS results must be corrected according to the abundance of the naturally occurring isotopes. However, this is a complex problem, and the valid method should be chosen for accurate results [49].

### Conclusion

Our study initially explored the effects of  $^{13}\text{C}$  labeling on the global metabolomic profiles of OA primary human chondrocytes via untargeted metabolomics. The results suggest that  $^{13}\text{C}$  compounds have minimal impact on overall chondrocyte metabolism, validating their use for heavy carbon labeling. Post-starvation metabolic activity revealed gradual metabolic restoration,

and 3 time-points in the span of 24-hr period showed TCA cycle activity and increased abundance of L-glutamic acid. These findings further support our direction to explore energy responses in OA articular chondrocytes.

Targeted metabolomic analysis has found important TCA metabolites and their isotopes in our dataset. It also highlighted significant differences between 2-h and 6-h timepoints and the different responses in labels. Shorter time windows were found to be more efficient in detecting metabolites of interest, with pronounced temporal and label changes with glutamine and oxaloacetate isotopes. Additionally, OA PHCs exhibited varied responses to different carbon sources, highlighting the importance of studying alternative carbon supplies and their effect on metabolism.

Overall, this work advances the understanding of OA chondrocyte metabolism and emphasizes the potential of heavy carbon labeling for future investigations. A quantified targeted analysis of similar samples can also be integrated with our model that is introduced in Chapter 3 for  $^{13}\text{C}$ -MFA analysis.

References

- [1] K. D. Allen, L. M. Thoma, and Y. M. Golightly, “Epidemiology of osteoarthritis,” *Osteoarthritis Cartilage*, vol. 30, no. 2, pp. 184–195, 2022, doi: 10.1016/j.joca.2021.04.020.
- [2] X. Ji and H. Zhang, “Current Strategies for the Treatment of Early Stage Osteoarthritis,” *Front Mech Eng*, vol. 5, p. 480160, Sep. 2019, doi: 10.3389/FMECH.2019.00057/BIBTEX.
- [3] J. W. J. Bijlsma, F. Berenbaum, and F. P. J. G. Lafèber, “Osteoarthritis: an update with relevance for clinical practice,” *The Lancet*, vol. 377, no. 9783, pp. 2115–2126, Jun. 2011, doi: 10.1016/S0140-6736(11)60243-2.
- [4] M. Lotz *et al.*, “Value of biomarkers in osteoarthritis: current status and perspectives,” *Ann Rheum Dis*, vol. 72, no. 11, p. 1756, 2013, doi: 10.1136/ANNRHEUMDIS-2013-203726.
- [5] S. Kundu *et al.*, “Enabling early detection of osteoarthritis from presymptomatic cartilage texture maps via transport-based learning,” *Proc Natl Acad Sci U S A*, vol. 117, no. 40, pp. 24709–24719, Oct. 2020, doi: 10.1073/PNAS.1917405117/SUPPL\_FILE/PNAS.1917405117.SAPP.PDF.
- [6] D. T. Felson and R. Hodgson, “Identifying and Treating Pre-Clinical and Early Osteoarthritis,” *Rheum Dis Clin North Am*, vol. 40, no. 4, p. 699, Nov. 2014, doi: 10.1016/J.RDC.2014.07.012.
- [7] E. G. L. Bywaters and M. MacKinnon, “The metabolism of joint tissues,” *J Pathol Bacteriol*, vol. 44, no. 1, pp. 247–268, Jan. 1937, doi: 10.1002/PATH.1700440119.
- [8] J. W. Kim and C. V. Dang, “Cancer’s Molecular Sweet Tooth and the Warburg Effect,” *Cancer Res*, vol. 66, no. 18, pp. 8927–8930, Sep. 2006, doi: 10.1158/0008-5472.CAN-06-1501.
- [9] H. K. Heywood, M. M. Knight, and D. A. Lee, “Both superficial and deep zone articular chondrocyte subpopulations exhibit the crabtree effect but have different basal oxygen consumption rates,” *J Cell Physiol*, vol. 223, no. 3, pp. 630–639, 2010, doi: 10.1002/jcp.22061.
- [10] P. C. Gomez-Contreras, P. N. Kluz, M. R. Hines, and M. C. Coleman, “Intersections Between Mitochondrial Metabolism and Redox Biology Mediate Posttraumatic Osteoarthritis,” *Curr Rheumatol Rep*, vol. 23, no. 5, 2021, doi: 10.1007/s11926-021-00994-z.

- [11] N. K. Goto and L. E. Kay, “New developments in isotope labeling strategies for protein solution NMR spectroscopy,” *Curr Opin Struct Biol*, vol. 10, no. 5, pp. 585–592, Oct. 2000, doi: 10.1016/S0959-440X(00)00135-4.
- [12] M. R. Antoniewicz, “A guide to <sup>13</sup>C metabolic flux analysis for the cancer biologist,” *Experimental & Molecular Medicine* 2018 50:4, vol. 50, no. 4, pp. 1–13, Apr. 2018, doi: 10.1038/s12276-018-0060-y.
- [13] P. Firdous, T. Hassan, S. Farooq, and K. Nissar, “Applications of proteomics in cancer diagnosis,” *Proteomics*, pp. 257–285, Jan. 2023, doi: 10.1016/B978-0-323-95072-5.00014-6.
- [14] P. P. Brahmachary, H. D. Welhaven, and R. K. June, “Metabolomic Profiling to Understand Chondrocyte Metabolism,” *Methods in Molecular Biology*, vol. 2598, pp. 141–156, 2023, doi: 10.1007/978-1-0716-2839-3\_11/FIGURES/5.
- [15] T. Pluskal, S. Castillo, A. Villar-Briones, and M. Orešič, “MZmine 2: modular framework for processing, visualizing, and analyzing mass spectrometry-based molecular profile data,” *BMC Bioinformatics*, vol. 11, Jul. 2010, doi: 10.1186/1471-2105-11-395.
- [16] C. Jang, L. Chen, and J. D. Rabinowitz, “Metabolomics and Isotope Tracing,” *Cell*, vol. 173, no. 4, pp. 822–837, 2018, doi: 10.1016/j.cell.2018.03.055.
- [17] R. Nilsson, “Validity of natural isotope abundance correction for metabolic flux analysis,” 2020, doi: 10.1101/2020.05.04.075838.

CHAPTER THREE

AN IMPROVED STOICHIOMETRIC MODEL OF CHONDROCYTE CENTRAL  
METABOLISM: FLUX BALANCE ANALYSIS AND INITIAL  
MECHANOTRANSDUCTION RESULTS

Contribution of Authors and Co-Authors

Manuscript in Chapter 2

Author: Ayten Ebru Erdogan

Contributions: Participated in manuscript preparation.

Co-Author: Adrienne Arnold

Contributions: Participated in manuscript preparation.

Co-Author: Erik Myers

Contributions: Participated in manuscript preparation.

Co-Author: Priyanka Brahmachary

Contributions: Participated in manuscript preparation

Co-Author: Donald Smith

Contributions: Participated in manuscript preparation

Co-Author: Ross Carlson

Contributions: Participated in manuscript preparation

Co-Author: Ronald K. June

Contributions: Participated in manuscript preparation

Manuscript Information

Ayten Ebru Erdogan, Adrienne Arnold, Erik Myers, Priyanka Brahmachary, Donald Smith, Ross  
Carlson, Ronald K. June

Status of Manuscript:

Prepared for submission to a peer-reviewed journal

Officially submitted to a peer-reviewed journal

Accepted by a peer-reviewed journal

Published in a peer-reviewed journal

Abstract

This study investigates how chondrocytes in articular cartilage respond to mechanical stimuli and how this process is altered in Osteoarthritis (OA). We focus on collagen's role, which depends on amino acids generated through metabolic pathways. We introduce a core metabolomic model of articular chondrocytes, which includes amino acid synthesis and collagen production. The findings highlight tradeoffs in collagen types based on oxygen availability and carbon sources. Experimental results, including gender-related differences in cellular metabolism, add to the model's insights. This work deepens our understanding of how cells, mechanics, and metabolism interplay in joint health and disease.

## Introduction

Osteoarthritis (OA) is a debilitating disease and one of the most common chronic health conditions. It causes joint pain and impacts physical function, while affecting mental health, sleep, work participation, and even mortality [1]. One of the most prominent consequences of OA is degradation of the articular cartilage, which covers the ends of bones that make up synovial joints such as the knee or the hip [2]. Cartilage functions to provide a low friction bearing surface for joints. Chondrocytes are the only cell types in articular cartilage, which consists of a dense extra cellular matrix (ECM), a less dense pericellular matrix (PCM), and multiple depth zones (superficial, middle, deep) [3]. Several biological pathways within the joint exhibit mechanosensitive properties (*e.g.* respond to mechanical loading). Therefore, there is therapeutic potential for using biomechanical stimuli for disease intervention [4]. However, the intracellular pathways behind chondrocytes sensing and responding to stimuli still have knowledge gaps and are being studied [5][6].

Therefore, it is critical to study mechanotransduction in chondrocytes, the sole cell type in articular cartilage. Chondrocytes form and maintain the ECM that is essential to the function cartilage. Developmentally, articular chondrocytes form their ECM during embryonic development, maintain it during most of the lifespan, remodel it during adaptative stages, and repair it as a response to diseases like OA [7]. The structural integrity and functionality of the articular cartilage relies on the chondrocytes' ability to maintain tissue homeostasis, including the ability to sense and respond to mechanical stimuli. Most of our daily activities that involve using our joints (*e.g.* walking, running, bending, etc) support cartilage homeostasis and have a

biochemical response involving mechanotransduction. Studies find this mechanotransduction is altered in OA [8][9].

Collagen is one of three main constituents that gives both ECM and PCM their mechanical properties and directly affect chondrocyte mechanotransduction. Type II Collagen comprises 90% to 95% of the total collagen in ECM and Type VI Collagen is an important regulator for PCM [10]. Key amino acid precursors that are responsible of producing these collagen types are generated in Glycolysis (for production of Pyruvate and 3-Phosphoglycerate), and the TCA cycle (for production of Oxaloacetate) (Figure 3.1). Pyruvate can be used to produce Leucine, 3-Phosphoglycerate for Glycine, and Oxaloacetate can produce both Proline and Hydroxyproline, which are needed for the production of collagens.

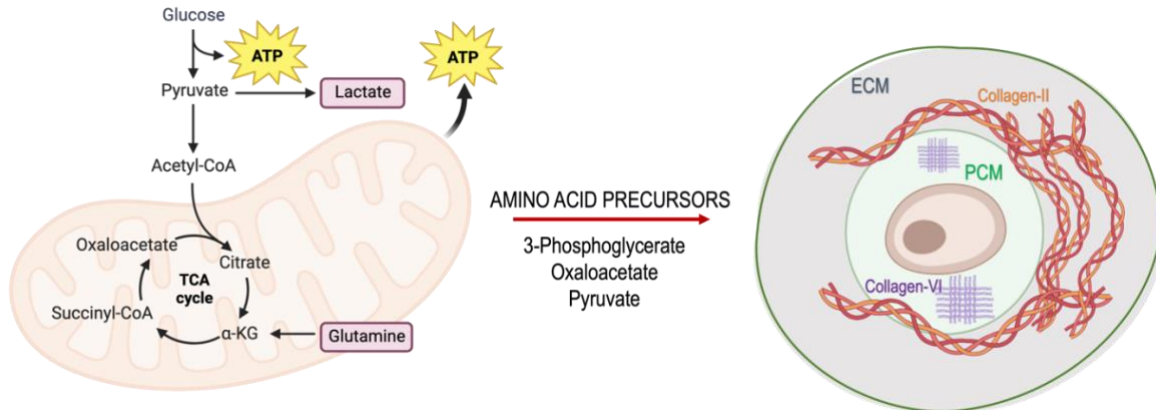


Figure 3.1. Key amino acid precursors produced by Glycolysis and TCA Cycle play an important role in the production and maintenance of Collagen. In turn, Collagen provides articular cartilage, that is degenerated in OA, with the necessary mechanical strength, flexibility, and resistance to mechanical forces.

Previous studies found that (i) dynamic compression plays a role in regulating energy-related metabolites and stimulates the accumulation of key amino acid precursors [11],

(ii) SW1353 chondrocytes respond to compression initially (0-15 minutes) by increasing glycolysis and respiration, then subsequently (15-30 minutes) by lowering the flux through these pathways [12], and (iii) even grade IV OA primary human chondrocytes are able to respond to physiological levels of compression by synthesizing precursors to non-essential amino acids [13]. The latter two studies utilized a relatively simple model of central carbon energy metabolism (CEM). In this paper, we introduce a novel expanded model of mammalian CEM that builds on these previous findings. Our model includes reactions of energy metabolism, amino acid synthesis, and amino acid degradation, as well as electron and energy component reactions that result in the production of Type II Collagen and Type VI Collagen.

To demonstrate the utility of this model, we then used Flux Balance Analysis (FBA) to assess tradeoffs for producing Type II Collagen and Type VI Collagen. Since these collagens have differing essential and non-essential amino acid content, we hypothesize that different costs will be expected for the production of the two collagen types based on (i) ATP needs, (ii) carbon source needs, and (iii) different oxidative stress conditions. We also present quantitative experimental results that can be integrated in the model later on and find experimental donor differences in key carbon sources in OA articular chondrocytes.

## Materials and Methods

### Stoichiometric Model Building

A core stoichiometric model of a human chondrocyte metabolism was constructed using human metabolic network data from HumanCyc [14]. The model consists of 152 metabolites and 140 reactions representing glycolysis, the citric acid cycle, the aerobic electron transport chain, lactate fermentation, the pentose phosphate pathway, uptake and synthesis of amino acids, and

synthesis of both Type II and Type VI collagen. CellNetAnalyzer was used to validate the model for mass, atom, and energy balance of each reaction [15]. Forward and reverse directions were determined using thermodynamic information from HumanCyc. Reversible transport reactions were included for protons, water, CO<sub>2</sub> and bicarbonate, and ammonium. Irreversible transport reactions were included for O<sub>2</sub>, the essential amino acids, glucose and glutamine uptake, urea excretion, lactate excretion, sodium export, and collagen production. Collagen composition was determined using the amino acid sequences of type II and type VI collagen from HumanCyc, scaled to 100 amino acids. A reaction representing ATP maintenance requirements was also included [16].

The model was constructed in CellNetAnalyzer 2019 and analyzed via flux balance analysis in CobraToolbox using MATLAB R2020a. Details on the composition of the metabolic model can be found in Appendix B.1. The code used to analyze the model can be found in Appendix B.2 and B.3.

### Chondrocyte Harvest and Culture

OA Human Primary Chondrocytes (OA-HPCs) were acquired from  $n = 10$  (5 male and 5 female) patients with Grade IV OA that underwent total joint replacement using an IRB-approved consent form. Cell harvest and culture have been described previously [17]. Briefly, the remaining cartilage was digested with Collagenase Type II (2 mg/mL) (Gibco, Waltham, MA, USA) for 12 h at 37°C and harvested cells were suspended in Dulbecco's Modified Eagle's medium (DMEM) (Gibco, Waltham, MA, USA). The isolated cells were then centrifuged and plated with complete media including Fetal Bovine Serum (FBS) (10% v/v) (Bio-Techne, Minneapolis, MN, USA), penicillin (10,000 I.U./mL), and streptomycin (10,000 µg/mL) in 5%

CO<sub>2</sub> at 37 °C. Chondrocytes were passaged at 90% confluency and released via trypsin digestion.

#### Agarose Encapsulation and Chondrocyte Loading

The OA-HPCs were suspended in high-stiffness (4.5% wt/vol final concentration) agarose using established methods in a cylindrical mold [18][19]. These molds were used to create a total of 115 hydrogels that were 12.7mm high and 7mm in diameter encapsulating approximately 500,000 live cells. A multi-modal loader machine developed in June Lab was used to apply compression and/or shear on the hydrogels.

115 hydrogels were divided among five different loading groups as followed: (A) unloaded control group, (B) 5% compression strain group, (C) 5% shear strain group, (D) 5% compression and shear strain group, and (E) 5% compression and shear strain applied out of phase from one another. Loading bouts were performed for 30 minutes at 37°C and 5% CO<sub>2</sub> concentration. Unloaded controls from each donor were used to established baseline metabolite levels for comparison of mechanical loads.

Table 3.3. List of targeted central carbon metabolism compounds.

<b>METABOLITE</b>	<b>EXACT MASS</b>	<b>IONIZATION</b>
<b>NADH</b>	665.125	Positive, Negative
<b>NADPH</b>	745.091	Positive, Negative
<b>HS-COA</b>	767.115	Positive, Negative
<b>ACETYLCOA</b>	809.125	Positive
<b>SUCCINYLCOA</b>	867.131	Positive
<b>PYRUVATE</b>	88.016	Negative
<b>PHOSPHOENOLPYRUVATE</b>	168.982	Negative
<b>LACTIC ACID</b>	90.032	Negative
<b>ALPHA-KETOGLUTARATE</b>	146.022	Negative
<b>GTP</b>	522.991	Negative
<b>OXALOACETATE</b>	132.006	Negative
<b>L-MALATE</b>	134.022	Negative
<b>GLUTAMATE</b>	147.053	Positive
<b>6-P-GLUCONATE</b>	276.025	Negative
<b>GLUCOSE</b>	180.063	Negative
<b>FRUCTOSE-6-PHOSPHATE</b>	260.03	Negative
<b>CITRATE</b>	192.027	Negative
<b>ISOCITRATE</b>	192.027	Negative
<b>SEDOHEPTULOSE-7-PHOSPHATE</b>	290.04	Negative
<b>GLYCERALDEHYDE 3-PHOSPHATE</b>	169.998	Negative

### LC-MS Method Development and Targeted Metabolomics

Initially, 20 analytical metabolite standards representing the key points in the novel stoichiometric model were chosen (Table 3.1). An LC-MS method was developed in the Mass Spectrometry facility at Montana State University to quantify these 20 targeted metabolites. Agilent 6538 UHD Accurate-Mass Q-TOF LC-MS coupled with HPLC was used for all trial experiments including standard pool trial runs and bovine cells with standard pool trial runs, to estimate the quantitation accuracy of the actual biological samples. After the initial method development period, using ammonium hydroxide in negative mode ESI deemed to be the most efficient mobile phase. A three-point standard curve was constructed to verify the accuracy of the quantification. The resulting concentrations of quantified standards were used to calculate metabolite accumulations using the following equation:

$$\Delta (\text{Accumulation}) = \frac{\text{Median Concentration of Condition} - \text{Median Concentration of Control}}{\text{Time}} \quad (\text{Eq 1})$$

## Results

### Model Predictions of ATP Yields

ATP yield model predictions for oxidative phosphorylation and the lack of oxidative phosphorylation were carried out for two carbon sources (Figure 3.2). When considering these carbon sources in the model, the uptake of either glucose or glutamine was prevented in the system to focus on each separately. ~26 ATPs were generated via glucose with oxidative phosphorylation, while ~2 ATPs were generated without available O<sub>2</sub>. For glutamine, ~14 molecules of ATP were generated with available O<sub>2</sub>, while in the lack of O<sub>2</sub> consumption FBA did not run.

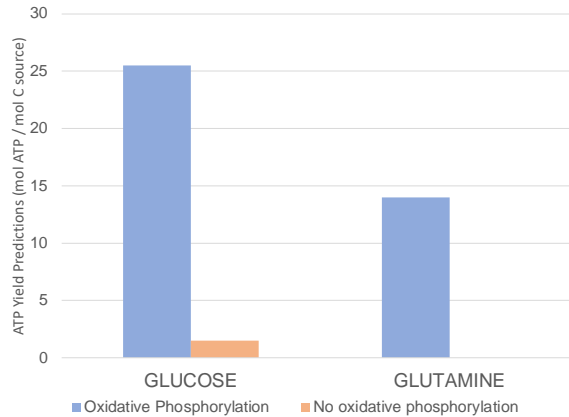


Figure 3.2. Carbon source dependent ATP yield predictions in the presence and absence of available O<sub>2</sub>.

### O<sub>2</sub> Dependent Type II Collagen and Type VI Collagen Predictions

Both Type II Collagen and Type VI Collagen were not produced when oxidative phosphorylation was blocked in the model. Figure 3.3 depicts the yield of two collagen types on oxidative phosphorylation. Glutamine was more efficient in both Type II Collagen and Type VI Collagen production, and while they followed similar trends, Type VI Collagen yields were relatively larger on both carbon sources.

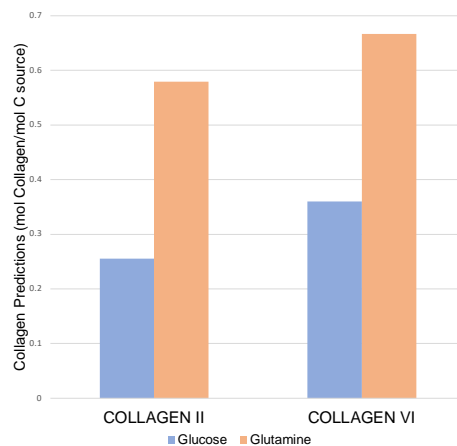


Figure 3.3. Yields of Collagen-II and Collagen-VI on Glucose and Glutamine with oxidative phosphorylation.

### Mapping Collagen Production on Lactate via FBA

Using CobraToolbox, predictions were run to maximize production of Type II Collagen and Type VI Collagen on glucose at varying levels of lactate fermentation (*i.e.*, flux through the terminal oxidase in the electron transport chain) (Figure 3.4 and Figure 3.5). The resulting fluxes were scaled to glucose uptake (mole/mole) to compare between the predictions. The collagen yield decreases as lactate production increases and O<sub>2</sub> levels decrease due to the lower availability of ATP.

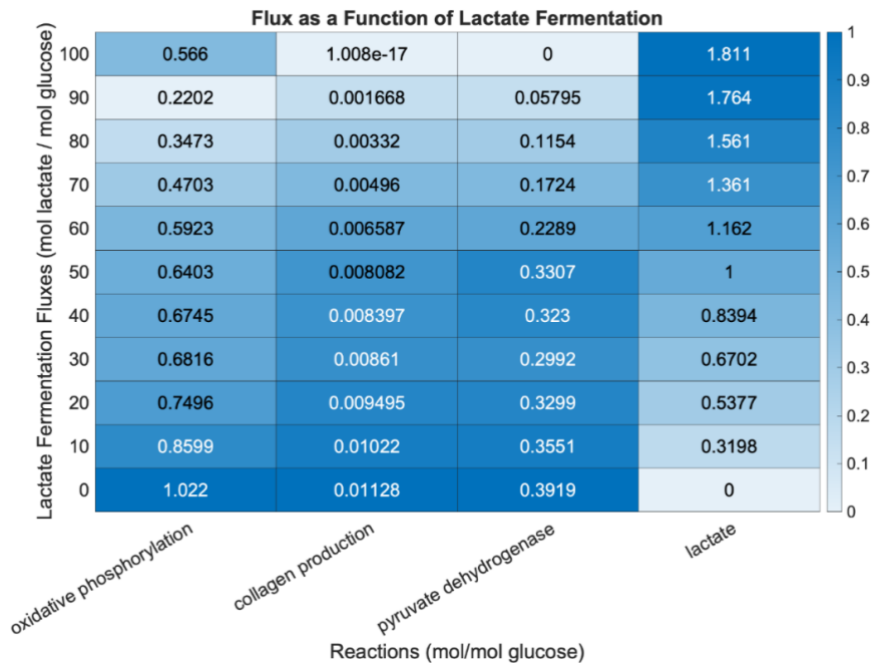


Figure 3.4. Maximized production of Collagen-II in varying levels of lactate production.

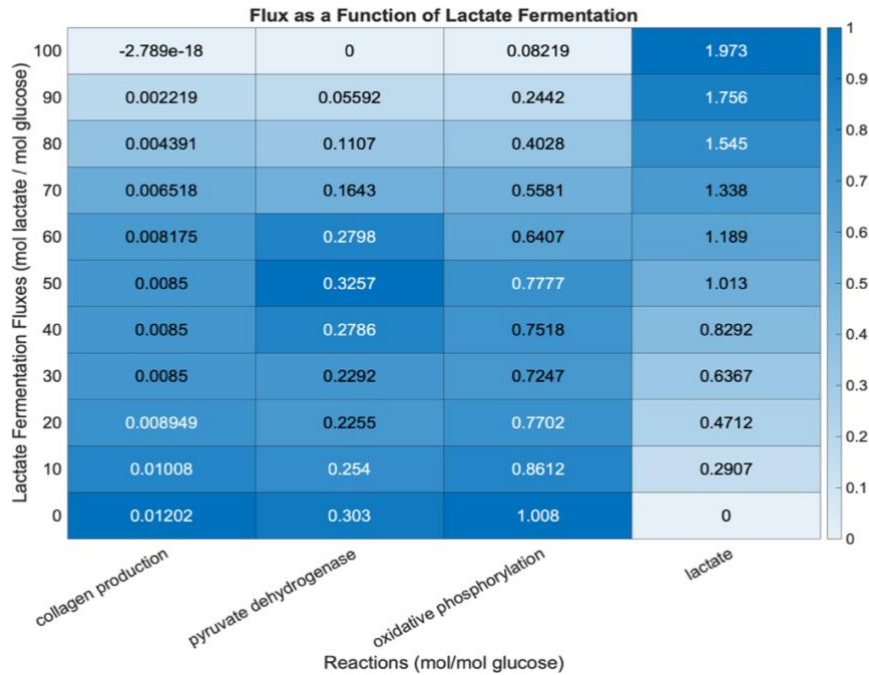


Figure 3.5. Maximized production of Collagen-VI in varying levels of lactate production.

#### Accumulation of Four Targets under OA Mechanotransduction

For the agarose encapsulated gels, 4 out of 20 metabolites were successfully detected and quantified (Figure 6). In males, glucose exhibited the most pronounced depletion within the 30-minute interval across all experimental conditions. In contrast, samples from female patients demonstrated a more distributed pattern of glucose levels. During the processes of glucose depletion induced by compression and shear, as well as during conditions involving out-of-phase compression/shear and combined compression with shear, female donor samples had a positive accumulation of glucose. For lactic acid, the male cohort exhibited relatively consistent values across all experimental conditions. In contrast, the female cohort exhibited a notably similar pattern in the temporal dynamics of lactic acid and glucose across the experimental conditions.

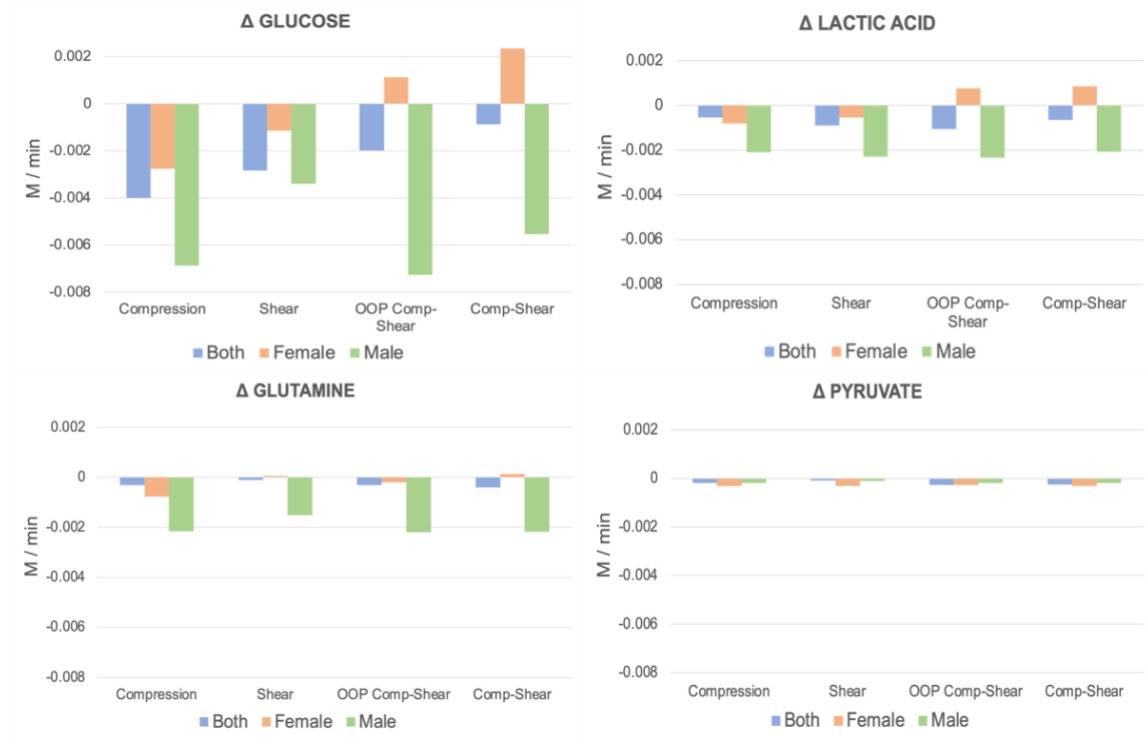


Figure 3.6. Accumulations of four targeted metabolites.

Meanwhile, the depletion of glutamine demonstrated relatively consistent accumulations within the male cohort across all conditions. The female cohort, again, displayed distinctive variations in response. Among the observed conditions, the most pronounced depletion was recorded under compression, followed sequentially by out-of-phase compression (OOP compression), and shear conditions. Pyruvate levels exhibited minimal fluctuation in both depletion and accumulation across all conditions for both male and female cohorts.

### Discussion

Metabolomics integrated with fluxomics has good potential for studying and interpreting metabolism within biological systems [20]. Mass spectrometry methods by themselves can report

the relatively downregulated and upregulated metabolite features. However even quantified analyses are not sufficient to accurately describe all of the complex reactions in play. For example, a depletion in the concentration of a metabolite can either be because of over-consumption or under-production [21]. To be able to accurately study these features, integration of experimental metabolite data with stoichiometric models is needed.

We built a model around central carbon metabolism and the production of essential and non-essential amino acids. Our model includes the key reactions of amino acid precursors, which play a major role in the production of two collagen types that are important for articular cartilage cells. The ATP predictions of the model are similar to established values. The Type II Collagen and Type VI Collagen predictions on glucose when lactate production is being gradually increased show that both the presence of oxygen and the utilization of oxidative phosphorylation are vital to collagen production for articular cartilage homeostasis. Even though the trends were similar, model results show that Type II- and Type VI Collagen have different production efficiencies for carbon sources of glucose and glutamine. This can be explained by different distributions of essential and non-essential amino acids for the two collagen types (Figure 3.7).

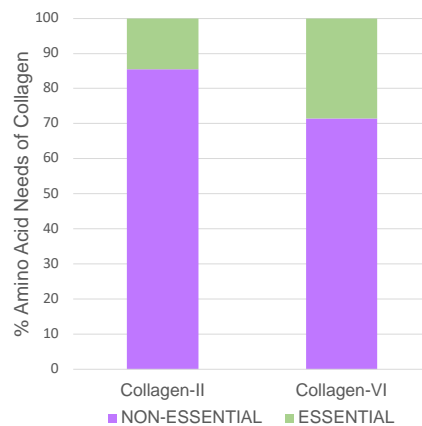


Figure 3.7. Essential and non-essential amino acid needs of Collagen-II and Collagen-VI.

From the experimental results, production of glucose by the female cohort is interesting. This phenomenon may potentially stem from an accelerated consumption of the finite glucose carbon source by the female group, causing the breakdown of stored glycogen molecules for additional energy production. Since the female population has increased incidence of OA compared to the male population, this observation along with the similar trend in lactic acid require further study.

While the lactic acid production in the female cohort may be an indicator of sexual dimorphism in OA, the depletion of lactic acid within other conditions in both males and females provides experimental evidence supporting the premise of mitochondrial activity as an early temporal response chondrocyte mechanotransduction. Comparing all quantified metabolites together, lactic acid can be another important source of carbon for OA chondrocytes. On the other hand, since Pyruvate is an important intermediate between Glycolysis and TCA cycle, the continual production and depletion may also explain the low levels of accumulation.

### Conclusion

We formulated a core metabolic model of chondrocytes centered around central carbon metabolism and the synthesis of both essential and non-essential amino acids, using collagen as biomass. The computational predictions for collagen production under varying conditions emphasizes the importance of oxygen availability and oxidative phosphorylation in sustaining collagen synthesis for maintaining articular cartilage homeostasis. The model also reveals how production of different collagen types have differing efficiencies in utilizing glucose and glutamine as carbon sources.

Experimental findings for OA human primary chondrocytes add data on central metabolism to a complex picture of chondrocyte mechanotransduction. Parallel trends in glucose and lactic acid production observed in females might be attributed to increased energy demands, potentially driving the utilization of stored glycogen reserves. Furthermore, the change in lactic acid levels across conditions in both genders can point towards mitochondrial activity as an early response mechanism in OA and a potential carbon source to investigate.

In the future, the model and the experimental results can be further integrated together to expand on these initial interpretations. Lactic acid can be studied via the model as an additional carbon source and the current method for extracting central carbon energy metabolism compounds can be optimized by changing the extraction buffers [22][23]. Improved extraction methods may allow detection of additional central metabolites. In conclusion, this study underscores the value of integrating diverse methodologies to unravel the complexities of metabolic processes. By bridging the gap between experimental data and computational models, this study provides a more nuanced understanding of metabolic dynamics in chondrocyte mechanotransduction, potentially providing a foundation for future targeted interventions in OA and related conditions. Further investigations, building upon these findings, hold the potential to reshape our strategies for managing and mitigating the impact of OA.

References

- [1] C. Cook, R. Pietrobon, and E. Hegedus, "Osteoarthritis and the impact on quality of life health indicators," *Rheumatol Int*, vol. 27, no. 4, pp. 315–321, Feb. 2007, doi: 10.1007/S00296-006-0269-2/TABLES/4.
- [2] R. F. Loeser, S. R. Goldring, C. R. Scanzello, and M. B. Goldring, "Osteoarthritis: A disease of the joint as an organ," *Arthritis Rheum*, vol. 64, no. 6, pp. 1697–1707, Jun. 2012, doi: 10.1002/art.34453.
- [3] A. J. Sophia Fox, A. Bedi, and S. A. Rodeo, "The basic science of articular cartilage: Structure, composition, and function," *Sports Health*, vol. 1, no. 6, pp. 461–468, 2009, doi: 10.1177/1941738109350438.
- [4] S. Glyn-Jones *et al.*, "Osteoarthritis," *The Lancet*, vol. 386, no. 9991, pp. 376–387, 2015, doi: 10.1016/S0140-6736(14)60802-3.
- [5] Z. Zhao, Y. Li, M. Wang, S. Zhao, Z. Zhao, and J. Fang, "Mechanotransduction pathways in the regulation of cartilage chondrocyte homeostasis," *J Cell Mol Med*, vol. 24, no. 10, pp. 5408–5419, May 2020, doi: 10.1111/JCMM.15204.
- [6] D. R. Haudenschild, J. Chen, N. Pang, M. K. Lotz, and D. D. D’Lima, "Rho kinase-dependent activation of SOX9 in chondrocytes," *Arthritis Rheum*, vol. 62, no. 1, pp. 191–200, Jan. 2010, doi: 10.1002/ART.25051.
- [7] J. D. Humphrey, E. R. Dufresne, and M. A. Schwartz, "Mechanotransduction and extracellular matrix homeostasis," *Nat Rev Mol Cell Biol*, vol. 15, no. 12, p. 802, Dec. 2014, doi: 10.1038/NRM3896.
- [8] W. Jiang, H. Liu, R. Wan, Y. Wu, Z. Shi, and W. Huang, "Mechanisms linking mitochondrial mechanotransduction and chondrocyte biology in the pathogenesis of osteoarthritis," *Ageing Res Rev*, vol. 67, May 2021, doi: 10.1016/J.ARR.2021.101315.
- [9] W. Lee *et al.*, "Inflammatory signaling sensitizes Piezo1 mechanotransduction in articular chondrocytes as a pathogenic feed-forward mechanism in osteoarthritis," *Proc Natl Acad Sci U S A*, vol. 118, no. 13, Mar. 2021, doi: 10.1073/PNAS.2001611118/-/DCSUPPLEMENTAL.

- [10] N. A. Zelenski *et al.*, “Type VI Collagen Regulates Pericellular Matrix Properties, Chondrocyte Swelling, and Mechanotransduction in Mouse Articular Cartilage,” *Arthritis Rheumatol*, vol. 67, no. 5, pp. 1286–1294, May 2015, doi: 10.1002/ART.39034.
- [11] D. L. Zignego, J. K. Hilmer, and R. K. June, “Mechanotransduction in primary human osteoarthritic chondrocytes is mediated by metabolism of energy, lipids, and amino acids,” *J Biomech*, vol. 48, no. 16, pp. 4253–4261, 2015, doi: 10.1016/j.jbiomech.2015.10.038.
- [12] D. Salinas, C. A. Minor, R. P. Carlson, C. N. McCutchen, B. M. Mumey, and R. K. June, “Combining targeted metabolomic data with a model of glucose metabolism: Toward progress in chondrocyte mechanotransduction,” *PLoS One*, vol. 12, no. 1, pp. 1–16, 2017, doi: 10.1371/journal.pone.0168326.
- [13] D. Salinas, B. M. Mumey, and R. K. June, “Physiological dynamic compression regulates central energy metabolism in primary human chondrocytes,” *Biomech Model Mechanobiol*, vol. 18, no. 1, pp. 69–77, 2019, doi: 10.1007/s10237-018-1068-x.
- [14] P. Romero, J. Wagg, M. L. Green, D. Kaiser, M. Krummenacker, and P. D. Karp, “Computational prediction of human metabolic pathways from the complete human genome.,” *Genome Biol*, vol. 6, no. 1, pp. 1–17, Dec. 2005, doi: 10.1186/GB-2004-6-1-R2/TABLES/7.
- [15] S. Klamt, J. Saez-Rodriguez, and E. D. Gilles, “Structural and functional analysis of cellular networks with CellNetAnalyzer,” *BMC Syst Biol*, vol. 1, no. 1, pp. 1–13, Jan. 2007, doi: 10.1186/1752-0509-1-2/FIGURES/6.
- [16] A. E. Beck, K. A. Hunt, and R. P. Carlson, “Measuring Cellular Biomass Composition for Computational Biology Applications,” *Processes 2018, Vol. 6, Page 38*, vol. 6, no. 5, p. 38, Apr. 2018, doi: 10.3390/PR6050038.
- [17] P. P. Brahmachary, H. D. Welhaven, and R. K. June, “Metabolomic Profiling to Understand Chondrocyte Metabolism,” *Methods in Molecular Biology*, vol. 2598, pp. 141–156, 2023, doi: 10.1007/978-1-0716-2839-3\_11/FIGURES/5.
- [18] A. A. Jutila, D. L. Zignego, W. J. Schell, and R. K. June, “Encapsulation of Chondrocytes in High-Stiffness Agarose Microenvironments for In Vitro Modeling of Osteoarthritic Mechanotransduction,” *Ann Biomed Eng*, vol. 43, no. 5, pp. 1132–1144, May 2015, doi: 10.1007/S10439-014-1183-5/FIGURES/6.

- [19] D. L. Zignego, A. A. Jutila, M. K. Gelbke, D. M. Gannon, and R. K. June, "The mechanical microenvironment of high concentration agarose for applying deformation to primary chondrocytes," *J Biomech*, vol. 47, no. 9, pp. 2143–2148, Jun. 2014, doi: 10.1016/J.JBIOMECH.2013.10.051.
- [20] A. H. Emwas, K. Szczepski, I. Al-Younis, J. I. Lachowicz, and M. Jaremko, "Fluxomics - New Metabolomics Approaches to Monitor Metabolic Pathways," *Front Pharmacol*, vol. 13, p. 805782, Mar. 2022, doi: 10.3389/FPHAR.2022.805782/BIBTEX.
- [21] C. Jang, L. Chen, and J. D. Rabinowitz, "Metabolomics and Isotope Tracing," *Cell*, vol. 173, no. 4, pp. 822–837, 2018, doi: 10.1016/j.cell.2018.03.055.
- [22] Z. Ser, X. Liu, N. N. Tang, and J. W. Locasale, "Extraction parameters for metabolomics from cell extracts," *Anal Biochem*, vol. 475, p. 22, Apr. 2015, doi: 10.1016/J.AB.2015.01.003.
- [23] C. Andresen *et al.*, "Comparison of extraction methods for intracellular metabolomics of human tissues," *Front Mol Biosci*, vol. 9, Aug. 2022, doi: 10.3389/FMOLB.2022.932261/FULL.

## CHAPTER FOUR

## CONCLUSION AND FUTURE WORK

This work highlights the importance of metabolomics and mathematical modeling for understanding OA primary human chondrocyte metabolism and filling the gaps in knowledge in the field. The results from Chapter 2 emphasizes the importance of the role of mitochondria and TCA cycle, that were previously disregarded in the literature. It also shows different carbon sources will play different roles in regulating central carbon metabolism thus the chondrocyte homeostasis that is related to collagen production. Chapter 3 introduces a core scale metabolic model of human articular chondrocytes, and the initial predictions via Flux Balance Analysis. It also presents initial mechanotransduction results of quantified accumulations for carbon sources of chondrocytes. The model and the accumulation results from different donors, once again, draw the attention to potential interventions that can stem from molecular level studies of OA chondrocytes. This way, novel intervention methods for a better understood biological system and its diseases can be investigated in the future.

For the future, metabolite extraction from agarose hydrogels can be optimized. The type of metabolites recovered from an extraction depends on the specific extraction method and solvents that were utilized [50]. For a robust analysis, one has to understand the possible modifications that can be implemented. Temperatures for precipitation and removal of macromolecules from 4°C to -80°C work well for a great range of metabolite classes (amino acids, carboxylic acids, fatty acids, hormones etc.) The samples need to be kept within this range including the centrifuging steps [51]. Another crucial step is the extraction buffer, where for a regular untargeted metabolomics analysis, 100% methanol is usually sufficient [50]. For more

specialized studies such as the ones we discussed here, i.e. using human primary articular chondrocyte cells extracted from cartilage tissue or agarose and targeting central carbon metabolism features, we found that different extraction buffers are needed to be compared to find the optimal method. Future experiments can build on the present results using these methodological improvements.

The core scale metabolic model introduced in Chapter 3 can also be used for further predictions of different carbon sources (e.g. lactic acid and pyruvate), as well as experimental data based predictions using both  $^{13}\text{C}$  isotopic labeling results and Mechanotransduction targeted results from OA primary human chondrocytes. Overall, this thesis and its potential future applications have great implications for a better understanding of OA metabolism and possible therapeutic routes to discover.

REFERENCES CITED

- [1] D. J. Hunter, L. March, and M. Chew, “Osteoarthritis in 2020 and beyond: a Lancet Commission,” *The Lancet*, vol. 396, no. 10264, pp. 1711–1712, 2020, doi: 10.1016/S0140-6736(20)32230-3.
- [2] J. S. Mort and C. J. Billington, “Articular cartilage and changes in arthritis matrix degradation,” *Arthritis Res*, vol. 3, no. 6, pp. 337–341, 2001, doi: 10.1186/ar325.
- [3] K. E. Barbour, C. G. Helmick, M. Boring, and T. J. Brady, “Vital Signs: Prevalence of Doctor-Diagnosed Arthritis and Arthritis-Attributable Activity Limitation — United States, 2013–2015,” *MMWR Morb Mortal Wkly Rep*, vol. 66, no. 9, pp. 246–253, 2017, doi: 10.15585/mmwr.mm6609e1.
- [4] A. J. Sophia Fox, A. Bedi, and S. A. Rodeo, “The basic science of articular cartilage: Structure, composition, and function,” *Sports Health*, vol. 1, no. 6, pp. 461–468, 2009, doi: 10.1177/1941738109350438.
- [5] D. D. Chan, L. Cai, K. D. Butz, S. B. Trippel, E. A. Nauman, and C. P. Neu, “In vivo articular cartilage deformation: Noninvasive quantification of intratissue strain during joint contact in the human knee,” *Sci Rep*, vol. 6, no. August 2015, pp. 1–14, 2016, doi: 10.1038/srep19220.
- [6] F. Meyer *et al.*, “Chondrocytes From Osteoarthritic and Chondrocalcinosis Cartilage Represent Different Phenotypes,” *Front Cell Dev Biol*, vol. 9, no. April, pp. 1–9, 2021, doi: 10.3389/fcell.2021.622287.
- [7] A. Villalvilla, R. Gómez, R. Largo, and G. Herrero-Beaumont, “Lipid transport and metabolism in healthy and osteoarthritic cartilage,” *Int J Mol Sci*, vol. 14, no. 10, pp. 20793–20808, 2013, doi: 10.3390/ijms141020793.
- [8] R. J. Goekoop *et al.*, “Determinants of absence of osteoarthritis in old age,” *Scand J Rheumatol*, vol. 40, no. 1, pp. 68–73, 2011, doi: 10.3109/03009742.2010.500618.
- [9] S. O., G. G., G. K., and M. F.D., “Investigation of the relationships between knee osteoarthritis and obesity via untargeted metabolomics analysis,” *Clin Rheumatol*, pp. 1351–1360, 2019, [Online]. Available: <http://www.embase.com/search/results?subaction=viewrecord&from=export&id=L625994783%0Ahttp://dx.doi.org/10.1007/s10067-019-04428-1>

- [10] K. M. Clements, Z. C. Bee, G. V. Crossingham, M. A. Adams, and M. Sharif, "How severe must repetitive loading be to kill chondrocytes in articular cartilage?," *Osteoarthritis Cartilage*, vol. 9, no. 5, pp. 499–507, 2001, doi: 10.1053/joca.2000.0417.
- [11] M. Tschon, D. Contartese, S. Pagani, V. Borsari, and M. Fini, "Gender and Sex Are Key Determinants in Osteoarthritis Not Only Confounding Variables. A Systematic Review of Clinical Data," *J Clin Med*, vol. 10, no. 14, p. 10, Jul. 2021, doi: 10.3390/JCM10143178.
- [12] N. Chinzei *et al.*, "Evidence for Genetic Contribution to Variation in Posttraumatic Osteoarthritis in Mice," *Arthritis and Rheumatology*, vol. 71, no. 3, pp. 370–381, 2019, doi: 10.1002/art.40730.
- [13] B. Mohajer *et al.*, "Metabolic Syndrome and Osteoarthritis Distribution in the Hand Joints: A Propensity Score Matching Analysis From the Osteoarthritis Initiative," *J Rheumatol*, vol. 48, no. 10, pp. 1608–1615, Oct. 2021, doi: 10.3899/JRHEUM.210189.
- [14] R. Lowe, N. Shirley, M. Bleackley, S. Dolan, and T. Shafee, "Transcriptomics technologies," *PLoS Comput Biol*, vol. 13, no. 5, pp. 1–23, 2017, doi: 10.1371/journal.pcbi.1005457.
- [15] S. Al-Amrani, Z. Al-Jabri, A. Al-Zaabi, J. Alshekaili, and M. Al-Khabori, "Proteomics: Concepts and applications in human medicine," *World J Biol Chem*, vol. 12, no. 5, pp. 57–69, 2021, doi: 10.4331/wjbc.v12.i5.57.
- [16] S. J. Kim, S. H. Kim, J. H. Kim, S. Hwang, and H. J. Yoo, "Understanding metabolomics in biomedical research," *Endocrinology and Metabolism*, vol. 31, no. 1, pp. 7–16, 2016, doi: 10.3803/EnM.2016.31.1.7.
- [17] B. Lin, "A roadmap for interpreting <sup>13</sup>C metabolite labeling patterns from cells," *Physiol Behav*, vol. 176, no. 12, pp. 139–148, 2017, doi: 10.1016/j.copbio.2015.02.003.A.
- [18] S. Edition, "The Expanding Role of Mass Spectrometry in Biotechnology, Second Edition [Paperback]," p. 257, 2006, [Online]. Available: [http://www.amazon.com/dp/0974245127/ref=cm\\_sw\\_su\\_dp](http://www.amazon.com/dp/0974245127/ref=cm_sw_su_dp)
- [19] A. H. M. Emwas, *The strengths and weaknesses of NMR spectroscopy and mass spectrometry with particular focus on metabolomics research*, vol. 1277. 2015. doi: 10.1007/978-1-4939-2377-9\_13.

- [20] R. E. Marcus and L. Sokoloff, "The effect of low oxygen concentration on growth, glycolysis, and sulfate incorporation by articular chondrocytes in monolayer culture," *Arthritis Rheum*, vol. 16, no. 5, pp. 646–656, 1973, doi: 10.1002/art.1780160509.
- [21] H. K. Heywood and D. A. Lee, "Monolayer expansion induces an oxidative metabolism and ROS in chondrocytes," *Biochem Biophys Res Commun*, vol. 373, no. 2, pp. 224–229, 2008, doi: 10.1016/j.bbrc.2008.06.011.
- [22] O. Rosentiial, M. A. Bowte, and G. Wagoner, "STUDIES I N T H E METABOLISM O F ARTICULAR CARTILAGE," pp. 221–233.
- [23] R. A. J. Windhaber, R. J. Wilkins, and D. Meredith, "Functional characterisation of glucose transport in bovine articular chondrocytes," *Pflugers Arch*, vol. 446, no. 5, pp. 572–577, 2003, doi: 10.1007/s00424-003-1080-5.
- [24] R. Terkeltaub, K. Johnson, A. Murphy, and S. Ghosh, "Invited review: The mitochondrion in osteoarthritis," *Mitochondrion*, vol. 1, no. 4, pp. 301–319, 2002, doi: 10.1016/S1567-7249(01)00037-X.
- [25] H. K. Heywood, M. M. Knight, and D. A. Lee, "Both superficial and deep zone articular chondrocyte subpopulations exhibit the crabtree effect but have different basal oxygen consumption rates," *J Cell Physiol*, vol. 223, no. 3, pp. 630–639, 2010, doi: 10.1002/jcp.22061.
- [26] M. C. Coleman *et al.*, "Targeting mitochondrial responses to intra-articular fracture to prevent posttraumatic osteoarthritis," *Sci Transl Med*, vol. 10, no. 427, pp. 1–15, 2018, doi: 10.1126/scitranslmed.aan5372.
- [27] J. A. Bolduc, J. A. Collins, and R. F. Loeser, "Reactive oxygen species, aging and articular cartilage homeostasis," *Free Radic Biol Med*, vol. 132, no. August 2018, pp. 73–82, 2019, doi: 10.1016/j.freeradbiomed.2018.08.038.
- [28] D. Salinas, C. A. Minor, R. P. Carlson, C. N. McCutchen, B. M. Mumey, and R. K. June, "Combining Targeted Metabolomic Data with a Model of Glucose Metabolism: Toward Progress in Chondrocyte Mechanotransduction," *PLoS One*, vol. 12, no. 1, Jan. 2017, doi: 10.1371/JOURNAL.PONE.0168326.
- [29] D. Salinas, C. A. Minor, R. P. Carlson, C. N. McCutchen, B. M. Mumey, and R. K. June, "Combining targeted metabolomic data with a model of glucose metabolism: Toward progress in

chondrocyte mechanotransduction,” *PLoS One*, vol. 12, no. 1, pp. 1–16, 2017, doi: 10.1371/journal.pone.0168326.

[30] D. Salinas, B. M. Mumey, and R. K. June, “Physiological dynamic compression regulates central energy metabolism in primary human chondrocytes,” *Biomech Model Mechanobiol*, vol. 18, no. 1, pp. 69–77, 2019, doi: 10.1007/s10237-018-1068-x.

[31] J. D. Humphrey, E. R. Dufresne, and M. A. Schwartz, “Mechanotransduction and extracellular matrix homeostasis,” *Nat Rev Mol Cell Biol*, vol. 15, no. 12, p. 802, Dec. 2014, doi: 10.1038/NRM3896.

[32] N. A. Zelenski *et al.*, “Type VI Collagen Regulates Pericellular Matrix Properties, Chondrocyte Swelling, and Mechanotransduction in Mouse Articular Cartilage,” *Arthritis Rheumatol*, vol. 67, no. 5, pp. 1286–1294, May 2015, doi: 10.1002/ART.39034.

[33] C. Jang, L. Chen, and J. D. Rabinowitz, “Metabolomics and Isotope Tracing,” *Cell*, vol. 173, no. 4, pp. 822–837, 2018, doi: 10.1016/j.cell.2018.03.055.

[34] U. Sauer, “Metabolic networks in motion: <sup>13</sup>C-based flux analysis,” *Mol Syst Biol*, vol. 2, pp. 1–10, 2006, doi: 10.1038/msb4100109.

[35] K. D. Allen, L. M. Thoma, and Y. M. Golightly, “Epidemiology of osteoarthritis,” *Osteoarthritis Cartilage*, vol. 30, no. 2, pp. 184–195, 2022, doi: 10.1016/j.joca.2021.04.020.

[36] X. Ji and H. Zhang, “Current Strategies for the Treatment of Early Stage Osteoarthritis,” *Front Mech Eng*, vol. 5, p. 480160, Sep. 2019, doi: 10.3389/FMECH.2019.00057/BIBTEX.

[37] J. W. J. Bijlsma, F. Berenbaum, and F. P. J. G. Lafeber, “Osteoarthritis: an update with relevance for clinical practice,” *The Lancet*, vol. 377, no. 9783, pp. 2115–2126, Jun. 2011, doi: 10.1016/S0140-6736(11)60243-2.

[38] M. Lotz *et al.*, “Value of biomarkers in osteoarthritis: current status and perspectives,” *Ann Rheum Dis*, vol. 72, no. 11, p. 1756, 2013, doi: 10.1136/ANNRHEUMDIS-2013-203726.

[39] S. Kundu *et al.*, “Enabling early detection of osteoarthritis from presymptomatic cartilage texture maps via transport-based learning,” *Proc Natl Acad Sci U S A*, vol. 117, no. 40, pp.

24709–24719, Oct. 2020, doi:

10.1073/PNAS.1917405117/SUPPL\_FILE/PNAS.1917405117.SAPP.PDF.

[40] D. T. Felson and R. Hodgson, “Identifying and Treating Pre-Clinical and Early Osteoarthritis,” *Rheum Dis Clin North Am*, vol. 40, no. 4, p. 699, Nov. 2014, doi: 10.1016/J.RDC.2014.07.012.

[41] E. G. L. Bywaters and M. MacKinnon, “The metabolism of joint tissues,” *J Pathol Bacteriol*, vol. 44, no. 1, pp. 247–268, Jan. 1937, doi: 10.1002/PATH.1700440119.

[42] J. W. Kim and C. V. Dang, “Cancer’s Molecular Sweet Tooth and the Warburg Effect,” *Cancer Res*, vol. 66, no. 18, pp. 8927–8930, Sep. 2006, doi: 10.1158/0008-5472.CAN-06-1501.

[43] P. C. Gomez-Contreras, P. N. Kluz, M. R. Hines, and M. C. Coleman, “Intersections Between Mitochondrial Metabolism and Redox Biology Mediate Posttraumatic Osteoarthritis,” *Curr Rheumatol Rep*, vol. 23, no. 5, 2021, doi: 10.1007/s11926-021-00994-z.

[44] N. K. Goto and L. E. Kay, “New developments in isotope labeling strategies for protein solution NMR spectroscopy,” *Curr Opin Struct Biol*, vol. 10, no. 5, pp. 585–592, Oct. 2000, doi: 10.1016/S0959-440X(00)00135-4.

[45] M. R. Antoniewicz, “A guide to <sup>13</sup>C metabolic flux analysis for the cancer biologist,” *Experimental & Molecular Medicine* 2018 50:4, vol. 50, no. 4, pp. 1–13, Apr. 2018, doi: 10.1038/s12276-018-0060-y.

[46] P. Firdous, T. Hassan, S. Farooq, and K. Nissar, “Applications of proteomics in cancer diagnosis,” *Proteomics*, pp. 257–285, Jan. 2023, doi: 10.1016/B978-0-323-95072-5.00014-6.

[47] P. P. Brahmachary, H. D. Welhaven, and R. K. June, “Metabolomic Profiling to Understand Chondrocyte Metabolism,” *Methods in Molecular Biology*, vol. 2598, pp. 141–156, 2023, doi: 10.1007/978-1-0716-2839-3\_11/FIGURES/5.

[48] T. Pluskal, S. Castillo, A. Villar-Briones, and M. Orešič, “MZmine 2: modular framework for processing, visualizing, and analyzing mass spectrometry-based molecular profile data,” *BMC Bioinformatics*, vol. 11, Jul. 2010, doi: 10.1186/1471-2105-11-395.

- [49] R. Nilsson, “Validity of natural isotope abundance correction for metabolic flux analysis,” 2020, doi: 10.1101/2020.05.04.075838.
- [50] Z. Ser, X. Liu, N. N. Tang, and J. W. Locasale, “Extraction parameters for metabolomics from cell extracts,” *Anal Biochem*, vol. 475, p. 22, Apr. 2015, doi: 10.1016/J.AB.2015.01.003.
- [51] C. Andresen *et al.*, “Comparison of extraction methods for intracellular metabolomics of human tissues,” *Front Mol Biosci*, vol. 9, Aug. 2022, doi: 10.3389/FMOLB.2022.932261/FULL.
- [52] K. D. Allen, L. M. Thoma, and Y. M. Golightly, “Epidemiology of osteoarthritis,” *Osteoarthritis Cartilage*, vol. 30, no. 2, pp. 184–195, 2022, doi: 10.1016/j.joca.2021.04.020.
- [53] X. Ji and H. Zhang, “Current Strategies for the Treatment of Early Stage Osteoarthritis,” *Front Mech Eng*, vol. 5, p. 480160, Sep. 2019, doi: 10.3389/FMECH.2019.00057/BIBTEX.
- [54] J. W. J. Bijlsma, F. Berenbaum, and F. P. J. G. Lafeber, “Osteoarthritis: an update with relevance for clinical practice,” *The Lancet*, vol. 377, no. 9783, pp. 2115–2126, Jun. 2011, doi: 10.1016/S0140-6736(11)60243-2.
- [55] M. Lotz *et al.*, “Value of biomarkers in osteoarthritis: current status and perspectives,” *Ann Rheum Dis*, vol. 72, no. 11, p. 1756, 2013, doi: 10.1136/ANNRHEUMDIS-2013-203726.
- [56] S. Kundu *et al.*, “Enabling early detection of osteoarthritis from presymptomatic cartilage texture maps via transport-based learning,” *Proc Natl Acad Sci U S A*, vol. 117, no. 40, pp. 24709–24719, Oct. 2020, doi: 10.1073/PNAS.1917405117/SUPPL\_FILE/PNAS.1917405117.SAPP.PDF.
- [57] D. T. Felson and R. Hodgson, “Identifying and Treating Pre-Clinical and Early Osteoarthritis,” *Rheum Dis Clin North Am*, vol. 40, no. 4, p. 699, Nov. 2014, doi: 10.1016/J.RDC.2014.07.012.
- [58] E. G. L. Bywaters and M. MacKinnon, “The metabolism of joint tissues,” *J Pathol Bacteriol*, vol. 44, no. 1, pp. 247–268, Jan. 1937, doi: 10.1002/PATH.1700440119.
- [59] J. W. Kim and C. V. Dang, “Cancer’s Molecular Sweet Tooth and the Warburg Effect,” *Cancer Res*, vol. 66, no. 18, pp. 8927–8930, Sep. 2006, doi: 10.1158/0008-5472.CAN-06-1501.

- [60] H. K. Heywood, M. M. Knight, and D. A. Lee, “Both superficial and deep zone articular chondrocyte subpopulations exhibit the crabtree effect but have different basal oxygen consumption rates,” *J Cell Physiol*, vol. 223, no. 3, pp. 630–639, 2010, doi: 10.1002/jcp.22061.
- [61] P. C. Gomez-Contreras, P. N. Kluz, M. R. Hines, and M. C. Coleman, “Intersections Between Mitochondrial Metabolism and Redox Biology Mediate Posttraumatic Osteoarthritis,” *Curr Rheumatol Rep*, vol. 23, no. 5, 2021, doi: 10.1007/s11926-021-00994-z.
- [62] N. K. Goto and L. E. Kay, “New developments in isotope labeling strategies for protein solution NMR spectroscopy,” *Curr Opin Struct Biol*, vol. 10, no. 5, pp. 585–592, Oct. 2000, doi: 10.1016/S0959-440X(00)00135-4.
- [63] M. R. Antoniewicz, “A guide to <sup>13</sup>C metabolic flux analysis for the cancer biologist,” *Experimental & Molecular Medicine* 2018 50:4, vol. 50, no. 4, pp. 1–13, Apr. 2018, doi: 10.1038/s12276-018-0060-y.
- [64] P. Firdous, T. Hassan, S. Farooq, and K. Nissar, “Applications of proteomics in cancer diagnosis,” *Proteomics*, pp. 257–285, Jan. 2023, doi: 10.1016/B978-0-323-95072-5.00014-6.
- [65] P. P. Brahmachary, H. D. Welhaven, and R. K. June, “Metabolomic Profiling to Understand Chondrocyte Metabolism,” *Methods in Molecular Biology*, vol. 2598, pp. 141–156, 2023, doi: 10.1007/978-1-0716-2839-3\_11/FIGURES/5.
- [66] T. Pluskal, S. Castillo, A. Villar-Briones, and M. Orešič, “MZmine 2: modular framework for processing, visualizing, and analyzing mass spectrometry-based molecular profile data,” *BMC Bioinformatics*, vol. 11, Jul. 2010, doi: 10.1186/1471-2105-11-395.
- [67] C. Jang, L. Chen, and J. D. Rabinowitz, “Metabolomics and Isotope Tracing,” *Cell*, vol. 173, no. 4, pp. 822–837, 2018, doi: 10.1016/j.cell.2018.03.055.
- [68] R. Nilsson, “Validity of natural isotope abundance correction for metabolic flux analysis,” 2020, doi: 10.1101/2020.05.04.075838.
- [69] C. Cook, R. Pietrobon, and E. Hegedus, “Osteoarthritis and the impact on quality of life health indicators,” *Rheumatol Int*, vol. 27, no. 4, pp. 315–321, Feb. 2007, doi: 10.1007/S00296-006-0269-2/TABLES/4.

[70] R. F. Loeser, S. R. Goldring, C. R. Scanzello, and M. B. Goldring, "Osteoarthritis: A disease of the joint as an organ," *Arthritis Rheum*, vol. 64, no. 6, pp. 1697–1707, Jun. 2012, doi: 10.1002/art.34453.

[71] A. J. Sophia Fox, A. Bedi, and S. A. Rodeo, "The basic science of articular cartilage: Structure, composition, and function," *Sports Health*, vol. 1, no. 6, pp. 461–468, 2009, doi: 10.1177/1941738109350438.

[72] S. Glyn-Jones *et al.*, "Osteoarthritis," *The Lancet*, vol. 386, no. 9991, pp. 376–387, 2015, doi: 10.1016/S0140-6736(14)60802-3.

[73] Z. Zhao, Y. Li, M. Wang, S. Zhao, Z. Zhao, and J. Fang, "Mechanotransduction pathways in the regulation of cartilage chondrocyte homeostasis," *J Cell Mol Med*, vol. 24, no. 10, pp. 5408–5419, May 2020, doi: 10.1111/JCMM.15204.

[74] D. R. Haudenschild, J. Chen, N. Pang, M. K. Lotz, and D. D. D’Lima, "Rho kinase-dependent activation of SOX9 in chondrocytes," *Arthritis Rheum*, vol. 62, no. 1, pp. 191–200, Jan. 2010, doi: 10.1002/ART.25051.

[75] J. D. Humphrey, E. R. Dufresne, and M. A. Schwartz, "Mechanotransduction and extracellular matrix homeostasis," *Nat Rev Mol Cell Biol*, vol. 15, no. 12, p. 802, Dec. 2014, doi: 10.1038/NRM3896.

[76] W. Jiang, H. Liu, R. Wan, Y. Wu, Z. Shi, and W. Huang, "Mechanisms linking mitochondrial mechanotransduction and chondrocyte biology in the pathogenesis of osteoarthritis," *Ageing Res Rev*, vol. 67, May 2021, doi: 10.1016/J.ARR.2021.101315.

[77] W. Lee *et al.*, "Inflammatory signaling sensitizes Piezo1 mechanotransduction in articular chondrocytes as a pathogenic feed-forward mechanism in osteoarthritis," *Proc Natl Acad Sci U S A*, vol. 118, no. 13, Mar. 2021, doi: 10.1073/PNAS.2001611118/-/DCSUPPLEMENTAL.

[78] N. A. Zelenski *et al.*, "Type VI Collagen Regulates Pericellular Matrix Properties, Chondrocyte Swelling, and Mechanotransduction in Mouse Articular Cartilage," *Arthritis Rheumatol*, vol. 67, no. 5, pp. 1286–1294, May 2015, doi: 10.1002/ART.39034.

- [79] D. L. Zignego, J. K. Hilmer, and R. K. June, "Mechanotransduction in primary human osteoarthritic chondrocytes is mediated by metabolism of energy, lipids, and amino acids," *J Biomech*, vol. 48, no. 16, pp. 4253–4261, 2015, doi: 10.1016/j.jbiomech.2015.10.038.
- [80] D. Salinas, C. A. Minor, R. P. Carlson, C. N. McCutchen, B. M. Mumey, and R. K. June, "Combining targeted metabolomic data with a model of glucose metabolism: Toward progress in chondrocyte mechanotransduction," *PLoS One*, vol. 12, no. 1, pp. 1–16, 2017, doi: 10.1371/journal.pone.0168326.
- [81] D. Salinas, B. M. Mumey, and R. K. June, "Physiological dynamic compression regulates central energy metabolism in primary human chondrocytes," *Biomech Model Mechanobiol*, vol. 18, no. 1, pp. 69–77, 2019, doi: 10.1007/s10237-018-1068-x.
- [82] P. Romero, J. Wagg, M. L. Green, D. Kaiser, M. Krummenacker, and P. D. Karp, "Computational prediction of human metabolic pathways from the complete human genome.," *Genome Biol*, vol. 6, no. 1, pp. 1–17, Dec. 2005, doi: 10.1186/GB-2004-6-1-R2/TABLES/7.
- [83] S. Klamt, J. Saez-Rodriguez, and E. D. Gilles, "Structural and functional analysis of cellular networks with CellNetAnalyzer," *BMC Syst Biol*, vol. 1, no. 1, pp. 1–13, Jan. 2007, doi: 10.1186/1752-0509-1-2/FIGURES/6.
- [16] A. E. Beck, K. A. Hunt, and R. P. Carlson, "Measuring Cellular Biomass Composition for Computational Biology Applications," *Processes 2018, Vol. 6, Page 38*, vol. 6, no. 5, p. 38, Apr. 2018, doi: 10.3390/PR6050038.
- [17] P. P. Brahmachary, H. D. Welhaven, and R. K. June, "Metabolomic Profiling to Understand Chondrocyte Metabolism," *Methods in Molecular Biology*, vol. 2598, pp. 141–156, 2023, doi: 10.1007/978-1-0716-2839-3\_11/FIGURES/5.
- [18] A. A. Jutila, D. L. Zignego, W. J. Schell, and R. K. June, "Encapsulation of Chondrocytes in High-Stiffness Agarose Microenvironments for In Vitro Modeling of Osteoarthritis Mechanotransduction," *Ann Biomed Eng*, vol. 43, no. 5, pp. 1132–1144, May 2015, doi: 10.1007/S10439-014-1183-5/FIGURES/6.
- [19] D. L. Zignego, A. A. Jutila, M. K. Gelbke, D. M. Gannon, and R. K. June, "The mechanical microenvironment of high concentration agarose for applying deformation to primary chondrocytes," *J Biomech*, vol. 47, no. 9, pp. 2143–2148, Jun. 2014, doi: 10.1016/J.JBIOMECH.2013.10.051.

- [20] A. H. Emwas, K. Szczepski, I. Al-Younis, J. I. Lachowicz, and M. Jaremko, "Fluxomics - New Metabolomics Approaches to Monitor Metabolic Pathways," *Front Pharmacol*, vol. 13, p. 805782, Mar. 2022, doi: 10.3389/FPHAR.2022.805782/BIBTEX.
- [21] C. Jang, L. Chen, and J. D. Rabinowitz, "Metabolomics and Isotope Tracing," *Cell*, vol. 173, no. 4, pp. 822–837, 2018, doi: 10.1016/j.cell.2018.03.055.
- [22] Z. Ser, X. Liu, N. N. Tang, and J. W. Locasale, "Extraction parameters for metabolomics from cell extracts," *Anal Biochem*, vol. 475, p. 22, Apr. 2015, doi: 10.1016/J.AB.2015.01.003.
- [23] C. Andresen *et al.*, "Comparison of extraction methods for intracellular metabolomics of human tissues," *Front Mol Biosci*, vol. 9, Aug. 2022, doi: 10.3389/FMOLB.2022.932261/FULL.

APPENDICES

APPENDIX A

SUPPLEMENTAL INFORMATION FOR CHAPTER 2

Table A.1. Library for targeted metabolites and their isotopes.

<b>ID</b>	<b>m/z</b>	<b>RT</b>
Pyruvate_H	87.0088	1.162
Pyruvate_H+1	88.0122	1.162
Pyruvate_H+2	89.0132	1.162
Pyruvate_H+3	90.0164	1.162
Pyruvate_H+4	91.0177	1.162
Pyruvate_H+5	92.0207	1.162
Pyruvate_Cl	122.9854	1.162
Pyruvate_Cl+1	123.9889	1.162
Pyruvate_Cl+2	124.9826	1.162
Pyruvate_Cl+3	125.9861	1.162
Pyruvate_Cl+4	126.987	1.162
Pyruvate_Cl+5	127.9902	1.162
Pyruvate_Cl+6	128.9914	1.162
Pyruvate_Cl+7	129.9945	1.162
Lactate_H	89.0244	1.162
Lactate_H+1	90.0279	1.162
Lactate_H+2	91.0288	1.162
Lactate_H+3	92.0321	1.162
Lactate_H+4	93.0333	1.162
Lactate_H+5	94.0364	1.162
Lactate_Cl	125.0011	1.162
Lactate_Cl+1	126.0045	1.162
Lactate_Cl+2	126.9983	1.162
Lactate_Cl+3	128.0017	1.162
Lactate_Cl+4	129.0026	1.162
Lactate_Cl+5	130.0059	1.162
Lactate_Cl+6	131.0071	1.162
Lactate_Cl+7	132.0102	1.162
Oxaloacetate_H	130.9986	1.113
Oxaloacetate_H+1	132.002	1.113
Oxaloacetate_H+2	133.003	1.113
Oxaloacetate_H+3	134.0063	1.113
Oxaloacetate_H+4	135.0075	1.113
Oxaloacetate_H+5	136.0106	1.113
Oxaloacetate_Cl	166.9753	1.113
Oxaloacetate_Cl+1	167.9787	1.113
Oxaloacetate_Cl+2	168.9726	1.113

Oxaloacetate_Cl+3	169.976	1.113
Oxaloacetate_Cl+4	170.9769	1.113
Oxaloacetate_Cl+5	171.9801	1.113
Oxaloacetate_Cl+6	172.9813	1.113
Oxaloacetate_Cl+7	173.9844	1.113
Malate_H	133.0142	1.121
Malate_H+1	134.0177	1.121
Malate_H+2	135.0187	1.121
Malate_H+3	136.022	1.121
Malate_H+4	137.0232	1.121
Malate_H+5	138.0262	1.121
Malate_Cl	168.9909	1.121
Malate_Cl+1	169.9944	1.121
Malate_Cl+2	170.9882	1.121
Malate_Cl+3	171.9916	1.121
Malate_Cl+4	172.9925	1.121
Malate_Cl+5	173.9958	1.121
Malate_Cl+6	174.997	1.121
Malate_Cl+7	176	1.121
Alpha-ketoglutarate_H	145.0142	1.104
Alpha-ketoglutarate_H+1	146.0177	1.104
Alpha-ketoglutarate_H+2	147.0188	1.104
Alpha-ketoglutarate_H+3	148.022	1.104
Alpha-ketoglutarate_H+4	149.0234	1.104
Alpha-ketoglutarate_H+5	150.0263	1.104
Alpha-ketoglutarate_Cl	180.9909	1.104
Alpha-ketoglutarate_Cl+1	181.9943	1.104
Alpha-ketoglutarate_Cl+2	182.9882	1.104
Alpha-ketoglutarate_Cl+3	183.9916	1.104
Alpha-ketoglutarate_Cl+4	184.9926	1.104
Alpha-ketoglutarate_Cl+5	185.9958	1.104
Alpha-ketoglutarate_Cl+6	186.9972	1.104
Alpha-ketoglutarate_Cl+7	188.0001	1.104
Glutamate_H	147.0532	1.179
Glutamate_H+1	148.0562	1.179
Glutamate_H+2	149.0577	1.179
Glutamate_H+3	150.0605	1.179
Glutamate_H+4	151.0622	1.179
Glutamate_H+5	152.0648	1.179

Glutamate_Cl	182.0226	1.179
Glutamate_Cl+1	183.0256	1.179
Glutamate_Cl+2	184.0198	1.179
Glutamate_Cl+3	185.0228	1.179
Glutamate_Cl+4	186.0242	1.179
Glutamate_Cl+5	187.027	1.179
Glutamate_Cl+6	188.0287	1.179
Glutamate_Cl+7	189.0313	1.179
Phosphoenolpyruvate_H	166.9751	1.088
Phosphoenolpyruvate_H+1	167.9785	1.088
Phosphoenolpyruvate_H+2	168.9794	1.088
Phosphoenolpyruvate_H+3	169.9828	1.088
Phosphoenolpyruvate_H+4	170.9838	1.088
Phosphoenolpyruvate_H+5	171.9871	1.088
Phosphoenolpyruvate_Cl	202.9518	1.088
Phosphoenolpyruvate_Cl+1	203.9552	1.088
Phosphoenolpyruvate_Cl+2	204.9491	1.088
Phosphoenolpyruvate_Cl+3	205.9525	1.088
Phosphoenolpyruvate_Cl+4	206.9533	1.088
Phosphoenolpyruvate_Cl+5	207.9567	1.088
Phosphoenolpyruvate_Cl+6	208.9576	1.088
Phosphoenolpyruvate_Cl+7	209.9609	1.088
Glyceraldehyde 3-phosphate_H	168.9907	0
Glyceraldehyde 3-phosphate_H+1	169.9942	0
Glyceraldehyde 3-phosphate_H+2	170.9951	0
Glyceraldehyde 3-phosphate_H+3	171.9985	0
Glyceraldehyde 3-phosphate_H+4	172.9995	0
Glyceraldehyde 3-phosphate_H+5	174.0027	0
Glyceraldehyde 3-phosphate_Cl	204.9674	0
Glyceraldehyde 3-phosphate_Cl+1	205.9709	0
Glyceraldehyde 3-phosphate_Cl+2	206.9648	0
Glyceraldehyde 3-phosphate_Cl+3	207.9682	0
Glyceraldehyde 3-phosphate_Cl+4	208.9689	0
Glyceraldehyde 3-phosphate_Cl+5	209.9723	0
Glyceraldehyde 3-phosphate_Cl+6	210.9733	0
Glyceraldehyde 3-phosphate_Cl+7	211.9765	0
Glucose_H	179.0561	0
Glucose_H+1	180.0595	0
Glucose_H+2	181.0607	0

Glucose_H+3	182.0639	0
Glucose_H+4	183.0654	0
Glucose_H+5	184.0683	0
Glucose_Cl	215.0328	0
Glucose_Cl+1	216.0362	0
Glucose_Cl+2	217.0302	0
Glucose_Cl+3	218.0336	0
Glucose_Cl+4	219.0346	0
Glucose_Cl+5	220.0377	0
Glucose_Cl+6	221.0392	0
Glucose_Cl+7	222.0421	0
Citrate_H	191.0197	1.113
Citrate_H+1	192.0231	1.113
Citrate_H+2	193.0243	1.113
Citrate_H+3	194.0275	1.113
Citrate_H+4	195.0289	1.113
Citrate_H+5	196.0318	1.113
Citrate_Cl	226.9964	1.113
Citrate_Cl+1	227.9998	1.113
Citrate_Cl+2	228.9938	1.113
Citrate_Cl+3	229.9972	1.113
Citrate_Cl+4	230.9982	1.113
Citrate_Cl+5	232.0014	1.113
Citrate_Cl+6	233.0027	1.113
Citrate_Cl+7	234.0056	1.113
Succinate_H	117.0193	1.137
Succinate_H+1	118.0228	1.137
Succinate_H+2	119.0238	1.137
Succinate_H+3	120.027	1.137
Succinate_H+4	121.0284	1.137
Succinate_H+5	122.0314	1.137
Succinate_Cl	152.996	1.137
Succinate_Cl+1	153.9994	1.137
Succinate_Cl+2	154.9933	1.137
Succinate_Cl+3	155.9967	1.137
Succinate_Cl+4	156.9976	1.137
Succinate_Cl+5	158.0008	1.137
Succinate_Cl+6	159.0021	1.137
Succinate_Cl+7	160.0051	1.137

Fructose-6-Phosphate_H	259.0224	0
Fructose-6-Phosphate_H+1	260.0259	0
Fructose-6-Phosphate_H+2	261.027	0
Fructose-6-Phosphate_H+3	262.0302	0
Fructose-6-Phosphate_H+4	263.0315	0
Fructose-6-Phosphate_H+5	264.0345	0
Fructose-6-Phosphate_Cl	294.9991	0
Fructose-6-Phosphate_Cl+1	296.0026	0
Fructose-6-Phosphate_Cl+2	296.9966	0
Fructose-6-Phosphate_Cl+3	298	0
Fructose-6-Phosphate_Cl+4	299.0009	0
Fructose-6-Phosphate_Cl+5	300.0041	0
Fructose-6-Phosphate_Cl+6	301.0053	0
Fructose-6-Phosphate_Cl+7	302.0084	0
6-P-gluconate_H	275.0174	1.154
6-P-gluconate_H+1	276.0208	1.154
6-P-gluconate_H+2	277.0219	1.154
6-P-gluconate_H+3	278.0251	1.154
6-P-gluconate_H+4	279.0264	1.154
6-P-gluconate_H+5	280.0294	1.154
6-P-gluconate_Cl	310.994	1.154
6-P-gluconate_Cl+1	311.9975	1.154
6-P-gluconate_Cl+2	312.9916	1.154
6-P-gluconate_Cl+3	313.995	1.154
6-P-gluconate_Cl+4	314.9958	1.154
6-P-gluconate_Cl+5	315.9991	1.154
6-P-gluconate_Cl+6	317.0002	1.154
6-P-gluconate_Cl+7	318.0033	1.154
Sedoheptulose-7-phosphate_H	289.033	1.104
Sedoheptulose-7-phosphate_H+1	290.0365	1.104
Sedoheptulose-7-phosphate_H+2	291.0376	1.104
Sedoheptulose-7-phosphate_H+3	292.0408	1.104
Sedoheptulose-7-phosphate_H+4	293.0421	1.104
Sedoheptulose-7-phosphate_H+5	294.0451	1.104
Sedoheptulose-7-phosphate_Cl	325.0097	1.104
Sedoheptulose-7-phosphate_Cl+1	326.0131	1.104
Sedoheptulose-7-phosphate_Cl+2	327.0072	1.104
Sedoheptulose-7-phosphate_Cl+3	328.0106	1.104
Sedoheptulose-7-phosphate_Cl+4	329.0116	1.104

Sedoheptulose-7-phosphate_Cl+5	330.0147	1.104
Sedoheptulose-7-phosphate_Cl+6	331.016	1.104
Sedoheptulose-7-phosphate_Cl+7	332.019	1.104
GTP_H	521.9834	0
GTP_H+1	522.9859	0
GTP_H+2	523.9878	0
GTP_H+3	524.9902	0
GTP_H+4	525.9922	0
GTP_H+5	526.9945	0
GTP_Cl	557.9601	0
GTP_Cl+1	558.9626	0
GTP_Cl+2	559.9579	0
GTP_Cl+3	560.9603	0
GTP_Cl+4	561.9619	0
GTP_Cl+5	562.9643	0
GTP_Cl+6	563.9662	0
GTP_Cl+7	564.9685	0
NADH_H	664.1175	1.154
NADH_H+1	665.1203	1.154
NADH_H+2	666.1224	1.154
NADH_H+3	667.1249	1.154
NADH_H+4	668.1271	1.154
NADH_H+5	669.1294	1.154
NADH_H+6	670.1316	1.154
NADH_Cl	700.0942	1.154
NADH_Cl+1	701.097	1.154
NADH_Cl+2	702.0925	1.154
NADH_Cl+3	703.0948	1.154
NADH_Cl+4	704.0967	1.154
NADH_Cl+5	705.099	1.154
NADH_Cl+6	706.1011	1.154
NADH_Cl+7	707.1034	1.154
NADH_Cl+8	708.1056	1.154
NADPH_H	743.076	0
NADPH_H+1	744.0788	0
NADPH_H+2	745.0809	0
NADPH_H+3	746.0833	0
NADPH_H+4	747.0855	0
NADPH_H+5	748.0878	0

NADPH_H+6	749.09	0
NADPH_Cl	779.0527	0
NADPH_Cl+1	780.0555	0
NADPH_Cl+2	781.0511	0
NADPH_Cl+3	782.0535	0
NADPH_Cl+4	783.0552	0
NADPH_Cl+5	784.0575	0
NADPH_Cl+6	785.0596	0
NADPH_Cl+7	786.0618	0
NADPH_Cl+8	787.064	0
HS-CoA_H	766.1079	1.054
HS-CoA_H+1	767.1106	1.054
HS-CoA_H+2	768.1092	1.054
HS-CoA_H+3	769.1109	1.054
HS-CoA_H+4	770.1118	1.054
HS-CoA_H+5	771.1136	1.054
HS-CoA_H+6	772.1151	1.054
HS-CoA_Cl	802.0846	1.054
HS-CoA_Cl+1	803.0873	1.054
HS-CoA_Cl+2	804.0828	1.054
HS-CoA_Cl+3	805.085	1.054
HS-CoA_Cl+4	806.0836	1.054
HS-CoA_Cl+5	807.0851	1.054
HS-CoA_Cl+6	808.0859	1.054
HS-CoA_Cl+7	809.0876	1.054
HS-CoA_Cl+8	810.0891	1.054
Acetyl-CoA_H	808.1185	1.054
Acetyl-CoA_H+1	809.1213	1.054
Acetyl-CoA_H+2	810.12	1.054
Acetyl-CoA_H+3	811.1217	1.054
Acetyl-CoA_H+4	812.1227	1.054
Acetyl-CoA_H+5	813.1244	1.054
Acetyl-CoA_H+6	814.126	1.054
Acetyl-CoA_Cl	844.0952	1.054
Acetyl-CoA_Cl+1	845.0979	1.054
Acetyl-CoA_Cl+2	846.0935	1.054
Acetyl-CoA_Cl+3	847.0957	1.054
Acetyl-CoA_Cl+4	848.0945	1.054
Acetyl-CoA_Cl+5	849.096	1.054

Acetyl-CoA_Cl+6	850.0969	1.054
Acetyl-CoA_Cl+7	851.0985	1.054
Acetyl-CoA_Cl+8	852.1001	1.054
Succinyl-CoA_H	866.124	0
Succinyl-CoA_H+1	867.1268	0
Succinyl-CoA_H+2	868.1259	0
Succinyl-CoA_H+3	869.1275	0
Succinyl-CoA_H+4	870.1285	0
Succinyl-CoA_H+5	871.1303	0
Succinyl-CoA_H+6	872.1319	0
Succinyl-CoA_Cl	902.1007	0
Succinyl-CoA_Cl+1	903.1035	0
Succinyl-CoA_Cl+2	904.0991	0
Succinyl-CoA_Cl+3	905.1014	0
Succinyl-CoA_Cl+4	906.1004	0
Succinyl-CoA_Cl+5	907.1018	0
Succinyl-CoA_Cl+6	908.1028	0
Succinyl-CoA_Cl+7	909.1044	0
Succinyl-CoA_Cl+8	910.1059	0
Glutamine_H	145.0619	0
Glutamine_H+1	146.0646	0
Glutamine_H+2	147.0663	0
Glutamine_H+3	148.0688	0
Glutamine_H+4	149.0708	0
Glutamine_H+5	150.0731	0
Glutamine_Cl	181.0385	0
Glutamine_Cl+1	182.0412	0
Glutamine_Cl+2	183.0358	0
Glutamine_Cl+3	184.0384	0
Glutamine_Cl+4	185.0401	0
Glutamine_Cl+5	186.0426	0
Glutamine_Cl+6	187.0446	0
Glutamine_Cl+7	188.0469	0
Fumarate_H	115.0037	0
Fumarate_H+1	116.0071	0
Fumarate_H+2	117.0082	0
Fumarate_H+3	118.0114	0
Fumarate_H+4	119.0127	0
Fumarate_H+5	120.0157	0

Fumarate_Cl	150.9804	0
Fumarate_Cl+1	151.9838	0
Fumarate_Cl+2	152.9776	0
Fumarate_Cl+3	153.981	0
Fumarate_Cl+4	154.982	0
Fumarate_Cl+5	155.9852	0
Fumarate_Cl+6	156.9865	0
Fumarate_Cl+7	157.9895	0

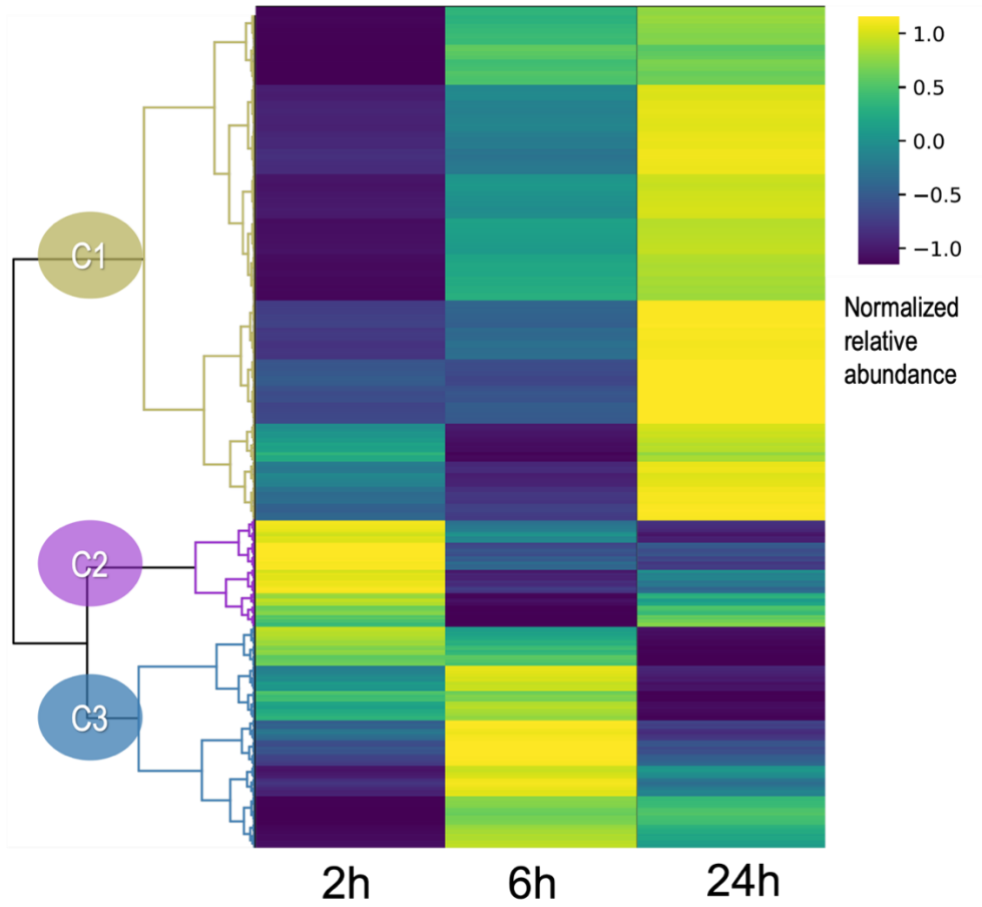


Figure A.1. Clustering of median metabolite intensities finds 3 distinct groups that vary between timepoints.

APPENDIX B

SUPPLEMENTAL INFORMATION FOR CHAPTER 3

## Appendix B.1

## BASIC TOPOLOGICAL NETWORK PROPERTIES:

-----

## EXTERNAL METABOLITES: 38

The following metabolites are marked as external (unbalanced) metabolites (38) :

ammonium\_ext

ATPm

CO2\_ext

collagen-VI\_ext

collagen-II\_ext

D-glucose\_ext

di-P\_ext

glycine\_ext

GTPm

H\_ext

H2O\_ext

HCO3\_ext

l-alanine\_ext

l-arginine\_ext

l-asparagine\_ext

l-aspartate\_ext

l-cysteine\_ext

l-glutamate\_ext

l-glutamine\_ext

l-histidine\_ext

l-isoleucine\_ext

l-leucine\_ext

l-lysine\_ext

l-methionine\_ext

l-phenylalanine\_ext

l-proline\_ext

l-serine\_ext

l-threonine\_ext

l-tryptophan\_ext

l-tyrosine\_ext

l-valine\_ext

lactate\_ext

O2\_ext

P\_ext

sodium\_ext

urea\_ext

pyruvate\_ext

formate\_ext

These metabolites are not considered in the following statistics.

INTERNAL METABOLITES WHICH CAN ONLY BE PRODUCED (SINKS) OR ONLY BE  
CONSUMED (SOURCES): 0

REACTIONS WITH EMPTY STOICHIOMETRY: 0

SIMPLE UPTAKE OF ONE METABOLITE: 3

T-O2 (species: O2)

T-Glucose-1 (species: D-glucose)

T-Glutamine-1 (species: l-glutamine)

SIMPLE EXCRETION OF ONE METABOLITE: 13

T-formate (species: formate)

T-Urea (species: urea)

cost\_alanine (species: l-alanine)

cost\_arginine (species: l-arginine)

cost\_asparagine (species: l-asparagine)

cost\_aspartate (species: l-aspartate)

cost\_cysteine (species: l-cysteine)

cost\_glutamate (species: l-glutamate)

cost\_glutamine (species: l-glutamine)

cost\_glycine (species: glycine)

cost\_proline (species: l-proline)

cost\_serine (species: l-serine)

cost\_tyrosine (species: l-tyrosine)

#### SIMPLE UPTAKE/EXCRETION OF ONE METABOLITE (REVERSIBLE): 7

T-Proton (species: H)

T-H<sub>2</sub>O (species: H<sub>2</sub>O)

T-CO<sub>2</sub> (species: CO<sub>2</sub>)

T-HCO<sub>3</sub> (species: HCO<sub>3</sub>)

T-Collagen-VI (species: collagen-VI)

T-Collagen-II (species: collagen-II)

T-Sodium (species: sodium)

Size of original network: 114 internal metabolites, 140 reactions

Size of compressed network: 53 internal metabolites, 91 reactions

#### COUPLED REACTIONS (ENZYME SUBSETS)

Found enzyme subset (irreversible): {G-3, G-4, G-5}

Found enzyme subset (reversible): {G-6, G-7}

Found enzyme subset (irreversible): {Glutaminase, ammonia\_spontaneous}

Found enzyme subset (reversible): {G-8, G-9}

Found enzyme subset (reversible): {PYR-2, T-Lactate}

Found enzyme subset (irreversible): {TCA-2, TCA-3}

Found enzyme subset (irreversible): {ETC-3, ETC-4}

Found enzyme subset (irreversible): {PPP-1, PPP-2, PPP-3, PPP-4, PPP-5, PPP-6, PPP-6.1, PPP-7}

Found enzyme subset (irreversible): {AA-Cys-1, AA-Cys-2, AA-Cys-3, AA-Cys-4, AA-Cys-5, 2-Oxob-Deg-2, 2-Oxob-Deg-3, 2-Oxob-Deg-4, 2-Oxob-Deg-5, Ade-1, Sarcosine}

Found enzyme subset (irreversible): {T-Collagen-II, CollagenII}

Found enzyme subset (irreversible): {T-Collagen-VI, CollagenVI}

Found enzyme subset (irreversible): {AA-Gly-1, Glyoxy-Bal}

Found enzyme subset (irreversible): {AA-Glu-1, T-Urea}

Found enzyme subset (irreversible): {AA-Tyr-1, AA-Tyr-2, AA-Tyr-3}

Found enzyme subset (irreversible): {AA-Arg-1, AA-Arg-2, AA-Arg-3, AA-Arg-4}

Found enzyme subset (irreversible): {AA-Pro-1, AA-Pro-2}

Found enzyme subset (irreversible): {AA-Ser-1, AA-Ser-2, AA-Ser-3}

Found enzyme subset (irreversible): {DiP, ATP-AMP-ADP}

Found enzyme subset (irreversible): {Gamma-Glutamyl-1, Gamma-Glutamyl-5, Gamma-Glutamyl-6}

Found enzyme subset (irreversible): {Gamma-Glutamyl-2, Gamma-Glutamyl-3, Gamma-Glutamyl-4}

Found enzyme subset (irreversible): {THF-1, THF-2, THF-3, T-formate}

Found enzyme subset (irreversible): {GABA-1, GABA-2, GABA-3}

Result: 22 enzyme subsets found (containing altogether 69 reactions)

#### ISOZYMES / PARALLEL REACTIONS

Found group of parallel reactions: {GTP-GDP, T-GTP}

1 groups of parallel reactions found (containing altogether 2 reactions)

Size of original network: 114 internal metabolites, 140 reactions

Size of compressed network: 22 internal metabolites, 60 reactions

STOICHIOMETRIC MATRIX (without external metabolites):

114 internal (balanced) metabolites (rows)

140 reactions (columns), thereof 42 reversible

Rank of stoichiometric matrix: 102

--> There are 12 independent conservation relation(s)!

--> You may compute elementary conservation relations (see menu)

Degrees of freedom: 38

Smallest (absolute) non-zero-value: 0.08

Largest (absolute) value: 297

Network can be compressed to (isozymes not considered):

22 metabolites

60 reactions (thereof 12 reversible)

0 reaction rates are currently defined

## Appendix B.2

```

%% Chondrocyte model, supplemental file for analysis in CobraToolbox
% Analysis begins with confirmation of basic model properties limodel_27july2023.xmlke
ATPchondrocyte_model_27july2023_v4_Ammonium_Source
% yield, collagen yield on glucose and glutamine. This analysis will
% demonstrate that the model is a realistic portrayal of chondrocyte
% metabolism. Note that glutamine is a nonessential amino acid but is
% present in the media that the experiments were run in.
%
% Then the analysis of cost of synthesis of individual nonessential amino acids and cost of transport of
individual essential amino acids
%
% Comparison of yields and amino acid costs with high and low O2
%
% Note that the dashes in the CNA model get turned into underscores
%%
initCobraToolbox()
%% Set some reaction names and variables
model =
readCbModel('/Users/ebruerdogan/Desktop/ADA_Code_July/chondrocyte_model_14aug2023_v5_Ammon
ium_Source_3H_pmf','fileType','SBML')

% biomass and ATP maintenance terms
collagenII = find(strcmp('T_Collagen_II',model.rxns));
collagenVI = find(strcmp('T_Collagen_VI',model.rxns));
O2 = find(strcmp('T_O2',model.rxns));
CO2 = find(strcmp('T_CO2',model.rxns));
HCO3 = find(strcmp('T_HCO3',model.rxns));

```

```
ATPm = find(strcmp('T_ATP',model.rxns));  
glucose_noCost = find(strcmp('T_Glucose_1',model.rxns));  
glucose_Na = find(strcmp('T_Glucose_2',model.rxns));  
glutamine_noCost = find(strcmp('T_Glutamine_1',model.rxns));  
glutamine_Na = find(strcmp('T_Glutamine_2',model.rxns));
```

```
alanine = find(strcmp('cost_alanine',model.rxns));  
arginine = find(strcmp('cost_arginine',model.rxns));  
asparagine = find(strcmp('cost_asparagine',model.rxns));  
aspartate = find(strcmp('cost_aspartate',model.rxns));  
cysteine = find(strcmp('cost_cysteine',model.rxns));  
glutamate = find(strcmp('cost_glutamate',model.rxns));  
glutamine = find(strcmp('cost_glutamine',model.rxns));  
glycine = find(strcmp('cost_glycine',model.rxns));  
proline = find(strcmp('cost_proline',model.rxns));  
serine = find(strcmp('cost_serine',model.rxns));  
tyrosine = find(strcmp('cost_tyrosine',model.rxns));  
phenylalanine = find(strcmp('T_Phe',model.rxns));
```

**% carbon content of each metabolite of interest**

```
Cmol_collagenII = 395;  
Cmol_collagenVI = 462;  
Cmol_glucose = 6;  
Cmol_glutamine = 5;  
  
Cmol_alanine = 3;  
Cmol_arginine = 6;  
Cmol_asparagine = 4;  
Cmol_aspartate = 4;  
Cmol_cysteine = 3;  
Cmol_glutamate = 5;  
Cmol_glycine = 2;
```

```

Cmol_proline = 5;
Cmol_serine = 3;
Cmol_tyrosine = 9;
Cmol_phenylalanine = 9;
%% Model predictions for ATPm production on glucose
% first, start with aerobic conditions, use the glucose transporter that
% requires Na+
model =
readCbModel('/Users/ebruerdogan/Desktop/ADA_Code_July/chondrocyte_model_27july2023_v4_Ammon
ium_Source','fileType','SBML')
% % prevent the export of nonessential amino acids; aren't needed for this
model = changeRxnBounds(model,'cost_alanine',0,'b');
model = changeRxnBounds(model,'cost_arginine',0,'b');
model = changeRxnBounds(model,'cost_asparagine',0,'b');
model = changeRxnBounds(model,'cost_aspartate',0,'b');
model = changeRxnBounds(model,'cost_cysteine',0,'b');
model = changeRxnBounds(model,'cost_glutamate',0,'b');
model = changeRxnBounds(model,'cost_glutamine',0,'b');
model = changeRxnBounds(model,'cost_glycine',0,'b');
model = changeRxnBounds(model,'cost_proline',0,'b');
model = changeRxnBounds(model,'cost_serine',0,'b');
model = changeRxnBounds(model,'cost_tyrosine',0,'b');
% turn off GTPm
model = changeRxnBounds(model,'T_GTP',0,'b');
% turn off pyruvate uptake
model = changeRxnBounds(model,'T_Pyruvate',0,'u');
% turn off lactate uptake
model = changeRxnBounds(model,'T_Lactate',0,'l');
% turn off CO2 uptake
model = changeRxnBounds(model,'T_CO2',0,'l');
% turn off HCO3 uptake
model = changeRxnBounds(model,'T_HCO3',1,'u');

```

```

% have to force transhydrogenase in the forward direction for the
% predictions to run properly. Otherwise, there seems to be an issue with
% Cobratoolbox predictions and ATP production is not actually maximized
model = changeRxnBounds(model,'TransHyd',0,'b');
% prevent glutamine uptake
model = changeRxnBounds(model,'T_Glutamine_1',0,'b');
model = changeRxnBounds(model,'T_Glutamine_2',0,'b');
% turn off glucose transporter that does not require sodium
model = changeRxnBounds(model,'T_Glucose_1',0,'b');
% prevent synthesis of collagen VI and collagen II
model = changeRxnBounds(model,'CollagenVI',0,'b');
model = changeRxnBounds(model,'CollagenII',0,'b');
% set maximization criteria to ATPm
model = changeObjective(model,'T_ATP');
% maximize production of ATP
FBAsolution1 = optimizeCbModel(model,'max');
% pull the important values
yield_ATPm_glucoseNa = ((FBAsolution1.v(ATPm))./(FBAsolution1.v(glucose_Na)));

% aerobic conditions but use glucose transporter with no cost
model =
readCbModel('/Users/ebruerdogan/Desktop/ADA_Code_July/chondrocyte_model_27july2023_v4_Ammon
ium_Source','fileType','SBML')
% % prevent the export of nonessential amino acids; aren't needed for this
model = changeRxnBounds(model,'cost_alanine',0,'b');
model = changeRxnBounds(model,'cost_arginine',0,'b');
model = changeRxnBounds(model,'cost_asparagine',0,'b');
model = changeRxnBounds(model,'cost_aspartate',0,'b');
model = changeRxnBounds(model,'cost_cysteine',0,'b');
model = changeRxnBounds(model,'cost_glutamate',0,'b');
model = changeRxnBounds(model,'cost_glutamine',0,'b');
model = changeRxnBounds(model,'cost_glycine',0,'b');

```

```
model = changeRxnBounds(model,'cost_proline',0,'b');
model = changeRxnBounds(model,'cost_serine',0,'b');
model = changeRxnBounds(model,'cost_tyrosine',0,'b');
% turn off GTPm
model = changeRxnBounds(model,'T_GTP',0,'b');
% turn off pyruvate uptake
model = changeRxnBounds(model,'T_Pyruvate',0,'u');
% turn off lactate uptake
model = changeRxnBounds(model,'T_Lactate',0,'l');
% turn off CO2 uptake
model = changeRxnBounds(model,'T_CO2',0,'l');
% turn off HCO3 uptake
model = changeRxnBounds(model,'T_HCO3',1,'u');
% have to force transhydrogenase in the forward direction for the
% predictions to run properly. Otherwise, there seems to be an issue with
% Cobratoolbox predictions and ATP production is not actually maximized
model = changeRxnBounds(model,'TransHyd',0,'b');
% prevent glutamine uptake
model = changeRxnBounds(model,'T_Glutamine_1',0,'b');
model = changeRxnBounds(model,'T_Glutamine_2',0,'b');
% turn off glucose transporter that requires sodium
model = changeRxnBounds(model,'T_Glucose_2',0,'b');
% prevent synthesis of collagen VI and collagen II
model = changeRxnBounds(model,'CollagenVI',0,'b');
model = changeRxnBounds(model,'CollagenII',0,'b');
% set maximization criteria to ATPm
model = changeObjective(model,'T_ATP');
% checking transhydrogenase reaction
model = changeRxnBounds(model,'TransHyd',0,'l');
% maximize production of collagen
FBAolution2 = optimizeCbModel(model,'max');
% pull the important values
```

```

yield_ATPm_glucosenoCost =((FBAsolution2.v(ATPm))./(FBAsolution2.v(glucose_noCost)));

% prevent use of O2 as terminal electron acceptor, use glucose transporter that requires Na+
model =
readCbModel('/Users/ebruerdogan/Desktop/ADA_Code_July/chondrocyte_model_27july2023_v4_Ammon
ium_Source','fileType','SBML')
% % prevent the export of nonessential amino acids; aren't needed for this
model = changeRxnBounds(model,'cost_alanine',0,'b');
model = changeRxnBounds(model,'cost_arginine',0,'b');
model = changeRxnBounds(model,'cost_asparagine',0,'b');
model = changeRxnBounds(model,'cost_aspartate',0,'b');
model = changeRxnBounds(model,'cost_cysteine',0,'b');
model = changeRxnBounds(model,'cost_glutamate',0,'b');
model = changeRxnBounds(model,'cost_glutamine',0,'b');
model = changeRxnBounds(model,'cost_glycine',0,'b');
model = changeRxnBounds(model,'cost_proline',0,'b');
model = changeRxnBounds(model,'cost_serine',0,'b');
model = changeRxnBounds(model,'cost_tyrosine',0,'b');
% turn off GTPm
model = changeRxnBounds(model,'T_GTP',0,'b');
% turn off pyruvate uptake
model = changeRxnBounds(model,'T_Pyruvate',0,'u');
% turn off lactate uptake
model = changeRxnBounds(model,'T_Lactate',0,'l');
% turn off CO2 uptake
model = changeRxnBounds(model,'T_CO2',0,'l');
% turn off HCO3 uptake
model = changeRxnBounds(model,'T_HCO3',1,'u');
% have to force transhydrogenase in the forward direction for the
% predictions to run properly. Otherwise, there seems to be an issue with
% Cobratoolbox predictions and ATP production is not actually maximized
model = changeRxnBounds(model,'TransHyd',0,'b');

```

```

% prevent glutamine uptake
model = changeRxnBounds(model,'T_Glutamine_1',0,'b');
model = changeRxnBounds(model,'T_Glutamine_2',0,'b');
% turn off glucose transporter that does not require sodium
model = changeRxnBounds(model,'T_Glucose_1',0,'b');
% prevent synthesis of collagen VI and collagen II
model = changeRxnBounds(model,'CollagenVI',0,'b');
model = changeRxnBounds(model,'CollagenII',0,'b');
% prevent use of aerobic electron transport chain
model = changeRxnBounds(model,'ETC_4',0,'b');
% set maximization criteria to ATPm
model = changeObjective(model,'T_ATP');
% maximize production of collagen
FBAolution3 = optimizeCbModel(model,'max');
% pull the important values
yield_ATPm_glucoseNa_noETC4 =((FBAolution3.v(ATPm))./(FBAolution3.v(glucose_Na)));

% no O2 as terminal electron acceptor; glucose transporter with no cost
model =
readCbModel('/Users/ebruerdogan/Desktop/ADA_Code_July/chondrocyte_model_27july2023_v4_Ammon
ium_Source','fileType','SBML')
% % prevent the export of nonessential amino acids; aren't needed for this
model = changeRxnBounds(model,'cost_alanine',0,'b');
model = changeRxnBounds(model,'cost_arginine',0,'b');
model = changeRxnBounds(model,'cost_asparagine',0,'b');
model = changeRxnBounds(model,'cost_aspartate',0,'b');
model = changeRxnBounds(model,'cost_cysteine',0,'b');
model = changeRxnBounds(model,'cost_glutamate',0,'b');
model = changeRxnBounds(model,'cost_glutamine',0,'b');
model = changeRxnBounds(model,'cost_glycine',0,'b');
model = changeRxnBounds(model,'cost_proline',0,'b');
model = changeRxnBounds(model,'cost_serine',0,'b');

```

```
model = changeRxnBounds(model,'cost_tyrosine',0,'b');
% turn off GTPm
model = changeRxnBounds(model,'T_GTP',0,'b');
% turn off pyruvate uptake
model = changeRxnBounds(model,'T_Pyruvate',0,'u');
% turn off lactate uptake
model = changeRxnBounds(model,'T_Lactate',0,'l');
% turn off CO2 uptake
model = changeRxnBounds(model,'T_CO2',0,'l');
% turn off HCO3 uptake
model = changeRxnBounds(model,'T_HCO3',1,'u');
% have to force transhydrogenase in the forward direction for the
% predictions to run properly. Otherwise, there seems to be an issue with
% Cobratoolbox predictions and ATP production is not actually maximized
model = changeRxnBounds(model,'TransHyd',0,'b');
% prevent glutamine uptake
model = changeRxnBounds(model,'T_Glutamine_1',0,'b');
model = changeRxnBounds(model,'T_Glutamine_2',0,'b');
% turn off glucose transporter that requires sodium
model = changeRxnBounds(model,'T_Glucose_2',0,'b');
% prevent use of O2 as terminal electron acceptor
model = changeRxnBounds(model,'ETC_4',0,'b');
% prevent synthesis of collagen VI and collagen II
model = changeRxnBounds(model,'CollagenVI',0,'b');
model = changeRxnBounds(model,'CollagenII',0,'b');
% set maximization criteria to ATPm
model = changeObjective(model,'T_ATP');
% maximize production of collagen
FBA_solution4 = optimizeCbModel(model,'max');
% pull the important values
yield_ATPm_glucosenoCost_noETC4 = ((FBA_solution4.v(ATPm))./(FBA_solution4.v(glucose_noCost)));
```

```
%% Model predictions for collagen II yields on glucose
```

```
% first, start with aerobic conditions, use the glucose transporter that
```

```
% requires Na+
```

```
model =
```

```
readCbModel('/Users/ebruerdogan/Desktop/ADA_Code_July/chondrocyte_model_27july2023_v4_Ammonium_Source','fileType','SBML')
```

```
% % prevent the export of nonessential amino acids; aren't needed for this
```

```
model = changeRxnBounds(model,'cost_alanine',0,'b');
```

```
model = changeRxnBounds(model,'cost_arginine',0,'b');
```

```
model = changeRxnBounds(model,'cost_asparagine',0,'b');
```

```
model = changeRxnBounds(model,'cost_aspartate',0,'b');
```

```
model = changeRxnBounds(model,'cost_cysteine',0,'b');
```

```
model = changeRxnBounds(model,'cost_glutamate',0,'b');
```

```
model = changeRxnBounds(model,'cost_glutamine',0,'b');
```

```
model = changeRxnBounds(model,'cost_glycine',0,'b');
```

```
model = changeRxnBounds(model,'cost_proline',0,'b');
```

```
model = changeRxnBounds(model,'cost_serine',0,'b');
```

```
model = changeRxnBounds(model,'cost_tyrosine',0,'b');
```

```
% turn off ATPm and GTPm
```

```
model = changeRxnBounds(model,'T_ATP',0,'b');
```

```
model = changeRxnBounds(model,'T_GTP',0,'b');
```

```
% turn off pyruvate uptake
```

```
model = changeRxnBounds(model,'T_Pyruvate',0,'u');
```

```
% turn off lactate uptake
```

```
model = changeRxnBounds(model,'T_Lactate',0,'l');
```

```
% turn off CO2 uptake
```

```
model = changeRxnBounds(model,'T_CO2',0,'l');
```

```
% turn off HCO3 uptake
```

```
model = changeRxnBounds(model,'T_HCO3',1,'u');
```

```
% have to force transhydrogenase in the forward direction for the
```

```
% predictions to run properly. Otherwise, there seems to be an issue with
```

```

% Cobratoolbox predictions and ATP production is not actually maximized
model = changeRxnBounds(model,'TransHyd',0,'b');
% prevent glutamine uptake
model = changeRxnBounds(model,'T_Glutamine_1',0,'b');
model = changeRxnBounds(model,'T_Glutamine_2',0,'b');
% turn off glucose transporter that does not require sodium
model = changeRxnBounds(model,'T_Glucose_1',0,'b');
% prevent synthesis of collagen VI
model = changeRxnBounds(model,'CollagenVI',0,'b');
% set maximization criteria to collagen II
model = changeObjective(model,'T_Collagen_II');
% maximize production of collagen
FBAsolution1 = optimizeCbModel(model,'max');
% pull the important values
yield_CollagenII_glucoseNa
=((FBAsolution1.v(collagenII)*Cmol_collagenII)/(FBAsolution1.v(glucose_Na)*Cmol_glucose));

% next, aerobic conditions, use the transporter with no cost
model =
readCbModel('/Users/ebruerdogan/Desktop/ADA_Code_July/chondrocyte_model_27july2023_v4_Ammon
ium_Source','fileType','SBML')
% prevent the export of nonessential amino acids; aren't needed for this
model = changeRxnBounds(model,'cost_alanine',0,'b');
model = changeRxnBounds(model,'cost_arginine',0,'b');
model = changeRxnBounds(model,'cost_asparagine',0,'b');
model = changeRxnBounds(model,'cost_aspartate',0,'b');
model = changeRxnBounds(model,'cost_cysteine',0,'b');
model = changeRxnBounds(model,'cost_glutamate',0,'b');
model = changeRxnBounds(model,'cost_glutamine',0,'b');
model = changeRxnBounds(model,'cost_glycine',0,'b');
model = changeRxnBounds(model,'cost_proline',0,'b');
model = changeRxnBounds(model,'cost_serine',0,'b');

```

```

model = changeRxnBounds(model,'cost_tyrosine',0,'b');
% turn off ATPm and GTPm
model = changeRxnBounds(model,'T_ATP',0,'b');
model = changeRxnBounds(model,'T_GTP',0,'b');
% turn off pyruvate uptake
model = changeRxnBounds(model,'T_Pyruvate',0,'u');
% turn off lactate uptake
model = changeRxnBounds(model,'T_Lactate',0,'l');
% turn off CO2 uptake
model = changeRxnBounds(model,'T_CO2',0,'l');
% turn off HCO3 uptake
model = changeRxnBounds(model,'T_HCO3',1,'u');
% have to force transhydrogenase in the forward direction for the
% predictions to run properly. Otherwise, there seems to be an issue with
% Cobratoolbox predictions and ATP production is not actually maximized
model = changeRxnBounds(model,'TransHyd',0,'b');
% prevent glutamine uptake
model = changeRxnBounds(model,'T_Glutamine_1',0,'b');
model = changeRxnBounds(model,'T_Glutamine_2',0,'b');
% turn off glucose transporter that requires sodium
model = changeRxnBounds(model,'T_Glucose_2',0,'b');
% prevent synthesis of collagen VI
model = changeRxnBounds(model,'CollagenVI',0,'b');
% set maximization criteria to collagen II
model = changeObjective(model,'T_Collagen_II');
% maximize production of collagen
FBAolution2 = optimizeCbModel(model,'max');
% pull the important values
yield_CollagenII_glucosenoCost
=((FBAolution2.v(collagenII)*Cmol_collagenII)/(FBAolution2.v(glucose_noCost)*Cmol_glucose));

% no O2 as terminal electron acceptor, use the glucose transporter that requires Na+

```

```
model =
readCbModel('/Users/ebruerdogan/Desktop/ADA_Code_July/chondrocyte_model_27july2023_v4_Ammonium_Source','fileType','SBML')
% prevent the export of nonessential amino acids; aren't needed for this
model = changeRxnBounds(model,'cost_alanine',0,'b');
model = changeRxnBounds(model,'cost_arginine',0,'b');
model = changeRxnBounds(model,'cost_asparagine',0,'b');
model = changeRxnBounds(model,'cost_aspartate',0,'b');
model = changeRxnBounds(model,'cost_cysteine',0,'b');
model = changeRxnBounds(model,'cost_glutamate',0,'b');
model = changeRxnBounds(model,'cost_glutamine',0,'b');
model = changeRxnBounds(model,'cost_glycine',0,'b');
model = changeRxnBounds(model,'cost_proline',0,'b');
model = changeRxnBounds(model,'cost_serine',0,'b');
model = changeRxnBounds(model,'cost_tyrosine',0,'b');
% turn off ATPm and GTPm
model = changeRxnBounds(model,'T_ATP',0,'b');
model = changeRxnBounds(model,'T_GTP',0,'b');
% turn off pyruvate uptake
model = changeRxnBounds(model,'T_Pyruvate',0,'u');
% turn off lactate uptake
model = changeRxnBounds(model,'T_Lactate',0,'l');
% turn off CO2 uptake
model = changeRxnBounds(model,'T_CO2',0,'l');
% turn off HCO3 uptake
model = changeRxnBounds(model,'T_HCO3',1,'u');
% have to force transhydrogenase in the forward direction for the
% predictions to run properly. Otherwise, there seems to be an issue with
% Cobratoolbox predictions and ATP production is not actually maximized
model = changeRxnBounds(model,'TransHyd',0,'b');
% prevent glutamine uptake
model = changeRxnBounds(model,'T_Glutamine_1',0,'b');
```

```

model = changeRxnBounds(model,'T_Glutamine_2',0,'b');
% turn off glucose transporter that does not require sodium
model = changeRxnBounds(model,'T_Glucose_1',0,'b');
% prevent synthesis of collagen VI
model = changeRxnBounds(model,'CollagenVI',0,'b');
% prevent use of O2 as terminal electron acceptor
model = changeRxnBounds(model,'ETC_4',0,'b');
% set maximization criteria to collagen II
model = changeObjective(model,'T_Collagen_II');
% maximize production of collagen
FBAolution3 = optimizeCbModel(model,'max');
% pull the important values
yield_CollagenII_glucoseNa_noETC4
=((FBAolution3.v(collagenII)*Cmol_collagenII)/(FBAolution3.v(glucose_Na)*Cmol_glucose));

% no O2 as terminal electron acceptor, use the no cost glucose transporter
model =
readCbModel('/Users/ebruerdogan/Desktop/ADA_Code_July/chondrocyte_model_27july2023_v4_Ammon
ium_Source','fileType','SBML')
% prevent the export of nonessential amino acids; aren't needed for this
model = changeRxnBounds(model,'cost_alanine',0,'b');
model = changeRxnBounds(model,'cost_arginine',0,'b');
model = changeRxnBounds(model,'cost_asparagine',0,'b');
model = changeRxnBounds(model,'cost_aspartate',0,'b');
model = changeRxnBounds(model,'cost_cysteine',0,'b');
model = changeRxnBounds(model,'cost_glutamate',0,'b');
model = changeRxnBounds(model,'cost_glutamine',0,'b');
model = changeRxnBounds(model,'cost_glycine',0,'b');
model = changeRxnBounds(model,'cost_proline',0,'b');
model = changeRxnBounds(model,'cost_serine',0,'b');
model = changeRxnBounds(model,'cost_tyrosine',0,'b');
% turn off ATPm and GTPm

```

```

model = changeRxnBounds(model,'T_ATP',0,'b');
model = changeRxnBounds(model,'T_GTP',0,'b');
% turn off pyruvate uptake
model = changeRxnBounds(model,'T_Pyruvate',0,'u');
% turn off lactate uptake
model = changeRxnBounds(model,'T_Lactate',0,'l');
% turn off CO2 uptake
model = changeRxnBounds(model,'T_CO2',0,'l');
% turn off HCO3 uptake
model = changeRxnBounds(model,'T_HCO3',1,'u');
% have to force transhydrogenase in the forward direction for the
% predictions to run properly. Otherwise, there seems to be an issue with
% Cobratoolbox predictions and ATP production is not actually maximized
model = changeRxnBounds(model,'TransHyd',0,'b');
% prevent glutamine uptake
model = changeRxnBounds(model,'T_Glutamine_1',0,'b');
model = changeRxnBounds(model,'T_Glutamine_2',0,'b');
% turn off glucose transporter that does not require sodium
model = changeRxnBounds(model,'T_Glucose_2',0,'b');
% prevent synthesis of collagen VI
model = changeRxnBounds(model,'CollagenVI',0,'b');
% prevent use of O2 as terminal electron acceptor
model = changeRxnBounds(model,'ETC_4',0,'b');
% set maximization criteria to collagen II
model = changeObjective(model,'T_Collagen_II');
% maximize production of collagen
FBA_solution4 = optimizeCbModel(model,'max');
% pull the important values
yield_CollagenII_glucosenoCost_noETC4
=((FBA_solution4.v(collagenII)*Cmol_collagenII)/(FBA_solution4.v(glucose_noCost)*Cmol_glucose));

%% Model predictions for collagen VI yields on glucose

```

```
% first, start with aerobic conditions, use the glucose transporter that
% requires Na+
model =
readCbModel('/Users/ebruerdogan/Desktop/ADA_Code_July/chondrocyte_model_27july2023_v4_Ammon
ium_Source','fileType','SBML')
% % prevent the export of nonessential amino acids; aren't needed for this
model = changeRxnBounds(model,'cost_alanine',0,'b');
model = changeRxnBounds(model,'cost_arginine',0,'b');
model = changeRxnBounds(model,'cost_asparagine',0,'b');
model = changeRxnBounds(model,'cost_aspartate',0,'b');
model = changeRxnBounds(model,'cost_cysteine',0,'b');
model = changeRxnBounds(model,'cost_glutamate',0,'b');
model = changeRxnBounds(model,'cost_glutamine',0,'b');
model = changeRxnBounds(model,'cost_glycine',0,'b');
model = changeRxnBounds(model,'cost_proline',0,'b');
model = changeRxnBounds(model,'cost_serine',0,'b');
model = changeRxnBounds(model,'cost_tyrosine',0,'b');
% turn off ATPm and GTPm
model = changeRxnBounds(model,'T_ATP',0,'b');
model = changeRxnBounds(model,'T_GTP',0,'b');
% turn off pyruvate uptake
model = changeRxnBounds(model,'T_Pyruvate',0,'u');
% turn off lactate uptake
model = changeRxnBounds(model,'T_Lactate',0,'l');
% turn off CO2 uptake
model = changeRxnBounds(model,'T_CO2',0,'l');
% turn off HCO3 uptake
model = changeRxnBounds(model,'T_HCO3',1,'u');
% have to force transhydrogenase in the forward direction for the
% predictions to run properly. Otherwise, there seems to be an issue with
% Cobratoolbox predictions and ATP production is not actually maximized
```

```

model = changeRxnBounds(model,'TransHyd',0,'b');
% prevent glutamine uptake
model = changeRxnBounds(model,'T_Glutamine_1',0,'b');
model = changeRxnBounds(model,'T_Glutamine_2',0,'b');
% turn off glucose transporter that does not require sodium
model = changeRxnBounds(model,'T_Glucose_1',0,'b');
% prevent synthesis of collagen II
model = changeRxnBounds(model,'CollagenII',0,'b');
% set maximization criteria to collagen VI
model = changeObjective(model,'T_Collagen_VI');
% maximize production of collagen
FBA_solution1 = optimizeCbModel(model,'max');
% pull the important values
yield_CollagenVI_glucoseNa
=((FBA_solution1.v(collagenVI)*Cmol_collagenVI)./(FBA_solution1.v(glucose_Na)*Cmol_glucose));

% next, aerobic conditions, use the transporter with no cost
model =
readCbModel('/Users/ebruerdogan/Desktop/ADA_Code_July/chondrocyte_model_27july2023_v4_Ammonium_Source','fileType','SBML')
% prevent the export of nonessential amino acids; aren't needed for this
model = changeRxnBounds(model,'cost_alanine',0,'b');
model = changeRxnBounds(model,'cost_arginine',0,'b');
model = changeRxnBounds(model,'cost_asparagine',0,'b');
model = changeRxnBounds(model,'cost_aspartate',0,'b');
model = changeRxnBounds(model,'cost_cysteine',0,'b');
model = changeRxnBounds(model,'cost_glutamate',0,'b');
model = changeRxnBounds(model,'cost_glutamine',0,'b');
model = changeRxnBounds(model,'cost_glycine',0,'b');
model = changeRxnBounds(model,'cost_proline',0,'b');
model = changeRxnBounds(model,'cost_serine',0,'b');
model = changeRxnBounds(model,'cost_tyrosine',0,'b');

```

```

% turn off ATPm and GTPm
model = changeRxnBounds(model,'T_ATP',0,'b');
model = changeRxnBounds(model,'T_GTP',0,'b');
% turn off pyruvate uptake
model = changeRxnBounds(model,'T_Pyruvate',0,'u');
% turn off lactate uptake
model = changeRxnBounds(model,'T_Lactate',0,'l');
% turn off CO2 uptake
model = changeRxnBounds(model,'T_CO2',0,'l');
% turn off HCO3 uptake
model = changeRxnBounds(model,'T_HCO3',1,'u');
% have to force transhydrogenase in the forward direction for the
% predictions to run properly. Otherwise, there seems to be an issue with
% Cobratoolbox predictions and ATP production is not actually maximized
model = changeRxnBounds(model,'TransHyd',0,'b');
% prevent glutamine uptake
model = changeRxnBounds(model,'T_Glutamine_1',0,'b');
model = changeRxnBounds(model,'T_Glutamine_2',0,'b');
% turn off glucose transporter that requires sodium
model = changeRxnBounds(model,'T_Glucose_2',0,'b');
% prevent synthesis of collagen II
model = changeRxnBounds(model,'CollagenII',0,'b');
% set maximization criteria to collagen VI
model = changeObjective(model,'T_Collagen_VI');
% maximize production of collagen
FBAolution2 = optimizeCbModel(model,'max');
% pull the important values
yield_CollagenVI_glucosenoCost
=((FBAolution2.v(collagenVI)*Cmol_collagenVI)./(FBAolution2.v(glucose_noCost)*Cmol_glucose));

% no O2 as terminal electron acceptor, use the glucose transporter that requires Na+

```

```
model =
readCbModel('/Users/ebruerdogan/Desktop/ADA_Code_July/chondrocyte_model_27july2023_v4_Ammon
ium_Source','fileType','SBML')
% prevent the export of nonessential amino acids; aren't needed for this
model = changeRxnBounds(model,'cost_alanine',0,'b');
model = changeRxnBounds(model,'cost_arginine',0,'b');
model = changeRxnBounds(model,'cost_asparagine',0,'b');
model = changeRxnBounds(model,'cost_aspartate',0,'b');
model = changeRxnBounds(model,'cost_cysteine',0,'b');
model = changeRxnBounds(model,'cost_glutamate',0,'b');
model = changeRxnBounds(model,'cost_glutamine',0,'b');
model = changeRxnBounds(model,'cost_glycine',0,'b');
model = changeRxnBounds(model,'cost_proline',0,'b');
model = changeRxnBounds(model,'cost_serine',0,'b');
model = changeRxnBounds(model,'cost_tyrosine',0,'b');
% turn off ATPm and GTPm
model = changeRxnBounds(model,'T_ATP',0,'b');
model = changeRxnBounds(model,'T_GTP',0,'b');
% turn off pyruvate uptake
model = changeRxnBounds(model,'T_Pyruvate',0,'u');
% turn off lactate uptake
model = changeRxnBounds(model,'T_Lactate',0,'l');
% turn off CO2 uptake
model = changeRxnBounds(model,'T_CO2',0,'l');
% turn off HCO3 uptake
model = changeRxnBounds(model,'T_HCO3',1,'u');
% have to force transhydrogenase in the forward direction for the
% predictions to run properly. Otherwise, there seems to be an issue with
% Cobratoolbox predictions and ATP production is not actually maximized
model = changeRxnBounds(model,'TransHyd',0,'b');
% prevent glutamine uptake
model = changeRxnBounds(model,'T_Glutamine_1',0,'b');
```

```

model = changeRxnBounds(model,'T_Glutamine_2',0,'b');
% turn off glucose transporter that does not require sodium
model = changeRxnBounds(model,'T_Glucose_1',0,'b');
% prevent synthesis of collagen II
model = changeRxnBounds(model,'CollagenII',0,'b');
% prevent use of O2 as terminal electron acceptor
model = changeRxnBounds(model,'ETC_4',0,'b');
% set maximization criteria to collagen VI
model = changeObjective(model,'T_Collagen_VI');
% maximize production of collagen
FBAolution3 = optimizeCbModel(model,'max');
% pull the important values
yield_CollagenVI_glucoseNa_noETC4
=((FBAolution3.v(collagenVI)*Cmol_collagenVI)/(FBAolution3.v(glucose_Na)*Cmol_glucose));

% no O2 as terminal electron acceptor, use the no cost glucose transporter
model =
readCbModel('/Users/ebruerdogan/Desktop/ADA_Code_July/chondrocyte_model_27july2023_v4_Ammon
ium_Source','fileType','SBML')
% prevent the export of nonessential amino acids; aren't needed for this
model = changeRxnBounds(model,'cost_alanine',0,'b');
model = changeRxnBounds(model,'cost_arginine',0,'b');
model = changeRxnBounds(model,'cost_asparagine',0,'b');
model = changeRxnBounds(model,'cost_aspartate',0,'b');
model = changeRxnBounds(model,'cost_cysteine',0,'b');
model = changeRxnBounds(model,'cost_glutamate',0,'b');
model = changeRxnBounds(model,'cost_glutamine',0,'b');
model = changeRxnBounds(model,'cost_glycine',0,'b');
model = changeRxnBounds(model,'cost_proline',0,'b');
model = changeRxnBounds(model,'cost_serine',0,'b');
model = changeRxnBounds(model,'cost_tyrosine',0,'b');
% turn off ATPm and GTPm

```

```

model = changeRxnBounds(model,'T_ATP',0,'b');
model = changeRxnBounds(model,'T_GTP',0,'b');
% turn off pyruvate uptake
model = changeRxnBounds(model,'T_Pyruvate',0,'u');
% turn off lactate uptake
model = changeRxnBounds(model,'T_Lactate',0,'l');
% turn off CO2 uptake
model = changeRxnBounds(model,'T_CO2',0,'l');
% turn off HCO3 uptake
model = changeRxnBounds(model,'T_HCO3',1,'u');
% have to force transhydrogenase in the forward direction for the
% predictions to run properly. Otherwise, there seems to be an issue with
% Cobratoolbox predictions and ATP production is not actually maximized
model = changeRxnBounds(model,'TransHyd',0,'b');
% prevent glutamine uptake
model = changeRxnBounds(model,'T_Glutamine_1',0,'b');
model = changeRxnBounds(model,'T_Glutamine_2',0,'b');
% turn off glucose transporter that does not require sodium
model = changeRxnBounds(model,'T_Glucose_2',0,'b');
% prevent synthesis of collagen II
model = changeRxnBounds(model,'CollagenII',0,'b');
% prevent use of O2 as terminal electron acceptor
model = changeRxnBounds(model,'ETC_4',0,'b');
% set maximization criteria to collagen VI
model = changeObjective(model,'T_Collagen_VI');
% maximize production of collagen
FBA_solution4 = optimizeCbModel(model,'max');
% pull the important values
yield_CollagenVI_glucosenoCost_noETC4
=((FBA_solution4.v(collagenVI)*Cmol_collagenVI)./(FBA_solution4.v(glucose_noCost)*Cmol_glucose));

%% Model predictions for ATPm production on glucose

```

```
% first, start with aerobic conditions, use the glucose transporter that
% requires Na+
model =
readCbModel('/Users/ebruerdogan/Desktop/ADA_Code_July/chondrocyte_model_27july2023_v4_Ammon
ium_Source', 'fileType', 'SBML')
% % prevent the export of nonessential amino acids; aren't needed for this
model = changeRxnBounds(model, 'cost_alanine', 0, 'b');
model = changeRxnBounds(model, 'cost_arginine', 0, 'b');
model = changeRxnBounds(model, 'cost_asparagine', 0, 'b');
model = changeRxnBounds(model, 'cost_aspartate', 0, 'b');
model = changeRxnBounds(model, 'cost_cysteine', 0, 'b');
model = changeRxnBounds(model, 'cost_glutamate', 0, 'b');
model = changeRxnBounds(model, 'cost_glutamine', 0, 'b');
model = changeRxnBounds(model, 'cost_glycine', 0, 'b');
model = changeRxnBounds(model, 'cost_proline', 0, 'b');
model = changeRxnBounds(model, 'cost_serine', 0, 'b');
model = changeRxnBounds(model, 'cost_tyrosine', 0, 'b');
% turn off GTPm
model = changeRxnBounds(model, 'T_GTP', 0, 'b');
% turn off pyruvate uptake
model = changeRxnBounds(model, 'T_Pyruvate', 0, 'u');
% turn off lactate uptake
model = changeRxnBounds(model, 'T_Lactate', 0, 'l');
% turn off CO2 uptake
model = changeRxnBounds(model, 'T_CO2', 0, 'l');
% turn off HCO3 uptake
model = changeRxnBounds(model, 'T_HCO3', 1, 'u');
% have to force transhydrogenase in the forward direction for the
% predictions to run properly. Otherwise, there seems to be an issue with
% Cobratoolbox predictions and ATP production is not actually maximized
model = changeRxnBounds(model, 'TransHyd', 0, 'b');
% prevent glucose uptake
```

```
model = changeRxnBounds(model,'T_Glucose_1',0,'b');
model = changeRxnBounds(model,'T_Glucose_2',0,'b');
% turn off glutamine transporter that does not require sodium
model = changeRxnBounds(model,'T_Glutamine_1',0,'b');
% prevent synthesis of collagen VI and collagen II
model = changeRxnBounds(model,'CollagenVI',0,'b');
model = changeRxnBounds(model,'CollagenII',0,'b');
% set maximization criteria to ATPm
model = changeObjective(model,'T_ATP');
% maximize production of collagen
FBAolution1 = optimizeCbModel(model,'max');
% pull the important values
yield_ATPm_glutamineNa =((FBAolution1.v(ATPm))./(FBAolution1.v(glutamine_Na)));

% aerobic conditions but use glucose transporter with no cost
model =
readCbModel('/Users/ebruerdogan/Desktop/ADA_Code_July/chondrocyte_model_27july2023_v4_Ammon
ium_Source','fileType','SBML')
% % prevent the export of nonessential amino acids; aren't needed for this
model = changeRxnBounds(model,'cost_alanine',0,'b');
model = changeRxnBounds(model,'cost_arginine',0,'b');
model = changeRxnBounds(model,'cost_asparagine',0,'b');
model = changeRxnBounds(model,'cost_aspartate',0,'b');
model = changeRxnBounds(model,'cost_cysteine',0,'b');
model = changeRxnBounds(model,'cost_glutamate',0,'b');
model = changeRxnBounds(model,'cost_glutamine',0,'b');
model = changeRxnBounds(model,'cost_glycine',0,'b');
model = changeRxnBounds(model,'cost_proline',0,'b');
model = changeRxnBounds(model,'cost_serine',0,'b');
model = changeRxnBounds(model,'cost_tyrosine',0,'b');
% turn offGTPm
model = changeRxnBounds(model,'T_GTP',0,'b');
```

```

% turn off pyruvate uptake
model = changeRxnBounds(model,'T_Pyruvate',0,'u');
% turn off lactate uptake
model = changeRxnBounds(model,'T_Lactate',0,'l');
% turn off CO2 uptake
model = changeRxnBounds(model,'T_CO2',0,'l');
% turn off HCO3 uptake
model = changeRxnBounds(model,'T_HCO3',1,'u');
% have to force transhydrogenase in the forward direction for the
% predictions to run properly. Otherwise, there seems to be an issue with
% Cobratoolbox predictions and ATP production is not actually maximized
model = changeRxnBounds(model,'TransHyd',0,'b');
% prevent glucose uptake
model = changeRxnBounds(model,'T_Glucose_1',0,'b');
model = changeRxnBounds(model,'T_Glucose_2',0,'b');
% turn off glucose transporter that requires sodium
model = changeRxnBounds(model,'T_Glutamine_2',0,'b');
% prevent synthesis of collagen VI and collagen II
model = changeRxnBounds(model,'CollagenVI',0,'b');
model = changeRxnBounds(model,'CollagenII',0,'b');
% set maximization criteria to ATPm
model = changeObjective(model,'T_ATP');
% checking transhydrogenase reaction
model = changeRxnBounds(model,'TransHyd',0,'l');
% maximize production of collagen
FBA_solution2 = optimizeCbModel(model,'max');
% pull the important values
yield_ATPm_glutaminenoCost = ((FBA_solution2.v(ATPm))./(FBA_solution2.v(glutamine_noCost)));

% prevent use of O2 as terminal electron acceptor, use glucose transporter that requires Na+

```

```

model =
readCbModel('/Users/ebruerdogan/Desktop/ADA_Code_July/chondrocyte_model_27july2023_v4_Ammon
ium_Source','fileType','SBML')
% % prevent the export of nonessential amino acids; aren't needed for this
model = changeRxnBounds(model,'cost_alanine',0,'b');
model = changeRxnBounds(model,'cost_arginine',0,'b');
model = changeRxnBounds(model,'cost_asparagine',0,'b');
model = changeRxnBounds(model,'cost_aspartate',0,'b');
model = changeRxnBounds(model,'cost_cysteine',0,'b');
model = changeRxnBounds(model,'cost_glutamate',0,'b');
model = changeRxnBounds(model,'cost_glutamine',0,'b');
model = changeRxnBounds(model,'cost_glycine',0,'b');
model = changeRxnBounds(model,'cost_proline',0,'b');
model = changeRxnBounds(model,'cost_serine',0,'b');
model = changeRxnBounds(model,'cost_tyrosine',0,'b');
% turn off GTPm
model = changeRxnBounds(model,'T_GTP',0,'b');
% turn off pyruvate uptake
model = changeRxnBounds(model,'T_Pyruvate',0,'u');
% turn off lactate uptake
model = changeRxnBounds(model,'T_Lactate',0,'l');
% turn off CO2 uptake
model = changeRxnBounds(model,'T_CO2',0,'l');
% turn off HCO3 uptake
model = changeRxnBounds(model,'T_HCO3',1,'u');
% have to force transhydrogenase in the forward direction for the
% predictions to run properly. Otherwise, there seems to be an issue with
% Cobratoolbox predictions and ATP production is not actually maximized
model = changeRxnBounds(model,'TransHyd',0,'b');
% prevent glucose uptake
model = changeRxnBounds(model,'T_Glucose_1',0,'b');
model = changeRxnBounds(model,'T_Glucose_2',0,'b');

```

```
% turn off glutamine transporter that does not require sodium
model = changeRxnBounds(model,'T_Glutamine_1',0,'b');
% prevent synthesis of collagen VI and collagen II
model = changeRxnBounds(model,'CollagenVI',0,'b');
model = changeRxnBounds(model,'CollagenIII',0,'b');
% prevent use of aerobic electron transport chain
model = changeRxnBounds(model,'ETC_4',0,'b');
% set maximization criteria to ATPm
model = changeObjective(model,'T_ATP');
% maximize production of collagen
FBAolution3 = optimizeCbModel(model,'max');
% pull the important values
yield_ATPm_glutamineNa_noETC4 =((FBAolution3.v(ATPm))./(FBAolution3.v(glutamine_Na)));

% no O2 as terminal electron acceptor; glucose transporter with no cost
model =
readCbModel('/Users/ebruerdogan/Desktop/ADA_Code_July/chondrocyte_model_27july2023_v4_Ammon
ium_Source','fileType','SBML')
% % prevent the export of nonessential amino acids; aren't needed for this
model = changeRxnBounds(model,'cost_alanine',0,'b');
model = changeRxnBounds(model,'cost_arginine',0,'b');
model = changeRxnBounds(model,'cost_asparagine',0,'b');
model = changeRxnBounds(model,'cost_aspartate',0,'b');
model = changeRxnBounds(model,'cost_cysteine',0,'b');
model = changeRxnBounds(model,'cost_glutamate',0,'b');
model = changeRxnBounds(model,'cost_glutamine',0,'b');
model = changeRxnBounds(model,'cost_glycine',0,'b');
model = changeRxnBounds(model,'cost_proline',0,'b');
model = changeRxnBounds(model,'cost_serine',0,'b');
model = changeRxnBounds(model,'cost_tyrosine',0,'b');
% turn offGTPm
model = changeRxnBounds(model,'T_GTP',0,'b');
```

```
% turn off pyruvate uptake
model = changeRxnBounds(model,'T_Pyruvate',0,'u');
% turn off lactate uptake
model = changeRxnBounds(model,'T_Lactate',0,'l');
% turn off CO2 uptake
model = changeRxnBounds(model,'T_CO2',0,'l');
% turn off HCO3 uptake
model = changeRxnBounds(model,'T_HCO3',1,'u');
% have to force transhydrogenase in the forward direction for the
% predictions to run properly. Otherwise, there seems to be an issue with
% Cobratoolbox predictions and ATP production is not actually maximized
model = changeRxnBounds(model,'TransHyd',0,'b');
% prevent glucose uptake
model = changeRxnBounds(model,'T_Glucose_1',0,'b');
model = changeRxnBounds(model,'T_Glucose_2',0,'b');
% turn off glutamine transporter that requires sodium
model = changeRxnBounds(model,'T_Glutamine_2',0,'b');
% prevent use of O2 as terminal electron acceptor
model = changeRxnBounds(model,'ETC_4',0,'b');
% prevent synthesis of collagen VI and collagen II
model = changeRxnBounds(model,'CollagenVI',0,'b');
model = changeRxnBounds(model,'CollagenII',0,'b');
% set maximization criteria to ATPm
model = changeObjective(model,'T_ATP');
% maximize production of collagen
FBA_solution4 = optimizeCbModel(model,'max');
% pull the important values
yield_ATPm_glutaminenoCost_noETC4 = ((FBA_solution4.v(ATPm))./(FBA_solution4.v(glutamine_noCost)));

%% Model predictions for collagen II yields on glutamine
```

```

% first, start with aerobic conditions, use the glutamine transporter that
% requires Na+
model =
readCbModel('/Users/ebruerdogan/Desktop/ADA_Code_July/chondrocyte_model_27july2023_v4_Ammon
ium_Source', 'fileType', 'SBML')
% % prevent the export of nonessential amino acids; aren't needed for this
model = changeRxnBounds(model, 'cost_alanine', 0, 'b');
model = changeRxnBounds(model, 'cost_arginine', 0, 'b');
model = changeRxnBounds(model, 'cost_asparagine', 0, 'b');
model = changeRxnBounds(model, 'cost_aspartate', 0, 'b');
model = changeRxnBounds(model, 'cost_cysteine', 0, 'b');
model = changeRxnBounds(model, 'cost_glutamate', 0, 'b');
model = changeRxnBounds(model, 'cost_glutamine', 0, 'b');
model = changeRxnBounds(model, 'cost_glycine', 0, 'b');
model = changeRxnBounds(model, 'cost_proline', 0, 'b');
model = changeRxnBounds(model, 'cost_serine', 0, 'b');
model = changeRxnBounds(model, 'cost_tyrosine', 0, 'b');
% turn off ATPm and GTPm
model = changeRxnBounds(model, 'T_ATP', 0, 'b');
model = changeRxnBounds(model, 'T_GTP', 0, 'b');
% turn off pyruvate uptake
model = changeRxnBounds(model, 'T_Pyruvate', 0, 'u');
% turn off lactate uptake
model = changeRxnBounds(model, 'T_Lactate', 0, 'l');
% turn off CO2 uptake
model = changeRxnBounds(model, 'T_CO2', 0, 'l');
% turn off HCO3 uptake
model = changeRxnBounds(model, 'T_HCO3', 1, 'u');
% have to force transhydrogenase in the forward direction for the
% predictions to run properly. Otherwise, there seems to be an issue with
% Cobratoolbox predictions and ATP production is not actually maximized
model = changeRxnBounds(model, 'TransHyd', 0, 'b');

```

```

% prevent glucose uptake
model = changeRxnBounds(model,'T_Glucose_1',0,'b');
model = changeRxnBounds(model,'T_Glucose_2',0,'b');
% turn off glutamine transporter that does not require sodium
model = changeRxnBounds(model,'T_Glutamine_1',0,'b');
% prevent synthesis of collagen VI
model = changeRxnBounds(model,'CollagenVI',0,'b');
% set maximization criteria to collagen II
model = changeObjective(model,'T_Collagen_II');
% maximize production of collagen
FBAsolution1 = optimizeCbModel(model,'max');
% pull the important values
yield_CollagenII_glutamineNa
=((FBAsolution1.v(collagenII)*Cmol_collagenII)./(FBAsolution1.v(glutamine_Na)*Cmol_glutamine));

% next, aerobic conditions, use the transporter with no cost
model =
readCbModel('/Users/ebruerdogan/Desktop/ADA_Code_July/chondrocyte_model_27july2023_v4_Ammon
ium_Source','fileType','SBML')
% prevent the export of nonessential amino acids; aren't needed for this
model = changeRxnBounds(model,'cost_alanine',0,'b');
model = changeRxnBounds(model,'cost_arginine',0,'b');
model = changeRxnBounds(model,'cost_asparagine',0,'b');
model = changeRxnBounds(model,'cost_aspartate',0,'b');
model = changeRxnBounds(model,'cost_cysteine',0,'b');
model = changeRxnBounds(model,'cost_glutamate',0,'b');
model = changeRxnBounds(model,'cost_glutamine',0,'b');
model = changeRxnBounds(model,'cost_glycine',0,'b');
model = changeRxnBounds(model,'cost_proline',0,'b');
model = changeRxnBounds(model,'cost_serine',0,'b');
model = changeRxnBounds(model,'cost_tyrosine',0,'b');
% turn off ATPm and GTPm

```

```

model = changeRxnBounds(model,'T_ATP',0,'b');
model = changeRxnBounds(model,'T_GTP',0,'b');
% turn off pyruvate uptake
model = changeRxnBounds(model,'T_Pyruvate',0,'u');
% turn off lactate uptake
model = changeRxnBounds(model,'T_Lactate',0,'l');
% turn off CO2 uptake
model = changeRxnBounds(model,'T_CO2',0,'l');
% turn off HCO3 uptake
model = changeRxnBounds(model,'T_HCO3',1,'u');
% have to force transhydrogenase in the forward direction for the
% predictions to run properly. Otherwise, there seems to be an issue with
% Cobratoolbox predictions and ATP production is not actually maximized
model = changeRxnBounds(model,'TransHyd',0,'b');
% prevent glucose uptake
model = changeRxnBounds(model,'T_Glucose_1',0,'b');
model = changeRxnBounds(model,'T_Glucose_2',0,'b');
% turn off glutamine transporter that requires sodium
model = changeRxnBounds(model,'T_Glutamine_2',0,'b');
% prevent synthesis of collagen VI
model = changeRxnBounds(model,'CollagenVI',0,'b');
% set maximization criteria to collagen II
model = changeObjective(model,'T_Collagen_II');
% maximize production of collagen
FBA_solution2 = optimizeCbModel(model,'max');
% pull the important values
yield_CollagenII_glutaminenoCost
=((FBA_solution2.v(collagenII)*Cmol_collagenII)./(FBA_solution2.v(glutamine_noCost)*Cmol_glutamine));

% no O2 as terminal electron acceptor, use the glucose transporter that requires Na+

```

```
model =
readCbModel('/Users/ebruerdogan/Desktop/ADA_Code_July/chondrocyte_model_27july2023_v4_Ammon
ium_Source','fileType','SBML')
% prevent the export of nonessential amino acids; aren't needed for this
model = changeRxnBounds(model,'cost_alanine',0,'b');
model = changeRxnBounds(model,'cost_arginine',0,'b');
model = changeRxnBounds(model,'cost_asparagine',0,'b');
model = changeRxnBounds(model,'cost_aspartate',0,'b');
model = changeRxnBounds(model,'cost_cysteine',0,'b');
model = changeRxnBounds(model,'cost_glutamate',0,'b');
model = changeRxnBounds(model,'cost_glutamine',0,'b');
model = changeRxnBounds(model,'cost_glycine',0,'b');
model = changeRxnBounds(model,'cost_proline',0,'b');
model = changeRxnBounds(model,'cost_serine',0,'b');
model = changeRxnBounds(model,'cost_tyrosine',0,'b');
% turn off ATPm and GTPm
model = changeRxnBounds(model,'T_ATP',0,'b');
model = changeRxnBounds(model,'T_GTP',0,'b');
% turn off pyruvate uptake
model = changeRxnBounds(model,'T_Pyruvate',0,'u');
% turn off lactate uptake
model = changeRxnBounds(model,'T_Lactate',0,'l');
% turn off CO2 uptake
model = changeRxnBounds(model,'T_CO2',0,'l');
% turn off HCO3 uptake
model = changeRxnBounds(model,'T_HCO3',1,'u');
% have to force transhydrogenase in the forward direction for the
% predictions to run properly. Otherwise, there seems to be an issue with
% Cobratoolbox predictions and ATP production is not actually maximized
model = changeRxnBounds(model,'TransHyd',0,'b');
% prevent glutamine uptake
model = changeRxnBounds(model,'T_Glucose_1',0,'b');
```

```

model = changeRxnBounds(model,'T_Glucose_2',0,'b');
% turn off glucose transporter that does not require sodium
model = changeRxnBounds(model,'T_Glutamine_1',0,'b');
% prevent synthesis of collagen VI
model = changeRxnBounds(model,'CollagenVI',0,'b');
% prevent use of O2 as terminal electron acceptor
model = changeRxnBounds(model,'ETC_4',0,'b');
% set maximization criteria to collagen II
model = changeObjective(model,'T_Collagen_II');
% maximize production of collagen
FBAolution3 = optimizeCbModel(model,'max');
% pull the important values
yield_CollagenII_glutamineNa_noETC4
=((FBAolution3.v(collagenII)*Cmol_collagenII)/(FBAolution3.v(glutamine_Na)*Cmol_glutamine));

% no O2 as terminal electron acceptor, use the no cost glucose transporter
model =
readCbModel('/Users/ebruerdogan/Desktop/ADA_Code_July/chondrocyte_model_27july2023_v4_Ammon
ium_Source','fileType','SBML')
% prevent the export of nonessential amino acids; aren't needed for this
model = changeRxnBounds(model,'cost_alanine',0,'b');
model = changeRxnBounds(model,'cost_arginine',0,'b');
model = changeRxnBounds(model,'cost_asparagine',0,'b');
model = changeRxnBounds(model,'cost_aspartate',0,'b');
model = changeRxnBounds(model,'cost_cysteine',0,'b');
model = changeRxnBounds(model,'cost_glutamate',0,'b');
model = changeRxnBounds(model,'cost_glutamine',0,'b');
model = changeRxnBounds(model,'cost_glycine',0,'b');
model = changeRxnBounds(model,'cost_proline',0,'b');
model = changeRxnBounds(model,'cost_serine',0,'b');
model = changeRxnBounds(model,'cost_tyrosine',0,'b');
% turn off ATPm and GTPm

```

```

model = changeRxnBounds(model,'T_ATP',0,'b');
model = changeRxnBounds(model,'T_GTP',0,'b');
% turn off pyruvate uptake
model = changeRxnBounds(model,'T_Pyruvate',0,'u');
% turn off lactate uptake
model = changeRxnBounds(model,'T_Lactate',0,'l');
% turn off CO2 uptake
model = changeRxnBounds(model,'T_CO2',0,'l');
% turn off HCO3 uptake
model = changeRxnBounds(model,'T_HCO3',1,'u');
% have to force transhydrogenase in the forward direction for the
% predictions to run properly. Otherwise, there seems to be an issue with
% Cobratoolbox predictions and ATP production is not actually maximized
model = changeRxnBounds(model,'TransHyd',0,'b');
% prevent glucose uptake
model = changeRxnBounds(model,'T_Glucose_1',0,'b');
model = changeRxnBounds(model,'T_Glucose_2',0,'b');
% turn off glutamine transporter that does not require sodium
model = changeRxnBounds(model,'T_Glutamine_2',0,'b');
% prevent synthesis of collagen VI
model = changeRxnBounds(model,'CollagenVI',0,'b');
% prevent use of O2 as terminal electron acceptor
model = changeRxnBounds(model,'ETC_4',0,'b');
% set maximization criteria to collagen II
model = changeObjective(model,'T_Collagen_II');
% maximize production of collagen
FBA_solution4 = optimizeCbModel(model,'max');
% pull the important values
yield_CollagenII_glutaminenoCost_noETC4
=((FBA_solution4.v(collagenII)*Cmol_collagenII)/(FBA_solution4.v(glutamine_noCost)*Cmol_glutamine));

%% Model predictions for collagen VI yields on glutamine

```

```
% first, start with aerobic conditions, use the glutamine transporter that
% requires Na+
model =
readCbModel('/Users/ebruerdogan/Desktop/ADA_Code_July/chondrocyte_model_27july2023_v4_Ammon
ium_Source', 'fileType', 'SBML')
% % prevent the export of nonessential amino acids; aren't needed for this
model = changeRxnBounds(model, 'cost_alanine', 0, 'b');
model = changeRxnBounds(model, 'cost_arginine', 0, 'b');
model = changeRxnBounds(model, 'cost_asparagine', 0, 'b');
model = changeRxnBounds(model, 'cost_aspartate', 0, 'b');
model = changeRxnBounds(model, 'cost_cysteine', 0, 'b');
model = changeRxnBounds(model, 'cost_glutamate', 0, 'b');
model = changeRxnBounds(model, 'cost_glutamine', 0, 'b');
model = changeRxnBounds(model, 'cost_glycine', 0, 'b');
model = changeRxnBounds(model, 'cost_proline', 0, 'b');
model = changeRxnBounds(model, 'cost_serine', 0, 'b');
model = changeRxnBounds(model, 'cost_tyrosine', 0, 'b');
% turn off ATPm and GTPm
model = changeRxnBounds(model, 'T_ATP', 0, 'b');
model = changeRxnBounds(model, 'T_GTP', 0, 'b');
% turn off pyruvate uptake
model = changeRxnBounds(model, 'T_Pyruvate', 0, 'u');
% turn off lactate uptake
model = changeRxnBounds(model, 'T_Lactate', 0, 'l');
% turn off CO2 uptake
model = changeRxnBounds(model, 'T_CO2', 0, 'l');
% turn off HCO3 uptake
model = changeRxnBounds(model, 'T_HCO3', 1, 'u');
% have to force transhydrogenase in the forward direction for the
% predictions to run properly. Otherwise, there seems to be an issue with
% Cobratoolbox predictions and ATP production is not actually maximized
```

```
model = changeRxnBounds(model,'TransHyd',0,'b');
% prevent glucose uptake
model = changeRxnBounds(model,'T_Glucose_1',0,'b');
model = changeRxnBounds(model,'T_Glucose_2',0,'b');
% turn off glutamine transporter that does not require sodium
model = changeRxnBounds(model,'T_Glutamine_1',0,'b');
% prevent synthesis of collagen II
model = changeRxnBounds(model,'CollagenII',0,'b');
% set maximization criteria to collagen VI
model = changeObjective(model,'T_Collagen_VI');
% maximize production of collagen
FBA_solution1 = optimizeCbModel(model,'max');
% pull the important values
yield_CollagenVI_glutamineNa
=((FBA_solution1.v(collagenVI)*Cmol_collagenVI)./(FBA_solution1.v(glutamine_Na)*Cmol_glutamine));

% next, aerobic conditions, use the transporter with no cost
model =
readCbModel('/Users/ebruerdogan/Desktop/ADA_Code_July/chondrocyte_model_27july2023_v4_Ammonium_Source','fileType','SBML')
% prevent the export of nonessential amino acids; aren't needed for this
model = changeRxnBounds(model,'cost_alanine',0,'b');
model = changeRxnBounds(model,'cost_arginine',0,'b');
model = changeRxnBounds(model,'cost_asparagine',0,'b');
model = changeRxnBounds(model,'cost_aspartate',0,'b');
model = changeRxnBounds(model,'cost_cysteine',0,'b');
model = changeRxnBounds(model,'cost_glutamate',0,'b');
model = changeRxnBounds(model,'cost_glutamine',0,'b');
model = changeRxnBounds(model,'cost_glycine',0,'b');
model = changeRxnBounds(model,'cost_proline',0,'b');
model = changeRxnBounds(model,'cost_serine',0,'b');
model = changeRxnBounds(model,'cost_tyrosine',0,'b');
```

```

% turn off ATPm and GTPm
model = changeRxnBounds(model,'T_ATP',0,'b');
model = changeRxnBounds(model,'T_GTP',0,'b');
% turn off pyruvate uptake
model = changeRxnBounds(model,'T_Pyruvate',0,'u');
% turn off lactate uptake
model = changeRxnBounds(model,'T_Lactate',0,'l');
% turn off CO2 uptake
model = changeRxnBounds(model,'T_CO2',0,'l');
% turn off HCO3 uptake
model = changeRxnBounds(model,'T_HCO3',1,'u');
% have to force transhydrogenase in the forward direction for the
% predictions to run properly. Otherwise, there seems to be an issue with
% Cobratoolbox predictions and ATP production is not actually maximized
model = changeRxnBounds(model,'TransHyd',0,'b');
% prevent glucose uptake
model = changeRxnBounds(model,'T_Glucose_1',0,'b');
model = changeRxnBounds(model,'T_Glucose_2',0,'b');
% turn off glutamine transporter that requires sodium
model = changeRxnBounds(model,'T_Glutamine_2',0,'b');
% prevent synthesis of collagen II
model = changeRxnBounds(model,'CollagenII',0,'b');
% set maximization criteria to collagen VI
model = changeObjective(model,'T_Collagen_VI');
% maximize production of collagen
FBAolution2 = optimizeCbModel(model,'max');
% pull the important values
yield_CollagenVI_glutaminenoCost
=((FBAolution2.v(collagenVI)*Cmol_collagenVI)./(FBAolution2.v(glutamine_noCost)*Cmol_glutamine));

% no O2 as terminal electron acceptor, use the glucose transporter that requires Na+

```

```
model =
readCbModel('/Users/ebruerdogan/Desktop/ADA_Code_July/chondrocyte_model_27july2023_v4_Ammon
ium_Source','fileType','SBML')
% prevent the export of nonessential amino acids; aren't needed for this
model = changeRxnBounds(model,'cost_alanine',0,'b');
model = changeRxnBounds(model,'cost_arginine',0,'b');
model = changeRxnBounds(model,'cost_asparagine',0,'b');
model = changeRxnBounds(model,'cost_aspartate',0,'b');
model = changeRxnBounds(model,'cost_cysteine',0,'b');
model = changeRxnBounds(model,'cost_glutamate',0,'b');
model = changeRxnBounds(model,'cost_glutamine',0,'b');
model = changeRxnBounds(model,'cost_glycine',0,'b');
model = changeRxnBounds(model,'cost_proline',0,'b');
model = changeRxnBounds(model,'cost_serine',0,'b');
model = changeRxnBounds(model,'cost_tyrosine',0,'b');
% turn off ATPm and GTPm
model = changeRxnBounds(model,'T_ATP',0,'b');
model = changeRxnBounds(model,'T_GTP',0,'b');
% turn off pyruvate uptake
model = changeRxnBounds(model,'T_Pyruvate',0,'u');
% turn off lactate uptake
model = changeRxnBounds(model,'T_Lactate',0,'l');
% turn off CO2 uptake
model = changeRxnBounds(model,'T_CO2',0,'l');
% turn off HCO3 uptake
model = changeRxnBounds(model,'T_HCO3',1,'u');
% have to force transhydrogenase in the forward direction for the
% predictions to run properly. Otherwise, there seems to be an issue with
% Cobratoolbox predictions and ATP production is not actually maximized
model = changeRxnBounds(model,'TransHyd',0,'b');
% prevent glutamine uptake
model = changeRxnBounds(model,'T_Glucose_1',0,'b');
```

```

model = changeRxnBounds(model,'T_Glucose_2',0,'b');
% turn off glucose transporter that does not require sodium
model = changeRxnBounds(model,'T_Glutamine_1',0,'b');
% prevent use of O2 as terminal electron acceptor
model = changeRxnBounds(model,'ETC_4',0,'b');
% prevent synthesis of collagen II
model = changeRxnBounds(model,'CollagenII',0,'b');
% set maximization criteria to collagen VI
model = changeObjective(model,'T_Collagen_VI');
% maximize production of collagen
FBA_solution3 = optimizeCbModel(model,'max');
% pull the important values
yield_CollagenVI_glutamineNa_noETC4
= ((FBA_solution3.v(collagenVI)*Cmol_collagenVI)/(FBA_solution3.v(glutamine_Na)*Cmol_glutamine));

% no O2 as terminal electron acceptor, use the no cost glucose transporter
model =
readCbModel('/Users/ebruerdogan/Desktop/ADA_Code_July/chondrocyte_model_27july2023_v4_Ammon
ium_Source','fileType','SBML')
% prevent the export of nonessential amino acids; aren't needed for this
model = changeRxnBounds(model,'cost_alanine',0,'b');
model = changeRxnBounds(model,'cost_arginine',0,'b');
model = changeRxnBounds(model,'cost_asparagine',0,'b');
model = changeRxnBounds(model,'cost_aspartate',0,'b');
model = changeRxnBounds(model,'cost_cysteine',0,'b');
model = changeRxnBounds(model,'cost_glutamate',0,'b');
model = changeRxnBounds(model,'cost_glutamine',0,'b');
model = changeRxnBounds(model,'cost_glycine',0,'b');
model = changeRxnBounds(model,'cost_proline',0,'b');
model = changeRxnBounds(model,'cost_serine',0,'b');
model = changeRxnBounds(model,'cost_tyrosine',0,'b');
% turn off ATPm and GTPm

```

```

model = changeRxnBounds(model,'T_ATP',0,'b');
model = changeRxnBounds(model,'T_GTP',0,'b');
% turn off pyruvate uptake
model = changeRxnBounds(model,'T_Pyruvate',0,'u');
% turn off lactate uptake
model = changeRxnBounds(model,'T_Lactate',0,'l');
% turn off CO2 uptake
model = changeRxnBounds(model,'T_CO2',0,'l');
% turn off HCO3 uptake
model = changeRxnBounds(model,'T_HCO3',1,'u');
% have to force transhydrogenase in the forward direction for the
% predictions to run properly. Otherwise, there seems to be an issue with
% Cobratoolbox predictions and ATP production is not actually maximized
model = changeRxnBounds(model,'TransHyd',0,'b');
% prevent glucose uptake
model = changeRxnBounds(model,'T_Glucose_1',0,'b');
model = changeRxnBounds(model,'T_Glucose_2',0,'b');
% turn off glutamine transporter that does not require sodium
model = changeRxnBounds(model,'T_Glutamine_2',0,'b');
% prevent use of O2 as terminal electron acceptor
model = changeRxnBounds(model,'ETC_4',0,'b');
% prevent synthesis of collagen II
model = changeRxnBounds(model,'CollagenII',0,'b');
% set maximization criteria to collagen VI
model = changeObjective(model,'T_Collagen_VI');
% maximize production of collagen
FBA_solution4 = optimizeCbModel(model,'max');
% pull the important values
yield_CollagenVI_glutaminenoCost_noETC4
=((FBA_solution4.v(collagenVI)*Cmol_collagenVI)./(FBA_solution4.v(glutamine_noCost)*Cmol_glutamine));

%% AMINO ACID YIELDS ON GLUCOSE, AEROBIC

```

```

% predict yields of individual amino acids on glucose. Use the glucose
% transporter that requires Na+. Aerobic conditions.
model =
readCbModel('/Users/ebruerdogan/Desktop/ADA_Code_July/chondrocyte_model_27july2023_v4_Ammon
ium_Source','fileType','SBML')

"error with cysteine--analysis for that amino acid will be incorrect"
%
% turn off ATPm and GTPm
model = changeRxnBounds(model,'T_GTP',0,'b');
model = changeRxnBounds(model,'T_ATP',0,'b');
% turn off pyruvate uptake
model = changeRxnBounds(model,'T_Pyruvate',0,'u');
% turn off lactate uptake
model = changeRxnBounds(model,'T_Lactate',0,'l');
% turn off CO2 uptake
model = changeRxnBounds(model,'T_CO2',0,'l');
% turn off HCO3 uptake
model = changeRxnBounds(model,'T_HCO3',1,'u');
% cysteine production is causing loops that result in CO2 fixation...turn
% it off
model = changeRxnBounds(model,'cost_cysteine',0,'b');
% have to force transhydrogenase in the forward direction for the
% predictions to run properly. Otherwise, there seems to be an issue with
% Cobratoolbox predictions and ATP production is not actually maximized
model = changeRxnBounds(model,'TransHyd',0,'b');
% prevent glutamine uptake
model = changeRxnBounds(model,'T_Glutamine_1',0,'b');
model = changeRxnBounds(model,'T_Glutamine_2',0,'b');
% turn off glucose transporter that does not require sodium
model = changeRxnBounds(model,'T_Glucose_1',0,'b');
% prevent synthesis of collagen VI and collagen II

```

```
model = changeRxnBounds(model,'CollagenVI',0,'b');
model = changeRxnBounds(model,'CollagenIII',0,'b');
% set maximization criteria to the amino acid
model = changeObjective(model,'cost_alanine');
% maximize production of objective
FBA_solution_alanine = optimizeCbModel(model,'max');
% pull the important values
yield_alanine_glucoseNa
=((FBA_solution_alanine.v(alanine)*Cmol_alanine)./(FBA_solution_alanine.v(glucose_Na)*Cmol_glucose));

% set maximization criteria to the amino acid
model = changeObjective(model,'cost_arginine');
% maximize production of objective
FBA_solution_arginine = optimizeCbModel(model,'max');
% pull the important values
yield_arginine_glucoseNa
=((FBA_solution_arginine.v(arginine)*Cmol_arginine)./(FBA_solution_arginine.v(glucose_Na)*Cmol_glucose
));

% set maximization criteria to the amino acid
model = changeObjective(model,'cost_asparagine');
% maximize production of objective
FBA_solution_asparagine = optimizeCbModel(model,'max');
% pull the important values
yield_asparagine_glucoseNa
=((FBA_solution_asparagine.v(asparagine)*Cmol_asparagine)./(FBA_solution_asparagine.v(glucose_Na)*C
mol_glucose));

% set maximization criteria to the amino acid
```

```

model = changeObjective(model,'cost_aspartate');
% maximize production of objective
FBA_solution_aspartate = optimizeCbModel(model,'max');
% pull the important values
yield_aspartate_glucoseNa
=((FBA_solution_aspartate.v(aspartate)*Cmol_aspartate)./(FBA_solution_aspartate.v(glucose_Na)*Cmol_glu
ucose));

% set maximization criteria to the amino acid
% getting an infinite yield still.. limit bicarb uptake at some point
model = changeRxnBounds(model,'cost_cysteine',100,'u');
model = changeObjective(model,'cost_cysteine');
% maximize production of objective
FBA_solution_cysteine = optimizeCbModel(model,'max');
% pull the important values
yield_cysteine_glucoseNa
=((FBA_solution_cysteine.v(cysteine)*Cmol_cysteine)./(FBA_solution_cysteine.v(glucose_Na)*Cmol_gluco
se));

% cysteine production is causing loops that result in CO2 fixation...turn
% it off
model = changeRxnBounds(model,'cost_cysteine',0,'b');

% set maximization criteria to the amino acid
model = changeObjective(model,'cost_glutamate');
% maximize production of objective
FBA_solution_glutamate = optimizeCbModel(model,'max');
% pull the important values
yield_glutamate_glucoseNa
=((FBA_solution_glutamate.v(glutamate)*Cmol_glutamate)./(FBA_solution_glutamate.v(glucose_Na)*Cmol_
glucose));

```

```
% set maximization criteria to the amino acid
model = changeObjective(model,'cost_glutamine');
% maximize production of objective
FBA_solutio_n_glutamine = optimizeCbModel(model,'max');
% pull the important values
yield_glutamine_glucoseNa
=((FBA_solutio_n_glutamine.v(glutamine)*Cmol_glutamine)./(FBA_solutio_n_glutamine.v(glucose_Na)*Cmol_g
lucose));
```

```
% set maximization criteria to the amino acid
model = changeObjective(model,'cost_glycine');
% maximize production of objective
FBA_solutio_n_glycine = optimizeCbModel(model,'max');
% pull the important values
yield_glycine_glucoseNa
=((FBA_solutio_n_glycine.v(glycine)*Cmol_glycine)./(FBA_solutio_n_glycine.v(glucose_Na)*Cmol_glucose));
```

```
% set maximization criteria to the amino acid
model = changeObjective(model,'cost_proline');
% maximize production of objective
FBA_solutio_n_proline = optimizeCbModel(model,'max');
% pull the important values
yield_proline_glucoseNa
=((FBA_solutio_n_proline.v(proline)*Cmol_proline)./(FBA_solutio_n_proline.v(glucose_Na)*Cmol_glucose));
```

```
% set maximization criteria to the amino acid
model = changeObjective(model,'cost_serine');
% maximize production of objective
FBA_solutio_n_serine = optimizeCbModel(model,'max');
% pull the important values
```

```

yield_serine_glucoseNa
=((FBA_solutio_n_serine.v(serine)*Cmol_serine)./(FBA_solutio_n_serine.v(glucose_Na)*Cmol_glucose));

% set maximization criteria to the amino acid
model = changeObjective(model,'cost_tyrosine');
% maximize production of objective
FBA_solutio_n_tyrosine = optimizeCbModel(model,'max');
% pull the important values
yield_tyrosine_glucoseNa
=((FBA_solutio_n_tyrosine.v(tyrosine)*Cmol_tyrosine)./(FBA_solutio_n_tyrosine.v(glucose_Na)*Cmol_glucose)
);
% pull the important values
yield_tyrosine_phenylalanine
=((FBA_solutio_n_tyrosine.v(tyrosine)*Cmol_tyrosine)./(FBA_solutio_n_tyrosine.v(phenylalanine)*Cmol_phenyl
alanine));

%% AMINO ACID YIELDS ON GLUCOSE, NO OXIDATIVE PHOSPHORYLATION
% predict yields of individual amino acids on glucose. Use the glucose
% transporter that requires Na+. Turn off ETC4 (terminal oxidase). These
% predictions are not anaerobic exactly--tyrosine production requires O2
model =
readCbModel('/Users/ebruerdogan/Desktop/ADA_Code_July/chondrocyte_model_27july2023_v4_Ammon
ium_Source','fileType','SBML')
%
% turn off ATPm and GTPm
model = changeRxnBounds(model,'T_GTP',0,'b');
model = changeRxnBounds(model,'T_ATP',0,'b');
% turn off pyruvate uptake
model = changeRxnBounds(model,'T_Pyruvate',0,'u');
% turn off lactate uptake
model = changeRxnBounds(model,'T_Lactate',0,'l');

```

```

% turn off CO2 uptake
model = changeRxnBounds(model,'T_CO2',0,'l');
% turn off HCO3 uptake
model = changeRxnBounds(model,'T_HCO3',1,'u');
% have to force transhydrogenase in the forward direction for the
% predictions to run properly. Otherwise, there seems to be an issue with
% Cobratoolbox predictions and ATP production is not actually maximized
model = changeRxnBounds(model,'TransHyd',0,'b');
% prevent glutamine uptake
model = changeRxnBounds(model,'T_Glutamine_1',0,'b');
model = changeRxnBounds(model,'T_Glutamine_2',0,'b');
% turn off glucose transporter that does not require sodium
model = changeRxnBounds(model,'T_Glucose_1',0,'b');
% prevent synthesis of collagen VI and collagen II
model = changeRxnBounds(model,'CollagenVI',0,'b');
model = changeRxnBounds(model,'CollagenII',0,'b');
% prevent use of ETC_4
model = changeRxnBounds(model,'ETC_4',0,'b');

% set maximization criteria to the amino acid
model = changeObjective(model,'cost_alanine');
% maximize production of objective
FBA_solution_alanine_noETC4 = optimizeCbModel(model,'max');
% pull the important values
yield_alanine_glucoseNa_noETC4
=((FBA_solution_alanine_noETC4.v(alanine)*Cmol_alanine)./(FBA_solution_alanine_noETC4.v(glucose_Na
)*Cmol_glucose));

% set maximization criteria to the amino acid
model = changeObjective(model,'cost_arginine');

```

```

% maximize production of objective
FBAsolution_arginine_noETC4 = optimizeCbModel(model,'max');
% pull the important values
yield_arginine_glucoseNa_noETC4
=((FBAsolution_arginine_noETC4.v(arginine)*Cmol_arginine)./(FBAsolution_arginine_noETC4.v(glucose_
Na)*Cmol_glucose));

% set maximization criteria to the amino acid
model = changeObjective(model,'cost_asparagine');
% maximize production of objective
FBAsolution_asparagine_noETC4 = optimizeCbModel(model,'max');
% pull the important values
yield_asparagine_glucoseNa_noETC4
=((FBAsolution_asparagine_noETC4.v(asparagine)*Cmol_asparagine)./(FBAsolution_asparagine_noETC
4.v(glucose_Na)*Cmol_glucose));

%turn off cost_tyrosine
model = changeRxnBounds(model,'cost_tyrosine',0,'l');
% set maximization criteria to the amino acid
model = changeObjective(model,'cost_aspartate');
% maximize production of objective
FBAsolution_aspartate_noETC4 = optimizeCbModel(model,'max');
% pull the important values
yield_aspartate_glucoseNa_noETC4
=((FBAsolution_aspartate_noETC4.v(aspartate)*Cmol_aspartate)./(FBAsolution_aspartate_noETC4.v(glu
cose_Na)*Cmol_glucose));

%turn on cost_tyrosine
model = changeRxnBounds(model,'cost_tyrosine',100,'u');
% set maximization criteria to the amino acid
model = changeObjective(model,'cost_cysteine');

```

```
% maximize production of objective
FBA_solution_cysteine_noETC4 = optimizeCbModel(model,'max');
% pull the important values
yield_cysteine_glucoseNa_noETC4
= ((FBA_solution_cysteine_noETC4.v(cysteine)*Cmol_cysteine)./(FBA_solution_cysteine_noETC4.v(glucose
_Na)*Cmol_glucose));

% set maximization criteria to the amino acid
model = changeObjective(model,'cost_glutamate');
% maximize production of objective
FBA_solution_glutamate_noETC4 = optimizeCbModel(model,'max');
% pull the important values
yield_glutamate_glucoseNa_noETC4
= ((FBA_solution_glutamate_noETC4.v(glutamate)*Cmol_glutamate)./(FBA_solution_glutamate_noETC4.v(gl
ucose_Na)*Cmol_glucose));

% set maximization criteria to the amino acid
model = changeObjective(model,'cost_glutamine');
% maximize production of objective
FBA_solution_glutamine_noETC4 = optimizeCbModel(model,'max');
% pull the important values
yield_glutamine_glucoseNa_noETC4
= ((FBA_solution_glutamine_noETC4.v(glutamine)*Cmol_glutamine)./(FBA_solution_glutamine_noETC4.v(gl
ucose_Na)*Cmol_glucose));

% set maximization criteria to the amino acid
model = changeObjective(model,'cost_glycine');
% maximize production of objective
FBA_solution_glycine_noETC4 = optimizeCbModel(model,'max');
% pull the important values
```

```

yield_glycine_glucoseNa_noETC4
=((FBA_solutio_n_glycine_noETC4.v(glycine)*Cmol_glycine)./(FBA_solutio_n_glycine_noETC4.v(glucose_Na)*
Cmol_glucose));

% set maximization criteria to the amino acid
model = changeObjective(model,'cost_proline');
% maximize production of objective
FBA_solutio_n_proline_noETC4 = optimizeCbModel(model,'max');
% pull the important values
yield_proline_glucoseNa_noETC4
=((FBA_solutio_n_proline_noETC4.v(proline)*Cmol_proline)./(FBA_solutio_n_proline_noETC4.v(glucose_Na)*
Cmol_glucose));

% set maximization criteria to the amino acid
model = changeObjective(model,'cost_serine');
% maximize production of objective
FBA_solutio_n_serine_noETC4 = optimizeCbModel(model,'max');
% pull the important values
yield_serine_glucoseNa_noETC4
=((FBA_solutio_n_serine_noETC4.v(serine)*Cmol_serine)./(FBA_solutio_n_serine_noETC4.v(glucose_Na)*Cm
ol_glucose));

% set maximization criteria to the amino acid
model = changeObjective(model,'cost_tyrosine');
% maximize production of objective
FBA_solutio_n_tyrosine_noETC4 = optimizeCbModel(model,'max');
% pull the important values
yield_tyrosine_glucoseNa_noETC4
=((FBA_solutio_n_tyrosine_noETC4.v(tyrosine)*Cmol_tyrosine)./(FBA_solutio_n_tyrosine_noETC4.v(glucose_
Na)*Cmol_glucose));
% pull the important values

```

```
yield_tyrosine_phenylalanine_noETC4
=((FBA_solutio_n_tyrosine_noETC4.v(tyrosine)*Cmol_tyrosine)./(FBA_solutio_n_tyrosine_noETC4.v(phenylala
nine)*Cmol_phenylalanine));
```

### Appendix B.3

```
%% heatmap comparing collagen II yields vs lactate fermentation
% first, run predictions that maximize lactate production. Pull max
% lactate flux. Use that value as the maximum, scale down lactate
% production, and run predictions for max collagen II as a function of
% lactate fermentation
% for each one, pull the fluxes through key reactions. Then, plot those
% fluxes as a heatmap

initCobraToolbox()

%% Set some reaction names and balance variables
model =
readCbModel('/Users/ebruerdogan/Desktop/ADA_Code_July/chondrocyte_model_27july2023_v2.xml','file
Type','SBML')

% biomass and ATP maintenance terms
collagenII = find(strcmp('T_Collagen_II',model.rxns));
collagenVI = find(strcmp('T_Collagen_VI',model.rxns));
O2 = find(strcmp('T_O2',model.rxns));
ATPm = find(strcmp('T_ATP',model.rxns));
glucose_noCost = find(strcmp('T_Glucose_1',model.rxns));
glucose_Na = find(strcmp('T_Glucose_2',model.rxns));
glutamine_noCost = find(strcmp('T_Glutamine_1',model.rxns));
glutamine_Na = find(strcmp('T_Glutamine_2',model.rxns));
pyruvate_dehydrogenase = find(strcmp('PYR_1', model.rxns));
oxidase = find(strcmp('ETC_4', model.rxns));
```

```
lactate_production = find(strcmp('T_Lactate', model.rxns));  
ATP_synthase = find(strcmp('ATP', model.rxns));  
pyruvate_transport = find(strcmp('T_Pyruvate', model.rxns));
```

```
alanine = find(strcmp('cost_alanine', model.rxns));  
arginine = find(strcmp('cost_arginine', model.rxns));  
asparagine = find(strcmp('cost_asparagine', model.rxns));  
aspartate = find(strcmp('cost_aspartate', model.rxns));  
cysteine = find(strcmp('cost_cysteine', model.rxns));  
glutamate = find(strcmp('cost_glutamate', model.rxns));  
glutamine = find(strcmp('cost_glutamine', model.rxns));  
glycine = find(strcmp('cost_glycine', model.rxns));  
proline = find(strcmp('cost_proline', model.rxns));  
serine = find(strcmp('cost_serine', model.rxns));  
tyrosine = find(strcmp('cost_tyrosine', model.rxns));  
phenylalanine = find(strcmp('T_Phe', model.rxns));
```

#### % carbon content of each metabolite of interest

```
Cmol_collagenII = 395;  
Cmol_collagenVI = 462;  
Cmol_glucose = 6;  
Cmol_glutamine = 5;  
  
Cmol_alanine = 3;  
Cmol_arginine = 6;  
Cmol_asparagine = 4;  
Cmol_aspartate = 4;  
Cmol_cysteine = 3;  
Cmol_glutamate = 5;  
Cmol_glycine = 2;  
Cmol_proline = 5;  
Cmol_serine = 3;
```

```
Cmol_tyrosine = 9;
Cmol_phenylalanine = 9;

%% run the first prediction that maximizes collagen production on glucose
% use the no cost glucose transporter
% aerobic conditions but use glucose transporter with no cost
model =
readCbModel('/Users/ebruerdogan/Desktop/ADA_Code_July/chondrocyte_model_27july2023_v2.xml','file
Type','SBML')
% % prevent the export of nonessential amino acids; aren't needed for this
model = changeRxnBounds(model,'cost_alanine',0,'b');
model = changeRxnBounds(model,'cost_arginine',0,'b');
model = changeRxnBounds(model,'cost_asparagine',0,'b');
model = changeRxnBounds(model,'cost_aspartate',0,'b');
model = changeRxnBounds(model,'cost_cysteine',0,'b');
model = changeRxnBounds(model,'cost_glutamate',0,'b');
model = changeRxnBounds(model,'cost_glutamine',0,'b');
model = changeRxnBounds(model,'cost_glycine',0,'b');
model = changeRxnBounds(model,'cost_proline',0,'b');
model = changeRxnBounds(model,'cost_serine',0,'b');
model = changeRxnBounds(model,'cost_tyrosine',0,'b');
% turn off GTPm
model = changeRxnBounds(model,'T_GTP',0,'b');
% turn off ATPm
model = changeRxnBounds(model,'T_ATP',0,'b');
% turn off pyruvate uptake
model = changeRxnBounds(model,'T_Pyruvate',0,'u');
% turn off lactate uptake
model = changeRxnBounds(model,'T_Lactate',0,'l');
% have to force transhydrogenase in the forward direction for the
% predictions to run properly. Otherwise, there seems to be an issue with
```

```

% Cobratoolbox predictions and ATP production is not actually maximized
model = changeRxnBounds(model,'TransHyd',0,'b');
% prevent glutamine uptake
model = changeRxnBounds(model,'T_Glutamine_1',0,'b');
model = changeRxnBounds(model,'T_Glutamine_2',0,'b');
% turn off glucose transporter that requires sodium
model = changeRxnBounds(model,'T_Glucose_2',0,'b');
% prevent synthesis of collagen VI and collagen II
model = changeRxnBounds(model,'CollagenVI',0,'b');
model = changeRxnBounds(model,'CollagenII',0,'b');
% set maximization criteria to lactate
model = changeObjective(model,'T_Lactate');
% maximize production of collagen II
FBAolution_max1 = optimizeCbModel(model,'max');
% pull the flux of O2 out
max_lactate = FBAolution_max1.v(lactate_production);

%% now, scale lactate flux to each of ten different values. This one has transhydrogenase forward only
% aerobic conditions but use glucose transporter with no cost
model =
readCbModel('/Users/ebruerdogan/Desktop/ADA_Code_July/chondrocyte_model_27july2023_v2.xml','file
Type','SBML')
% % prevent the export of nonessential amino acids; aren't needed for this
model = changeRxnBounds(model,'cost_alanine',0,'b');
model = changeRxnBounds(model,'cost_arginine',0,'b');
model = changeRxnBounds(model,'cost_asparagine',0,'b');
model = changeRxnBounds(model,'cost_aspartate',0,'b');
model = changeRxnBounds(model,'cost_cysteine',0,'b');
model = changeRxnBounds(model,'cost_glutamate',0,'b');
model = changeRxnBounds(model,'cost_glutamine',0,'b');
model = changeRxnBounds(model,'cost_glycine',0,'b');
model = changeRxnBounds(model,'cost_proline',0,'b');

```

```

model = changeRxnBounds(model,'cost_serine',0,'b');
model = changeRxnBounds(model,'cost_tyrosine',0,'b');
% turn off GTPm
model = changeRxnBounds(model,'T_GTP',0,'b');
% turn off ATPm
model = changeRxnBounds(model,'T_ATP',0,'b');
% turn off pyruvate uptake
model = changeRxnBounds(model,'T_Pyruvate',0,'u');
% turn off lactate uptake
model = changeRxnBounds(model,'T_Lactate',0,'l');
% have to force transhydrogenase in the forward direction for the
% predictions to run properly. Otherwise, there seems to be an issue with
% Cobratoolbox predictions and ATP production is not actually maximized
model = changeRxnBounds(model,'TransHyd',0,'b');
% prevent glutamine uptake
model = changeRxnBounds(model,'T_Glutamine_1',0,'b');
model = changeRxnBounds(model,'T_Glutamine_2',0,'b');
% turn off glucose transporter that requires sodium
model = changeRxnBounds(model,'T_Glucose_2',0,'b');
% prevent synthesis of collagen II
model = changeRxnBounds(model,'CollagenII',0,'b');
% set maximization criteria to Collagen VI
model = changeObjective(model,'CollagenVI');

lactate_values = [max_lactate, 0.9*max_lactate, 0.8*max_lactate, 0.7*max_lactate,
0.6*max_lactate,0.5*max_lactate,0.4*max_lactate,0.3*max_lactate,0.2*max_lactate,0.1*max_lactate,0];
heatmap_matrix = zeros([11,4])
for i = 1:11
    % set lactate flux
    model = changeRxnBounds(model,'T_Lactate',lactate_values(i),'b');
    lactate_values(i)
    % maximize production of collagen II

```

```

FBAolution = optimizeCbModel(model,'max');
% get the values for the fluxes through reactions of interest. Scale to
% glucose uptake
flux_oxidase =((FBAolution.v(oxidase))./(FBAolution.v(glucose_noCost)));
heatmap_matrix(i,1) = flux_oxidase;
flux_collagen =((FBAolution.v(collagenVI))./(FBAolution.v(glucose_noCost)));
heatmap_matrix(i,2) = flux_collagen;
flux_pyruvatedehydrogenase
= ((FBAolution.v(pyruvate_dehydrogenase))./(FBAolution.v(glucose_noCost)));
heatmap_matrix(i,3) = flux_pyruvatedehydrogenase;
flux_lactate =((FBAolution.v(lactate_production))./(FBAolution.v(glucose_noCost)));
heatmap_matrix(i,4) = flux_lactate;
end

% plot the data as a heatmap
x_names = ["oxidative phosphorylation"; "collagen production"; 'pyruvate dehydrogenase'; 'lactate'];
%y_label = str(O2_values);
figure(1)
set(gca, 'fontsize', 55)
h = heatmap(x_names, lactate_values, heatmap_matrix)
h.XLabel = "Reactions (mol/mol glucose)"
h.YLabel = "Lactate Fermentation Fluxes (mol lactate / mol glucose)"
h.Title = "Flux as a Function of Lactate Fermentation"
h.ColorScaling = 'scaledcolumns'

```